DOT/FAA/PS-88/12

Project Report
ATC-161

Observability of Microbursts Using Doppler Weather Radar and Surface Anemometers During 1987 in Denver, CO

J. T. DiStefano

29 December 1988

Lincoln Laboratory
MASSACHUSETTS INSTITUTE OF TECHNOLOGY
LEXINGTON, MASSACHUSETTS

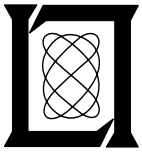

Prepared for the Federal Aviation Administration,
Washington, D.C. 20591

This document is available to the public through
the National Technical Information Service,
Springfield, VA 22161

TECHNICAL REPORT STANDARD TITLE PAGE

1. Report No.	2. Government Accession No.	3. Recipient's Catalog No.
DOT/FAA/RD/PS-88/12		

4. Title and Subtitle	5. Report Date
Observability of Microbursts Using Doppler Weather Radar and Surface Anemometers During 1987 in Denver, CO	29 December 1988
	6. Performing Organization Code

7. Author(s)	8. Performing Organization Report No.
John T. DiStefano	ATC-161

9. Performing Organization Name and Address	10. Work Unit No. (TRAIS)
Lincoln Laboratory, MIT P.O. Box 73 Lexington, MA 02173-0073	11. Contract or Grant No. DTFA-01L-83-4-10579
	13. Type of Report and Period Covered
12. Sponsoring Agency Name and Address Department of Transportation Federal Aviation Administration 800 Independence Avenue, SW Washington, DC 20591	Project Report
	14. Sponsoring Agency Code

15. Supplementary Notes

The work reported in this document was performed at Lincoln Laboratory, a center for research operated by Massachusetts Institute of Technology under Air Force Contract F19628-85-C-0002.

16. Abstract

This report focuses on the observability of microbursts using pulse Doppler weather radars and surface anemometers respectively by an experienced meteorologist. The data used for this study were collected in the Denver, Colorado area during the FAA Terminal Doppler Weather Radar (TDWR) measurement program in 1987. The methods used for declaring a microburst from both Doppler radar and surface anemometer data are described.

The main objective of this report is to compare the 1987 radar observed microbursts (which impacted the area covered by a surface anemometer system) with the surface mesonet observed microbursts. Of the 66 microbursts for which radar and mesonet data were available, 4 were not observed by the radar and 1 was not observed by the mesonet. All four microbursts not observed by the radar were classified as "dry" events with low surface reflectivities and with three of the four being relatively weak (peak velocity differences $\leq$ 20 m/s) shear events. Possible reasons as to why these microbursts were not observed are discussed in detail. The strongest event exceeded 20 m/s (differential velocity) for two minutes and appears to have been missed due to a combination of very low reflectivity and a very shallow depth overflow.

17. Key Words		18. Distribution Statement
Terminal Doppler Weather Radar	dry microburst	Document is available to the public through the National Technical Information Service, Springfield, VA 22161.
mesonet	surface anemometers	
observability	low level windshear	
microburst	radar/mesonet comparison	

19. Security Classif. (of this report)	20. Security Classif. (of this page)	21. No. of Pages	22. Price
Unclassified	Unclassified	114	

FORM DOT F 1700.7 (8-69)

ABSTRACT

This report focuses on the observability of microbursts using pulse Doppler weather radars and surface anemometers respectively by an experienced meteorologist. The data used for this study were collected in the Denver, Colorado area during the FAA Terminal Doppler Weather Radar (TDWR) measurement program in 1987. The methods used for declaring a microburst from both Doppler radar and surface anemometer data are described.

The main objective of this report is to compare the 1987 radar observed microbursts (which impacted the area covered by a surface anemometer system) with the surface mesonet observed microbursts. Of the 66 microbursts for which radar and mesonet data were available, 4 were not observed by the radar and 1 was not observed by the mesonet. All four microbursts not observed by the radar were classified as "dry" events with low surface reflectivities and with three of the four being relatively weak (peak velocity differences $\leq$ 20 m/s) shear events. Possible reasons as to why these microbursts were not observed are discussed in detail. The strongest event exceeded 20 m/s (differential velocity) for two minutes and appears to have been missed due to a combination of very low reflectivity and a very shallow depth outflow.

TABLE OF CONTENTS

LIST OF ILLUSTRATIONS

LIST OF TABLES

ACRONYMS

AGL	Above Ground Level
FAA	Federal Aviation Administration
FLOWS	FAA/Lincoln Laboratory Observational Weather Studies
FL-2	FAA/Lincoln Laboratory Test-bed Doppler Radar
GAO	General Accounting Office
JAWS	Joint Airport Weather Studies
LLWAS	Low-Level Windshear Alert System
Mesonet	Refers to a network of automatic weather stations with a close, i.e., a "mesoscale" spacing
MSL	Mean Sea Level
NEXRAD	Next Generation Weather Radar
NWSFO	National Weather Service Forecast Office
PROBE	Portable Remote OBservations of the Environment
SNR	Signal-to-Noise Ratio
TDWR	Terminal Doppler Weather Radar
UND	University of North Dakota
UT	Universal Time

I. INTRODUCTION

In 1987, Denver, Colorado was the site for the FAA Terminal Doppler Weather Radar (TDWR) measurement program. During this time, Doppler weather radar and surface data were collected on low-level wind shear events, in particular microbursts and gust fronts that occurred within the area. It has been shown that microbursts pose a potential hazard to aviation [Fujita, 1980; 1983; National Research Council, 1983; Fujita, 1985; 1986]. The use of Doppler radar has been presented as an effective means for identifying such events [Wilson, et al., 1984]. This report focuses on the observability of Denver microbursts using pulse Doppler weather radars and surface anemometers. Similar studies were done on data collected in Memphis, Tennessee [DiStefano, 1987] and Huntsville, Alabama [Clark, 1988].

The radars used in collecting data during this program were an S-band radar (FL-2), which was developed and operated by Lincoln Laboratory for the FAA [Evans and Turnbull, 1985], and a C-band radar that was operated by the University of North Dakota (UND). These two radars, FL-2 and UND, were located approximately 15 km southeast and 15 km northeast of Denver's Stapleton International Airport, respectively (see Figure I-1).

The mesonet system, from which surface meteorological data was collected, consisted of:

(1) 30 PROBE (Portable Remote OBservations of the Environment) weather stations [Wolfson, et al., 1986], and

(2) an enhanced 12 station Low-Level Wind Shear Alert System (LLWAS).

The PROBE stations collected data on several meteorological parameters (barometric pressure, relative humidity, temperature, precipitation rates, average and peak wind speed and direction) while the LLWAS sensors recorded only wind speed and direction. The locations of these 42 sensors are also shown in Figure I-1. All these surface sensors, except for stations 29 and 30, which are situated at the radar sites, are located in a 150 square km area centered about the airport. The typical station spacing of the sensors in this area is approximately 2.3 km. This is approximately the same value used for the station spacing of the enhanced LLWAS at Denver.

The analysis performed during this study determined, through comparison with surface mesonet observations, the probability of microburst events that are observable in the radar field (either over or in close proximity to the mesonet) by expert humans. Other studies of radar data compare algorithm detected microbursts [Merritt, 1987; Campbell, 1987] to those determined by expert humans from radar observations alone. Figure I-2 shows a diagram that compares these two comparative studies, with the former identified

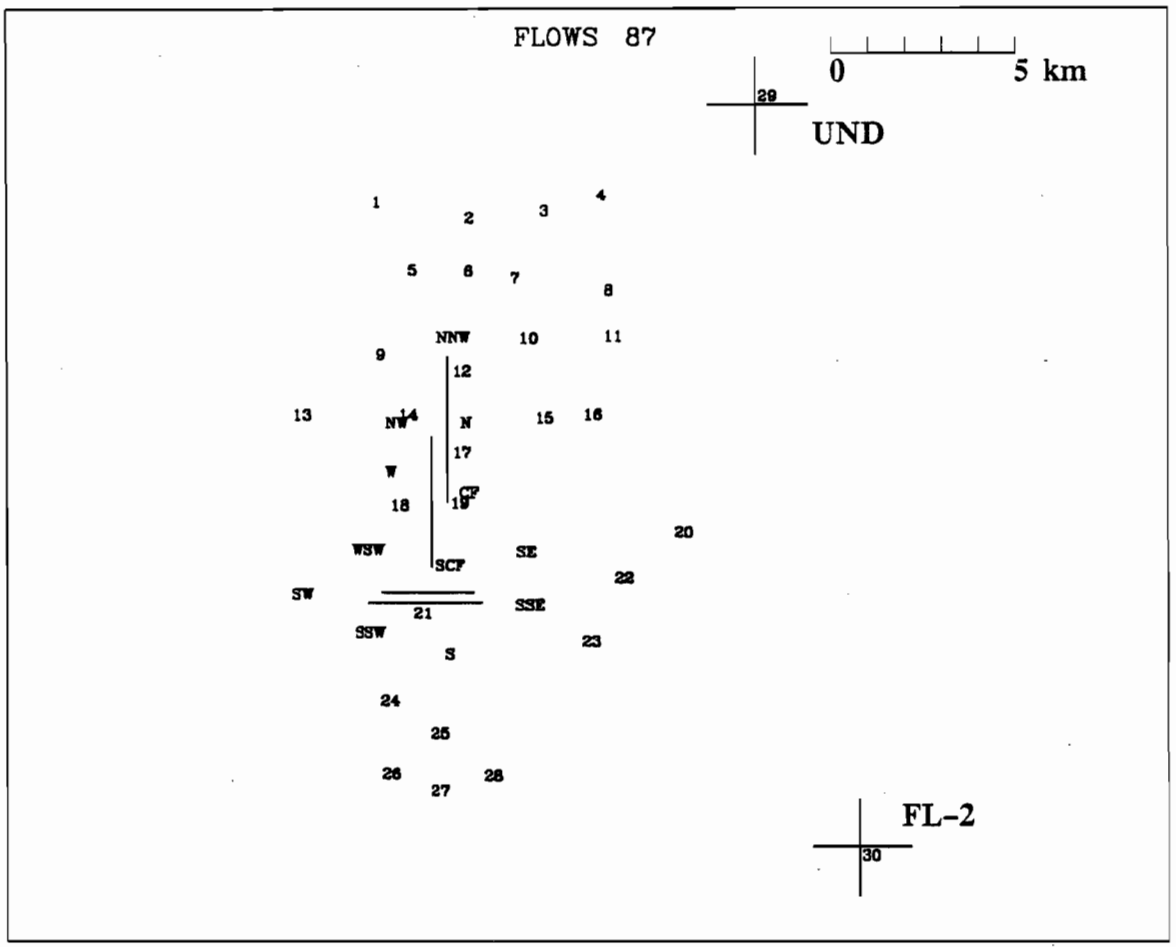

Figure I-1. *The 1987 TDWR testbed mesonet in Denver, Colorado (2 radars, 30 PROBE stations (numbered 1-30), and 12 LLWAS sensors (labelled with 1-3 letter identifiers)). The runways of Denver's Stapleton International Airport are denoted by straight lines.*

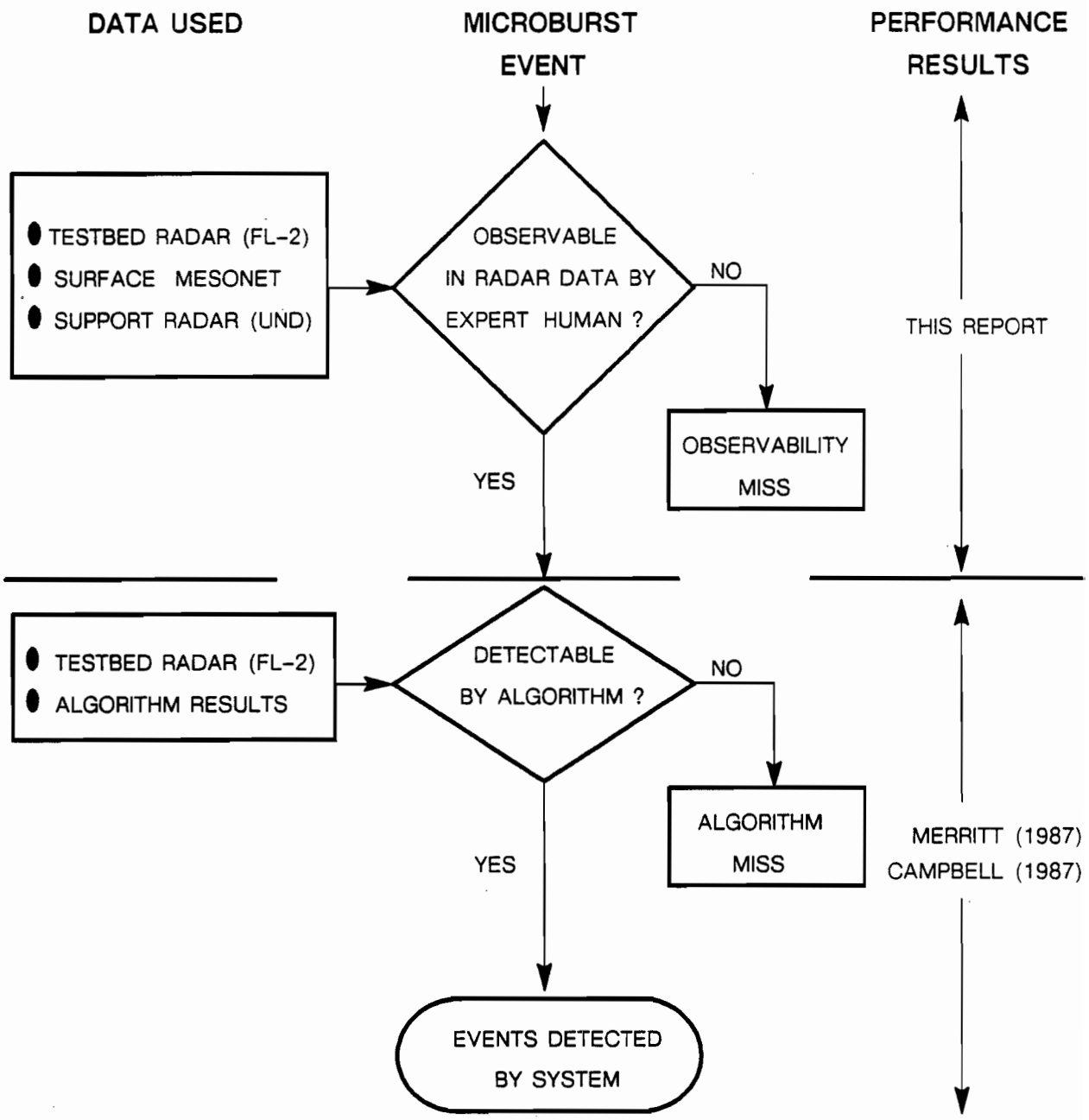

Figure I-2. *Relationship of microburst detection studies*

by the top and the latter by the bottom. The analysis reported in this study addresses the possibility that microbursts are not observed by the radar due to:

(1) low SNR (signal-to-noise ratio),

(2) the radar beam looking too high above the surface (i.e., looking above events that have very shallow outflows),

(3) blockage of the beam, and/or

(4) asymmetry in the surface wind field causing radar to significantly underestimate the magnitude of the surface wind shear [Eilts and Doviak,1987; GAO, 1987].

These potential problems indicate why, for this study, the radar data was compared with surface mesonet data. Also addressed is the possibility that microbursts are not observed by the mesonet surface sensors (e.g., due to too large a station spacing or microburst outflows not reaching the surface due to a dense layer of cold air).

The second chapter of this report describes the methodology used for declaring a microburst from Doppler radar and surface mesonet data. Chapter III identifies the procedure in comparing radar and mesonet data, while Chapter IV provides an overall listing of microburst observations and results from the radar/mesonet comparison study. Chapter V details specific cases in which missed microburst events were identified. A case is also given exemplifying the observability of a rather weak microburst by both the radar and mesonet sensors. Chapter VI summarizes the results while the last chapter discusses some future plans for data analysis.

II. METHODOLOGY USED IN DECLARING A MICROBURST

Fujita describes a downburst as a strong downdraft which induces a microburst of damaging* winds on or near the ground. The outburst winds, either straight or curved, are highly divergent [Fujita, 1985]. He subdivides the downburst into two categories depending on the outbursts' horizontal scale:

(1) macroburst – a large downburst with its outburst winds extending in excess of 4 km in the horizontal direction, and

(2) microburst – a small downburst with its outburst winds extending only 4 km or less in the horizontal (see Figure II–1).

This divergent outburst, which was the main microburst identifying feature, was searched for in both the FL–2 and surface mesonet data sets.

A. Using Doppler Radar Data

In both real time and playback modes, the microburst signature was identified in the Doppler velocity field by a divergent outflow at or near the surface. The observed minimum differential velocity values within this outflow had to reach 10 m/s within a range extent of 4 km for at least one low–level scan during the microburst's history. This criteria differs somewhat with that used in the detection algorithms. Merritt (1987) used a similar microburst definition where a wind speed difference of 10 m/s over a distance of no more than 4 km must be exhibited, but he also imposed spacial and temporal requirements on this divergent outflow signature. The current TDWR microburst detection algorithm [Campbell and Merritt (1987)] uses a similar definition of a microburst as observed in the surface velocity field (with a slightly lower threshold), but requires that a surface outflow whose radial mean velocity difference is less than 10 m/s (but $\geq$ 7.5 m/s) be associated with meteorological phenomena aloft. Also, microburst truthers, those experienced radar meteorologists who determine the existence of microbursts from radar data to assist the algorithm developers with their evaluation, have been less stringent in their identification of microbursts. The group developing truth for the TDWR performance assessment has agreed that a differential velocity of 10 m/s does not necessarily need to occur along a single radial, but could be skewed** to allow for asymmetry in microburst outflows.

---

* It should be noted that the wind shear which accompanies these events may be hazardous to aviation but may not necessarily produce damage to impacted structures or landscapes.

** Skewed here would mean that the differential velocity could be measured along a line somewhat off–set/slanted from a single radial.

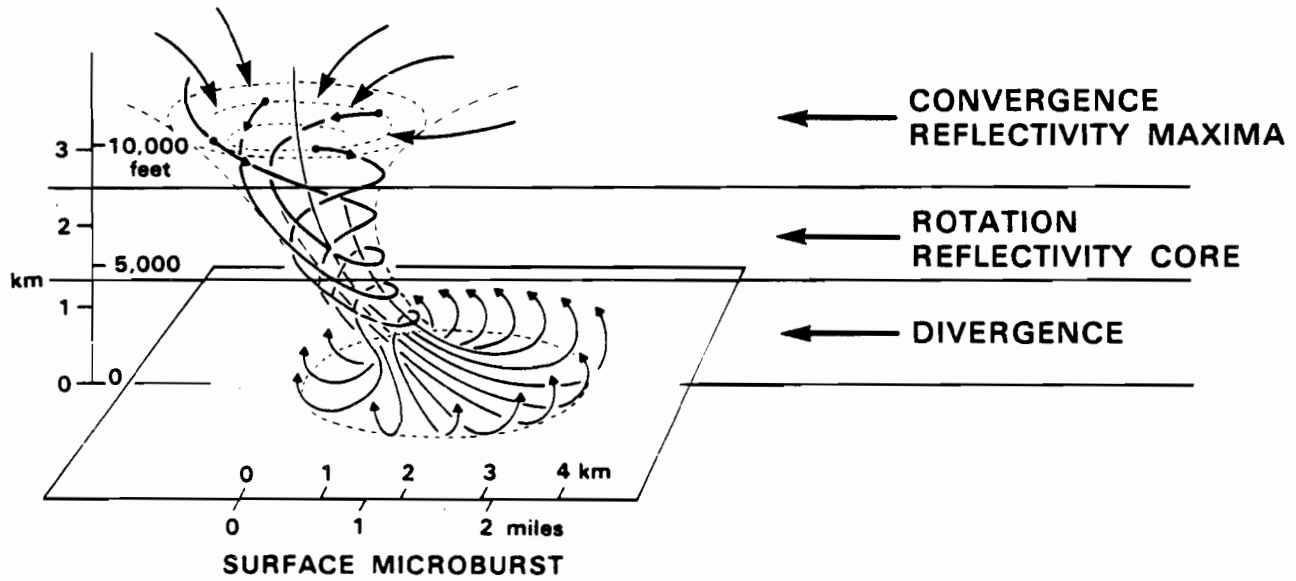

Figure II-1. Generalized model of a microburst.

Figure II–2 portrays an ideal surface divergent signature produced by a microburst outflow. The radar in this figure observes a radial velocity couplet, where the negative values are velocities approaching the radar while positive values are receding. Realistically, however, not all microbursts demonstrate this clear signature. For those that did not, further analysis involving a hierarchy of the radar's higher intrinsic resolution were performed. It should also be noted that FL–2 was the primary source of radar data used for identifying microbursts during this study. The UND radar was a back–up source for information and to be used if:

(1) there are no available FL–2 data, or

(2) the FL–2 radar data showed no clear microburst signature.

Although the microburst signature is ultimately identified in the Doppler velocity field, more supportive information can be found in the reflectivity field. In order for a wind shear event to be classified a microburst, a parent cloud must first exist from which this event can emanate [Fujita, 1985]. Therefore, there should be evidence in the reflectivity field of an existing cell. In Denver, during this 1987 data collection period, it was not always obvious from the low–level radar reflectivity field that a cell existed even though a

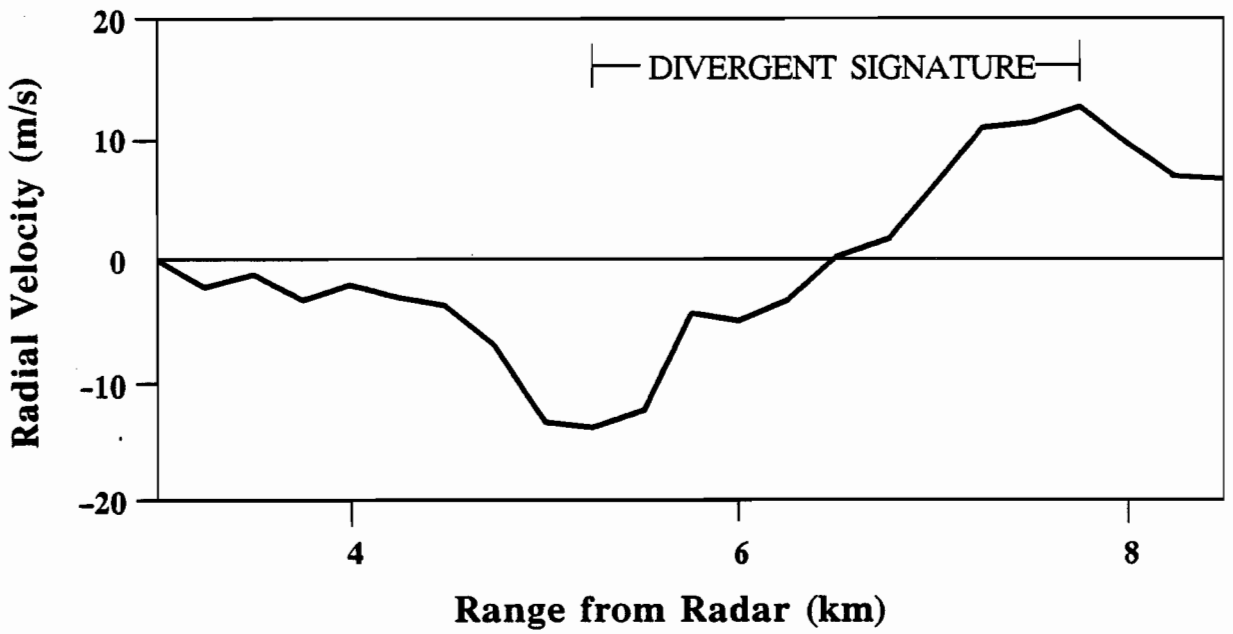

Figure II – 2. *Microburst divergent outflow signature.*

distinct microburst signature in the Doppler velocity field would suggest that there was one. In cases such as this, it was necessary to look aloft in order to clearly identify the cell. Fujita (1985) has made reference to similar types of microbursts which have been observed in the Denver area during the Joint Airport Weather Studies (JAWS) Project of 1982. These events are classified as "dry microbursts" and are commonly seen in dry regions (i.e., Denver) where the convective clouds have deep (several km's) sub-cloud layers. The precipitation which is observed falling from this type of cloud often evaporates completely before reaching the ground (i.e., virga), hence, the low or negligible reflectivity values at the surface. During 1987 in Denver, only one event, which occurred on July 6, indicated a surface divergent signature where differential velocity values of 10–15 m/s were observed for a short period, but where no parent cell existed. In this case, a wind shear event was evident but, according to the above definition, was not a microburst.

B. Using Surface Mesonet Data

Once the surface mesonet data have been received at Lincoln Laboratory and converted to a common format, they are inventoried and plotted for immediate analysis. From this initial look at the data and from the FLOWS operational field logs, the days and times on which microbursts (and other wind shear events) may have occurred over the mesonet are determined [Wolfson, *et al.*, 1986]. A primary indicator of the microburst, through this initial analysis, is given by the profile of the wind speed where an isolated peak may be identified. Other parameters (along with wind speed) such as wind direction, barometric pressure, temperature, precipitation rate, and relative humidity may also aid in the declaration process for a microburst. Statistics on these identifying parameters are discussed by Fujita (1985) and Rinehart, et al. (1986).

Several steps, involving both objective and subjective analysis, are then taken to confirm and classify the event(s) [Wolfson, *et al.*, 1986]. Probably the most important part of this analysis is identifying the surface divergence over the mesonet. Once this surface signature, such as seen in Figure II–1, is identified, the strength of the event as observed by the differential velocity is noted through an objective shear analysis scheme. In order for the event to be classified as a microburst, it should attain a differential velocity value of 10 m/s within a distance of 4 km. This is the same threshold value used in identifying a microburst from the analysis of Doppler velocity fields. However, due to the undersampling of the surface mesonet field, it is not always possible to calculate the differential velocity of an event within the suggested 4 km distance. For example, if an event affects stations 23 and 30 or stations 1 and 13 (see Figure I–1) with differential velocities in excess of the threshold value of 10 m/s, but obviously not within the specified distance of 4 km, then a more subjectively arrived at determination, by the author, would be made concerning the classification of the event. Clark (1988) indicates the reliability of this methodology as a suitable approach for microburst identification.

III. COMPARING RADAR AND MESONET DATA

Comparison of the Doppler radar detected microbursts, which occurred over (or in close proximity to) the surface mesonet, with the mesonet detected microburst was the prime objective of this 1987 evaluation. The procedure during this evaluation was straight forward. If a microburst signature was observed by the mesonet surface sensors, it would be checked against the corresponding Doppler radar data and a determination regarding the classification of the event would be made. Likewise, microburst signatures that were identified from radar data during real and/or post-real time analysis were also checked against their complimenting data set (the mesonet) in order to make a similar determination.

Upon comparing this data, there were four categories for which classifications could be identified. They were:

(1) a microburst detection by both the radar and mesonet,

(2) a missed microburst detection by the mesonet,

(3) a missed microburst detection by the radar, or

(4) no microburst event at all*.

The only discrepancy during this process occurred when Doppler radar detected microbursts were located outside the mesonet (i.e., not observed between two or more surface mesonet stations). For these cases, if the criteria mentioned in the previous chapter were met by the mesonet in determining a microburst, the events were included in the overall results. However, if this criteria (involving the mesonet sensors) was not met, the results were not included. It would be a misrepresentation to classify these as having been misdetected by the mesonet when, in fact, a major portion of the event would actually go unsampled (by the mesonet). Similarly, mesonet impacting events not observed by the radar because it was scanning in a different sector have not been included.

---

* It was possible for an apparent microburst signature to be observed by the surface mesonet and then discounted after analyzing the corresponding radar data as discussed in section II. This catagory will not be included in the overall results, since the results deal only with confirmed microburst events.

IV. OVERALL RESULTS

During the 1987 data collection season, it was estimated based on Doppler radar and mesonet surface data that 102 microbursts impacted* the mesonet. These microbursts were observed during the period June 6 through October 5 when both radar and surface data were available. It is possible that there may have been more events since not all of the radar data collected have been exhaustively examined.

Of the 102 known microburst events, 66 of these (64.7%) occurred when data were available from both the radar and mesonet surface sensors. From the remaining 36 events, 29 were without radar data while 7 occurred without enough supporting mesonet data (see Figure IV-1). An incomplete surface network or inadequate surface coverage were the reasons that contributed to the lack of mesonet support for these 7 events. Relevant to this study, however, were the 66 microbursts which had radar and mesonet data that could be compared, and of these:

(1) 61 (92.4%) were observed by both the radar** and mesonet,

(2) 1 (1.5%) which occurred entirely within the mesonet dense coverage sector was unobserved by the mesonet surface sensors†, and

(3) 4 (6.1%) were unobserved by the radar, corresponding to a radar observed percentage of 93.9%.

Table IV-1 categorizes these 66 microbursts according to their observed strength. Approximately 47% of these events were identified by maximum velocity differences of at least 20 m/s. The P_D (probability of detection) for these stronger microbursts was 0.97 (where $P_D = \frac{\text{No. of detected events}}{\text{No. of events}}$).

The microburst that was unobserved by the mesonet surface sensors occurred on September 16 while the four microbursts, which were not observed by the radar but were identified by the mesonet, occurred on August 29, September 2 (two events), and Septem-

---

* Recall, from the previous chapters, that a microburst did not have to be positioned directly over a specific station or even within the bounds of the mesonet in order to be impacting. It may be peripherally outside the mesonet.

** 58 of these 61 microbursts were observed by FL-2 and the mesonet while the remaining three were observed by UND and the mesonet (no FL-2 data for these three events).

† There were at least eight (8) additional events at the mesonet periphery for which mesonet detections may be ambiguous. These have not been included.

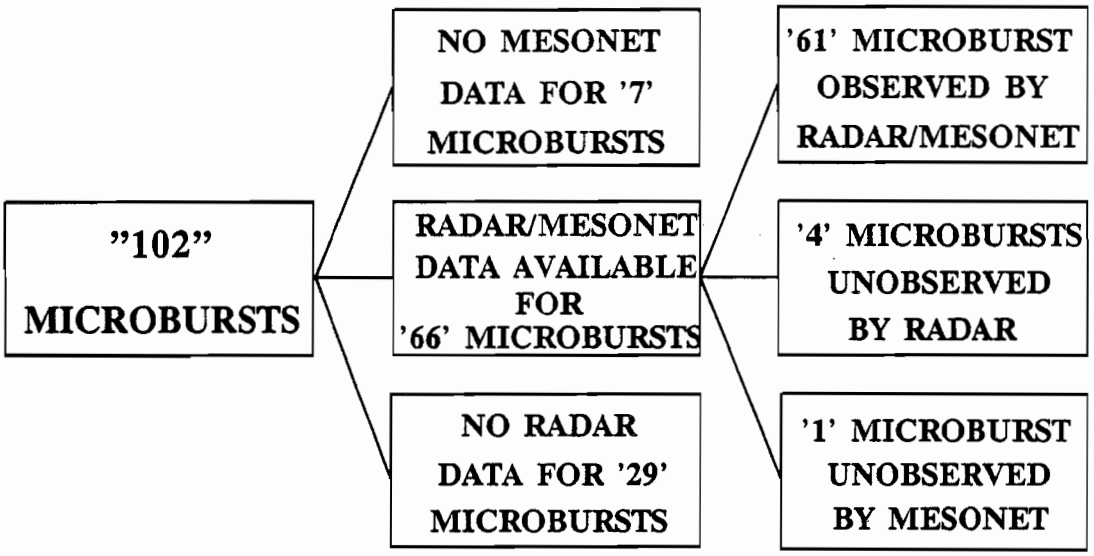

Figure IV – 1. *A breakdown of the 1987 mesonet impacting microbursts in Denver.*

Table IV – 1. *Catagorical distribution according to the strength of the mesonet impacting microbursts that occurred in Denver during 1987 when radar and mesonet data were simultaeously available.*

	Maximum Differential Velocity (m/s)		
	<15	$15 \leq dV < 20$	≥ 20
Number of Microbursts	18	17	31

ber 13. Table IV-2 presents some pertinent information regarding these events, as well as for all the other mesonet impacting microbursts. The approximate location of each of these microbursts, with respect to the mesonet, is depicted in Figure IV-2. These locations identify at what point the microbursts, while impacting the mesonet, were observed to be at maximum strength. Where possible, radar data was used in determining the microburst locations. Otherwise, the surface mesonet data was used.

Table IV-2(a). *1987 mesonet impacting microbursts. Maximum velocity differentials observed by the radar for each event are given. The third column, labeled 'Time (UT)' refers to the time at which the microburst (MB) was observed by the surface mesonet (MESO). (Y=Yes, N=No, DIV*=DIVergence, ND=No Data, BD=Bad Data, NA=Not Applicable.)*

MB#	Date	Time (UT)	Detected By: MESO	FL-2	UND	Approx. Max dV (m/s)	Approx. Couplet (m/s)	Time Max dV Observed By Radar (UT)
1	9 Jun	0424–0436	Y	ND	ND	--	---	-----
2	10 Jun	2230–2300	Y	Y	NA	23	11/–12	2251
3	10 Jun	2232–2244	*Y	Y	NA	22	9/–13	2229
4	10 Jun	-----	ND	Y	NA	11	8/–3	2235
5	10 Jun	2240–2245	Y	Y	NA	16	8/–8	2238
6	10 Jun	-----	ND	Y	NA	17	10/–7	2244
7	12 Jun	0646–0709	Y	ND	ND	--	---	-----
8	12 Jun	-----	ND	Y	NA	16	7/–9	2135
9	12 Jun	2254–2307	Y	Y	NA	24	9/–15	2258
10	12 Jun	-----	ND	Y	NA	17	12/–5	2301
11	12 Jun	2308–2318	Y	Y	NA	24	9/–15	2308
12	12 Jun	2308–2318	Y	Y	NA	32	13/–19	2308
13	12 Jun	2325–2342	Y	Y	NA	14	12/–2	2331
14	17 Jun	2145–2150	Y	Y	NA	24	12/–12	2149
15	17 Jun	2219–2247	Y	Y	NA	32	16/–16	2227
16	18 Jun	2328–2342	Y	Y	NA	24	13/–11	2333

* Divergence here indicates that a divergent signature was observed but it was not strong enough to be classified (by the mesonet surface stations) as a microburst.

Table IV-2(a) (continued)

MB#	Date	Time (UT)	Detected By: MESO	FL-2	UND	Approx. Max dV (m/s)	Approx. Couplet (m/s)	Time Max dV Observed By Radar (UT)
17	18 Jun	2346–2359	Y	Y	NA	22	15/–7	2352
18	19 Jun	0403–0409	Y	ND	ND	--	---	----
19	21 Jun	0000–0005	Y	Y	NA	15	3/–12	2359
20	22 Jun	2140–2153	Y	Y	NA	14	6/–8	2141
21	22 Jun	2145–2208	Y	Y	NA	18	4/–14	2144
22	22 Jun	2206–2223	Y	Y	NA	15	7/–8	2207
23	23 Jun	2147–2205	Y	Y	NA	18	6/–12	2152
24	23 Jun	2205–2223	Y	Y	NA	22	9/–13	2205
25	27 Jun	2322–2329	Y	ND	ND	--	---	----
26	27 Jun	2333–0022	Y	ND	ND	--	---	----
27	27 Jun	2347–2356	Y	ND	ND	--	---	----
28	27 Jun	2357–2358	Y	ND	ND	--	---	----
29	28 Jun	2043–2052	Y	ND	ND	--	---	----
30	28 Jun	2122–2136	Y	ND	ND	--	---	----
31	28 Jun	2135–2151	Y	ND	ND	--	---	----
32	28 Jun	2142–2156	Y	ND	ND	--	---	----
33	28 Jun	2157–2218	Y	ND	ND	--	---	----
34	28 Jun	2214–2226	Y	ND	ND	--	---	----
35	2 Jul	2114–2122	Y	Y	NA	14	7/–7	2120

Table IV-2(a) (continued)

MB#	Date	Time (UT)	Detected By: MESO	FL-2	UND	Approx. Max dV (m/s)	Approx. Couplet (m/s)	Time Max dV Observed By Radar (UT)
36	2 Jul	2127-2143	Y	Y	NA	16	9/-7	2132
37	4 Jul	1949-2000	Y	ND	ND	--	---	----
38	4 Jul	2002-2012	Y	ND	ND	--	---	----
39	4 Jul	2003-2009	Y	ND	ND	--	---	----
40	4 Jul	2039-2047	Y	ND	Y	14	7/-7	2037
41	4 Jul	2130-2151	Y	ND	Y	20	5/-15	2141
42	4 Jul	2248-2254	Y	ND	Y	26	9/-17	2249
43	8 Jul	0211-0244	Y	ND	ND	--	---	----
44	8 Jul	0219-0229	Y	ND	ND	--	---	----
45	8 Jul	------	ND	Y	NA	23	13/-10	2340
46	9 Jul	0017-0036	Y	Y	NA	16	1/-15	0022
47	9 Jul	0018-0034	Y	Y	NA	18	6/-12	0022
48	9 Jul	0026-0031	Y	Y	NA	14	3/-11	0022
49	9 Jul	2249-2301	Y	Y	NA	12	5/-7	2251
50	10 Jul	0046-0104	Y	Y	NA	13	4/-9	0054
51	10 Jul	------	ND	Y	NA	27	15/-12	0054
52	10 Jul	0144-0150	Y	Y	NA	22	12/-10	0149
53	11 Jul	0846-0853	Y	ND	ND	--	---	----
54	12 Jul	0125-0133	Y	ND	ND	--	---	----
55	12 Jul	0132-0143	Y	ND	ND	--	---	----

Table IV-2(a) (continued)

MB#	Date	Time (UT)	Detected By: MESO	FL-2	UND	Approx. Max dV (m/s)	Approx. Couplet (m/s)	Time Max dV Observed By Radar (UT)
56	12 Jul	0135-0144	Y	ND	ND	--	---	----
57	12 Jul	0159-0209	Y	ND	ND	--	---	----
58	20 Jul	0100-0106	Y	ND	ND	--	---	----
59	24 Jul	0544-0554	Y	ND	ND	--	---	----
60	24 Jul	2205-2241	Y	Y	NA	24	14/-10	2220
61	24 Jul	2245-2256	Y	Y	NA	24	17/-7	2249
62	29 Jul	2302-2312	Y	Y	NA	11	9/-2	2301
63	29 Jul	2313-2335	Y	Y	NA	25	7/-18	2321
64	29 Jul	2326-2336	Y	Y	NA	17	8/-9	2334
65	31 Jul	2322-2345	Y	Y	NA	29	9/-20	2325
66	2 Aug	2155-2215	Y	Y	NA	13	8/-5	2202
67	2 Aug	------	ND	Y	NA	20	7/-13	2303
68	6 Aug	2023-2035	Y	Y	NA	14	6/-8	2033
69	20 Aug	0100-0113	Y	ND	ND	--	---	----
70	20 Aug	2114-2128	Y	ND	ND	--	---	----
71	20 Aug	2117-2125	Y	ND	BD	--	---	----
72	25 Aug	2321-2348	Y	Y	NA	22	11/-11	2319
73	26 Aug	0026-0100	Y	Y	NA	22	8/-14	0037
74	26 Aug	0041-0055	Y	Y	NA	14	7/-7	0047
75	29 Aug	0113-0123	Y	Y	NA	14	9/-5	0112

Table IV-2(a) (continued)

MB#	Date	Time (UT)	Detected By: MESO	FL-2	UND	Approx. Max dV (m/s)	Approx. Couplet (m/s)	Time Max dV Observed By Radar (UT)
76	29 Aug	0121-0125	Y	N	BD	--	---	----
77	2 Sep	2235-2241	Y	Y	NA	22	8/-14	2239
78	2 Sep	2242-2253	Y	N	BD	--	---	----
79	2 Sep	2244-2251	Y	Y	NA	20	10/-10	2245
80	2 Sep	2250-2257	Y	Y	NA	20	10/-10	2249
81	2 Sep	2253-2304	Y	N	BD	--	---	----
82	2 Sep	2253-2257	Y	Y	NA	18	9/-9	2252
83	2 Sep	2253-2300	Y	Y	NA	20	10/-10	2252
84	4 Sep	2010-2031	Y	Y	NA	20	13/-7	2022
85	4 Sep	2013-2017	Y	Y	NA	18	12/-6	2010
86	4 Sep	2019-2025	Y	Y	NA	18	13/-5	2023
87	4 Sep	2050-2114	Y	Y	NA	18	4/-14	2055
88	13 Sep	2105-2114	Y	Y	NA	25	12/-13	2104
89	13 Sep	2113-2118	Y	N	N	--	---	----
90	13 Sep	2118-2126	Y	Y	NA	15	8/-7	2119
91	13 Sep	2122-2129	Y	Y	NA	15	9/-6	2121
92	13 Sep	2123-2130	Y	Y	NA	22	6/-16	2124
93	13 Sep	2127-2140	Y	Y	NA	20	12/-8	2126
94	14 Sep	0050-0054	Y	Y	NA	12	-2/-14	0054
95	14 Sep	0104-0120	Y	Y	NA	25	11/-14	0109

Table IV-2(a) (continued)

MB#	Date	Time (UT)	Detected By: MESO	FL-2	UND	Approx. Max dV (m/s)	Approx. Couplet (m/s)	Time Max dV Observed By Radar (UT)
96	14 Sep	0105–0111	Y	Y	NA	20	9/–11	0104
97	14 Sep	0110–0113	Y	Y	NA	20	9/–11	0111
98	14 Sep	0111–0122	Y	Y	NA	12	6/–6	0111
99	14 Sep	0111–0122	Y	Y	NA	14	6/–8	0114
100	16 Sep	2216–2218	DIV	Y	NA	12	5/–7	2216
101	16 Sep	2236–2249	Y	Y	NA	18	5/–13	2238
102	17 Sep	0830–0846	Y	ND	ND	--	---	----

Table IV-2(b). *Locations of the 1987 mesonet impacting microbursts (relative to the FL-2 and UND radar sites). These locations indicate where the maximum strength was observed, either by FL-2, UND, or the mesonet surface sensors*.*

MB#	Date	FL-2		UND	
		Ran(km)	Az(°)	Ran(km)	Az(°)
1	9 Jun	10.0	310	14.0	197
2	10 Jun	22.0	337	5.0	274
3	10 Jun	13.0	272	21.5	206
4	10 Jun	18.0	308	14.0	231
5	10 Jun	15.0	320	10.0	217
6	10 Jun	8.0	323	13.0	186
7	12 Jun	11.5	290	17.5	205
8	12 Jun	16.0	293	17.5	220
9	12 Jun	17.0	306	14.0	227
10	12 Jun	17.0	330	7.0	225
11	12 Jun	12.5	311	13.0	207
12	12 Jun	14.0	283	19.5	212
13	12 Jun	10.0	301	15.5	199
14	17 Jun	18.0	278	22.5	220
15	17 Jun	22.5	327	9.0	265
16	18 Jun	5.0	302	17.0	183
17	18 Jun	6.0	280	19.0	187

* The mesonet surface sensors are used to indicate the locations of the microbursts*only* for cases where no radar data are available or the radars did not detect the event.

Table IV-2(b) (continued)

MB#	Date	FL-2 Ran(km)	FL-2 Az(°)	UND Ran(km)	UND Az(°)
18	19 Jun	12.5	280	19.5	207
19	21 Jun	14.0	300	15.5	214
20	22 Jun	11.0	285	18.0	203
21	22 Jun	21.0	322	10.0	252
22	22 Jun	12.0	292	17.0	207
23	23 Jun	14.0	290	18.0	213
24	23 Jun	6.0	281	18.5	187
25	27 Jun	12.5	285	18.5	208
26	27 Jun	12.0	300	15.5	207
27	27 Jun	15.0	307	13.5	219
28	27 Jun	15.0	315	11.5	218
29	28 Jun	14.0	293	17.0	213
30	28 Jun	15.0	315	11.5	218
31	28 Jun	10.0	323	12.0	192
32	28 Jun	14.0	305	14.0	214
33	28 Jun	17.0	308	13.5	227
34	28 Jun	15.0	330	8.0	211
35	2 Jul	18.0	310	13.0	232
36	2 Jul	19.0	311	13.0	236
37	4 Jul	12.5	310	13.0	208

Table IV-2(b) (continued)

MB#	Date	FL-2 Ran(km)	FL-2 Az(°)	UND Ran(km)	UND Az(°)
38	4 Jul	12.0	290	17.5	207
39	4 Jul	8.5	325	13.0	186
40	4 Jul	19.5	302	16.0	235
41	4 Jul	15.0	302	15.0	218
42	4 Jul	9.0	273	20.0	196
43	8 Jul	19.0	315	12.0	238
44	8 Jul	12.5	290	17.5	208
45	8 Jul	0.8	334	19.0	171
46	9 Jul	7.0	248	22.5	188
47	9 Jul	17.5	300	16.0	227
48	9 Jul	16.0	328	8.0	219
49	9 Jul	22.0	326	9.0	261
50	10 Jul	16.0	305	14.0	222
51	10 Jul	7.0	310	15.0	187
52	10 Jul	10.0	320	12.5	194
53	11 Jul	12.5	285	18.5	208
54	12 Jul	18.0	320	10.0	234
55	12 Jul	15.0	327	8.5	213
56	12 Jul	18.0	315	11.5	233
57	12 Jul	12.0	282	19.0	206

Table IV-2(b) (continued)

MB#	Date	FL-2 Ran(km)	FL-2 Az(°)	UND Ran(km)	UND Az(°)
58	20 Jul	14.5	302	15.0	216
59	24 Jul	11.0	315	12.5	200
60	24 Jul	16.0	353	4.0	158
61	24 Jul	20.0	327	8.0	249
62	29 Jul	18.0	335	5.0	231
63	29 Jul	20.0	307	14.5	239
64	29 Jul	21.5	312	13.5	247
65	31 Jul	7.0	280	19.0	190
66	2 Aug	12.0	302	15.0	207
67	2 Aug	3.0	291	18.5	178
68	6 Aug	20.5	340	3.5	263
69	20 Aug	16.0	330	7.5	218
70	20 Aug	13.5	310	13.0	212
71	20 Aug	15.0	290	18.0	216
72	25 Aug	4.0	305	17.5	179
73	26 Aug	19.0	295	18.0	230
74	26 Aug	16.0	330	7.5	218
75	29 Aug	22.0	318	12.0	253
76	29 Aug	18.0	303	15.0	230
77	2 Sep	19.0	313	12.5	237

Table IV-2(b) (continued)

MB#	Date	FL-2 Ran(km)	FL-2 Az(°)	UND Ran(km)	UND Az(°)
78	2 Sep	18.0	305	14.5	230
79	2 Sep	17.0	322	9.5	228
80	2 Sep	16.5	325	8.5	224
81	2 Sep	18.0	310	13.0	232
82	2 Sep	16.0	334	6.5	214
83	2 Sep	12.0	312	13.0	205
84	4 Sep	17.0	335	5.5	221
85	4 Sep	13.0	275	21.0	207
86	4 Sep	17.0	321	9.5	228
87	4 Sep	20.0	320	10.5	245
88	13 Sep	12.5	274	21.0	206
89	13 Sep	17.5	325	8.5	231
90	13 Sep	16.0	296	16.5	221
91	13 Sep	18.0	335	5.5	231
92	13 Sep	16.0	322	9.5	222
93	13 Sep	12.0	310	13.5	206
94	14 Sep	21.0	320	10.5	250
95	14 Sep	8.0	305	15.5	192
96	14 Sep	17.5	300	16.0	227
97	14 Sep	10.0	330	11.0	188

Table IV-2(b) (continued)

MB#	Date	FL-2 Ran(km)	FL-2 Az(°)	UND Ran(km)	UND Az(°)
98	14 Sep	13.5	322	10.5	208
99	14 Sep	18.0	322	9.5	234
100	16 Sep	11.0	305	14.5	202
101	16 Sep	23.0	316	13.0	256
102	17 Sep	14.0	303	14.5	214

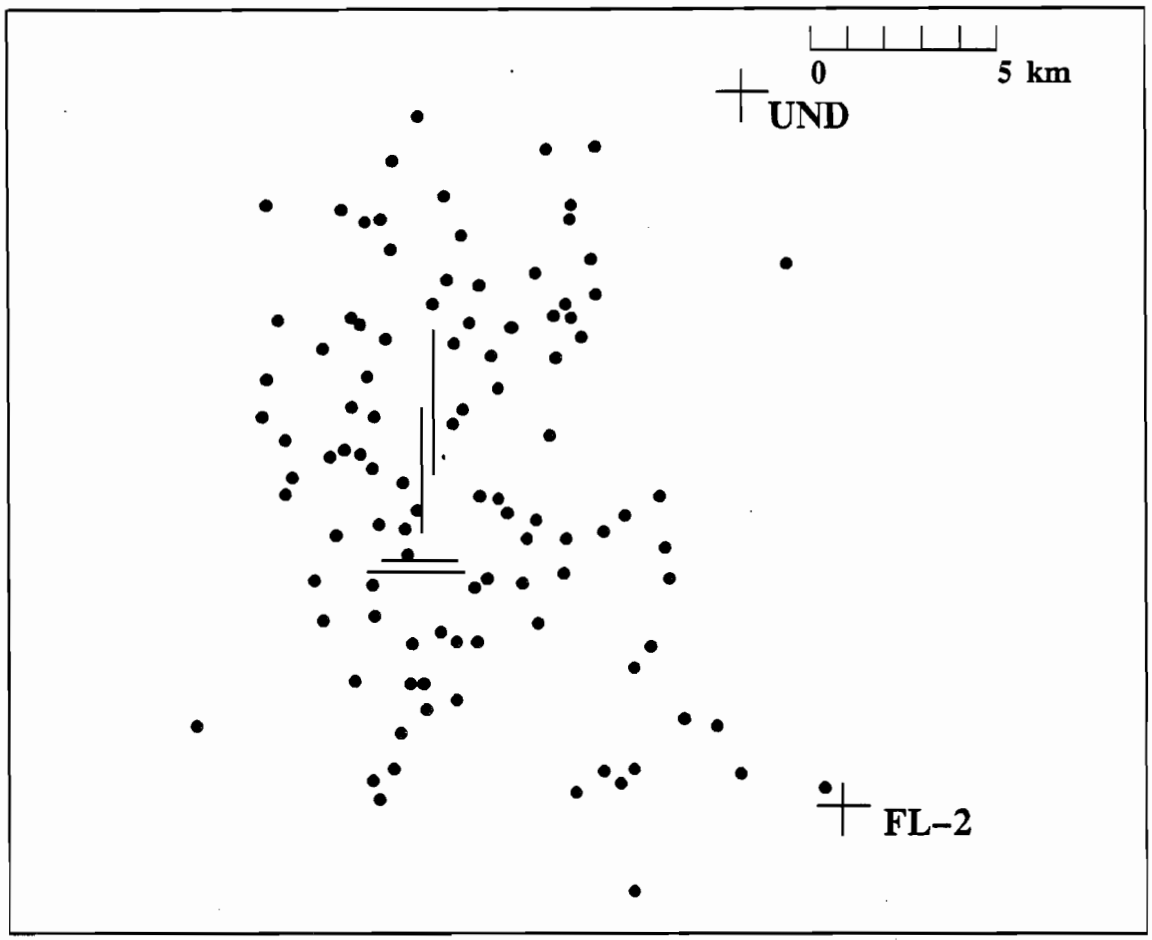

Figure IV–2. *Locations of the 1987 mesonet impacting microbursts.*

V. SPECIFIC CASE EXAMPLES

A. A Microburst Detection By Both the Radar and Mesonet Sensors

As mentioned in Chapter IV, a total of 61 mesonet impacting microbursts were observed by both the radar and mesonet. According to the radar data, the strongest event was identified as having a 32 m/s differential velocity (dV) while the weakest showed an 11 m/s dV (see Table IV-2). Figure V-1 shows the distribution of radar identified maximum dV values for these microbursts. The event that occurred on 6 August 1987 (microburst #68) had a radar measured maximum dV of 14 m/s (relatively weak) and is presented here as an example of observability by both sensors.

The mesonet surface plots from 6 August 1987 depict a microburst as it entered the northwestern portion of the network and then moved east-northeastward. Figure V-2 shows the track of this microburst as it impacted the mesonet during the period 2018-2039 (UT). The divergent outflow signature in the northern portion of the network was clearly identified in Figures V-3 and V-4. Differential velocities, as observed by the surface sensors for this impacting microburst, exceeded 10 m/s for more than 10 minutes and attained a maximum at 2030(UT) of approximately 18 m/s (Figure V-5).

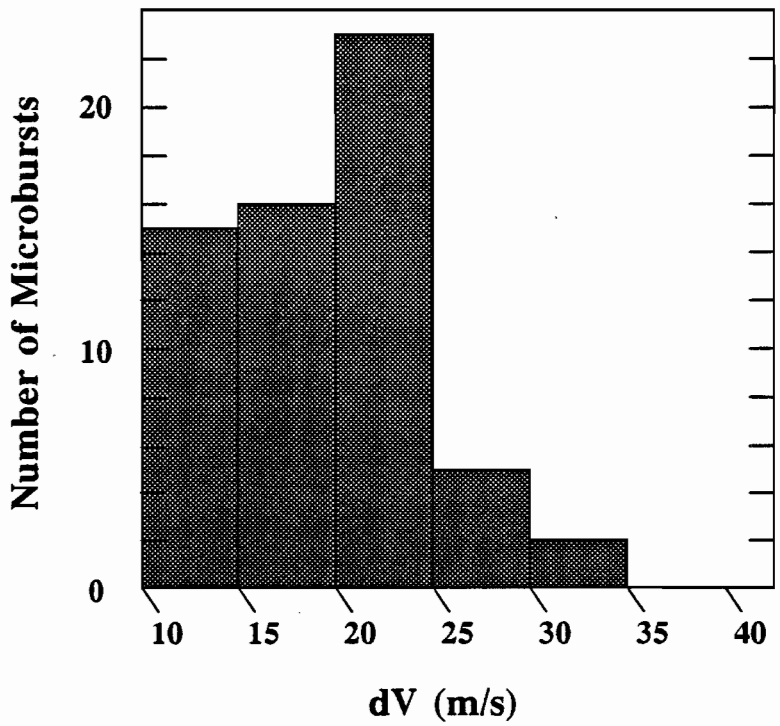

Figure V-1. *The distribution of radar identified maximum differential (dV) values for the 61 mesonet impacting microbursts that were observed by both radar and surface sensors.*

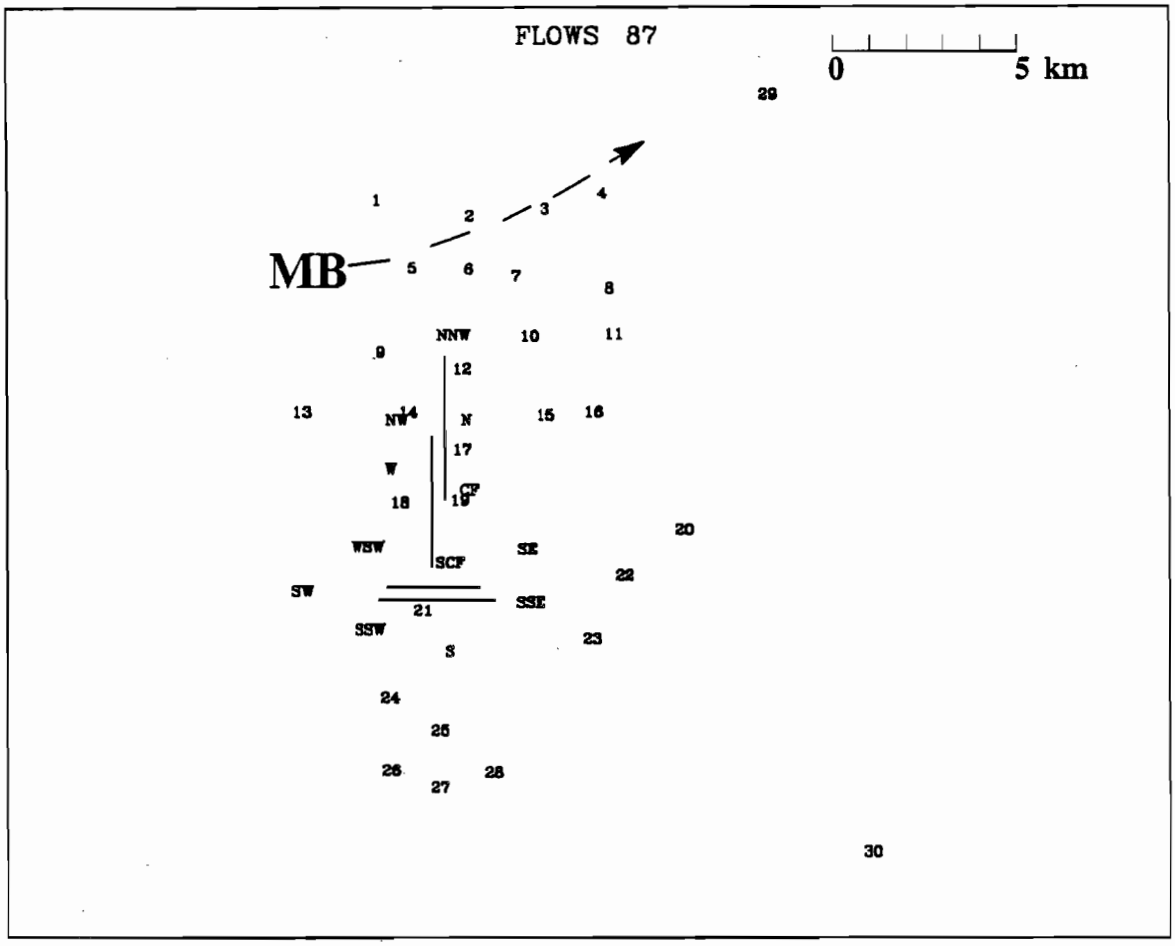

Figure V–2. *Track of the August 6th microburst as it impacted the mesonet between 2018–2039 (UT).*

AUG 06 2026(UT)

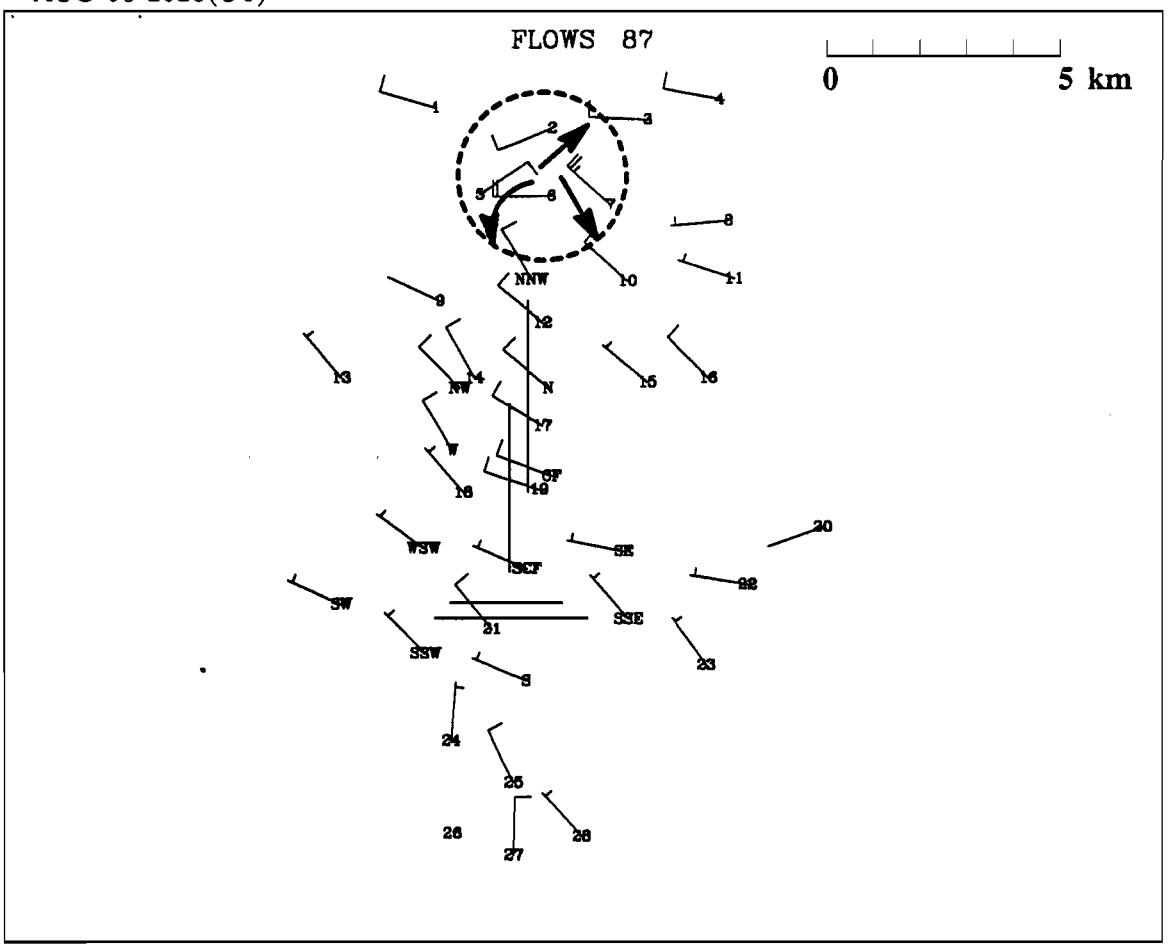

Figure V-3. *Mesonet plots showing the surface wind field at 2026 (UT) on August 6, 1987. Microburst outflow boundary denoted by a dashed line. Full barb represents 5 m/s and half-barb 2.5 m/s.*

AUG 06 2031(UT)

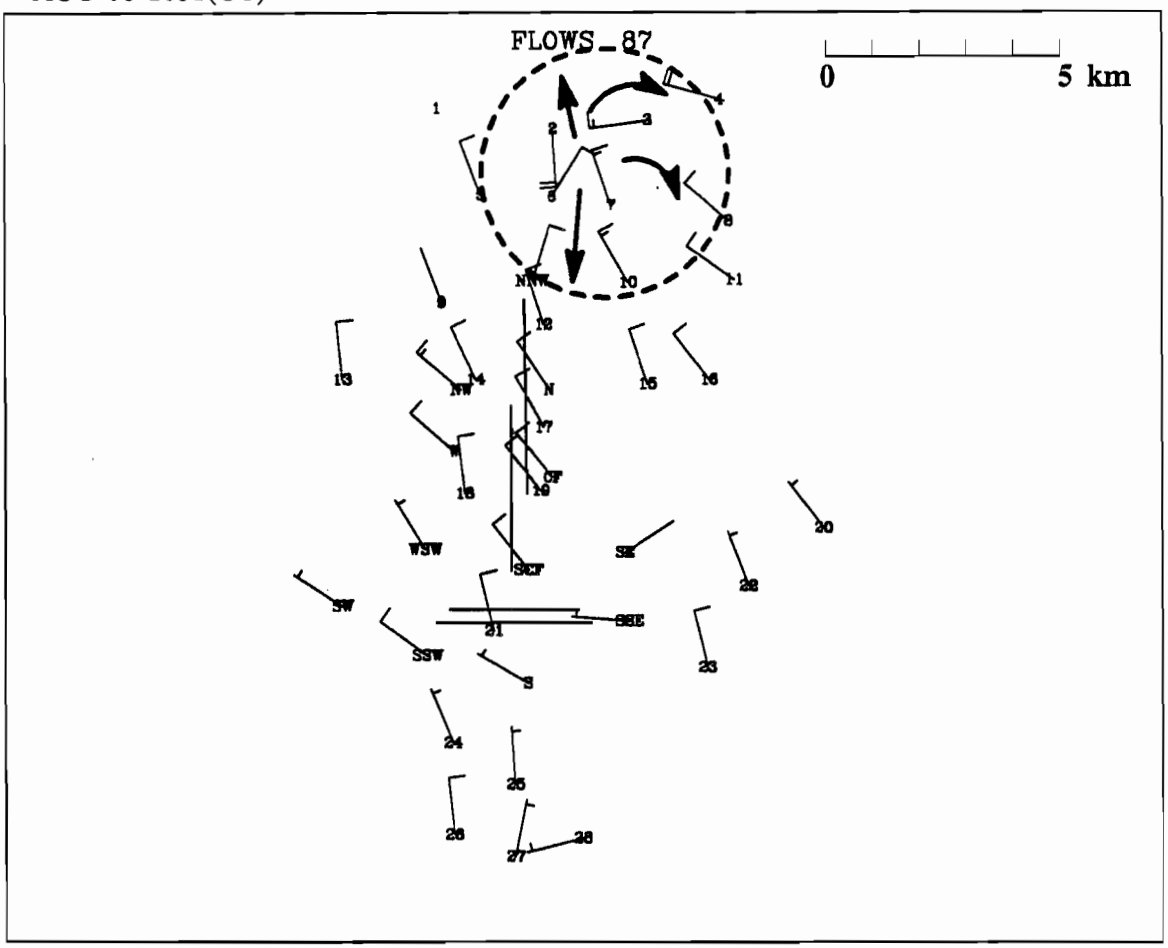

Figure V–4. *Same as figure V–3 except at 2031 (UT).*

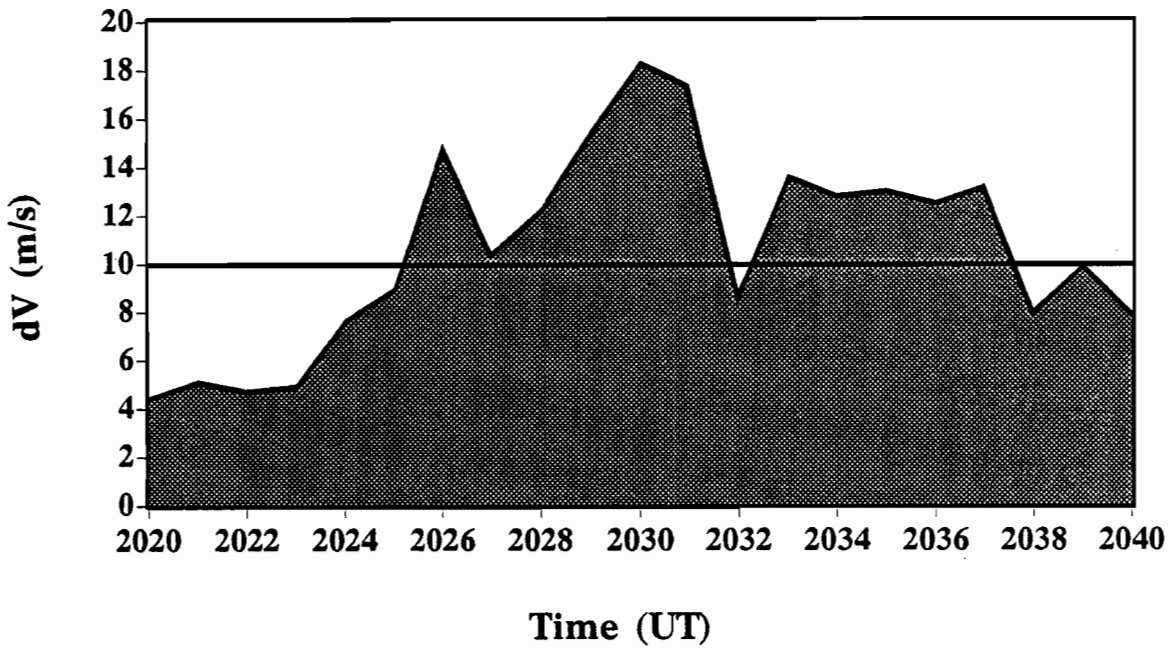

Figure V–5. *Maximum dV values that were computed over the mesonet using the actual measured winds for a specified period during August 6,1987.*

Resampled FL–2 radar data also showed a clear picture of this microburst as it moved through the northern portion of the mesonet. Although a weak event, where dV's of only 11–14 m/s were observed as it impacted the network, its velocity signature was extremely visible. Figures V–6 and V–7 show the divergent velocity couplet as it moved east–northeastward from near mesonet stations 2, 6 and 7 to a position just north of station 4 (20 km's from FL–2). The reflectivity field in these figures did not identify any clear cellular development (especially in Figure V–6). The elevation angle of the radar was at 0.4° for these tilts, which, at 20 km, would place the center of the beam at approximately 150 m AGL (well below the cloud base of 2.6 km AGL which was identified from thermodynamic data furnished by the National Weather Service Forecast Office (NWSFO) in Denver). However, at an elevation angle of 6.7°, the center of the beam, in the vicinity of the microburst, was approximately 2.5 km's AGL. Therefore, a better representation of the reflectivity field for this event was obtained (see Figure V–8 and note that the times correspond with the plots in Figures V–6 and V–7).

B. A Missed Detection By the Mesonet Surface Sensors

On September 16 at 2218(UT), the mesonet surface sensors showed no signatures of any important shear events (Figure V–9). However, very weak divergence (well below the microburst threshold level) had developed between station 23 and LLWAS sensor 'SSE'. The FL–2 Doppler velocity field revealed a weak, but well defined, microburst event at approximately 11 km northwest of the radar between 2215 and 2217(UT) (see Figures V–10, and 11). Differential velocity values for this event reached 12 m/s at each of these times.

The reason this event was missed by the mesonet sensors became apparent upon closer examination of the Doppler velocity fields. It was observed that the area of strongest receding (positive) values was contained predominantly between the three LLWAS sensors that were positioned just northwest of station 23 ('SCF', 'SE' and 'SSE'). Even though these surface stations were separated, on the average, by less than 2 km's, the microburst was still effectively small enough to remain unobserved by the mesonet sensors. This was the only missed detection by the surface mesonet where the microburst lay totally within the mesonet dense coverage region.

C. Missed Detections by the Radar

1. Case 1: 29 August 1987

On August 29, the surface mesonet system identified a microburst in the western portion of the network. This event was observed by the surface sensors between 0121 and 0125(UT). Figures V–12 and V–13 showed the microburst to be just a couple of kilometers south of station 13. It was a weak event, whereby maximum differential velocities, as observed by the actual wind field, exceeded the threshold of 10 m/s for only three minutes and, during this time, failed even to reach a value of 12 m/s (Figure V–14). Looking

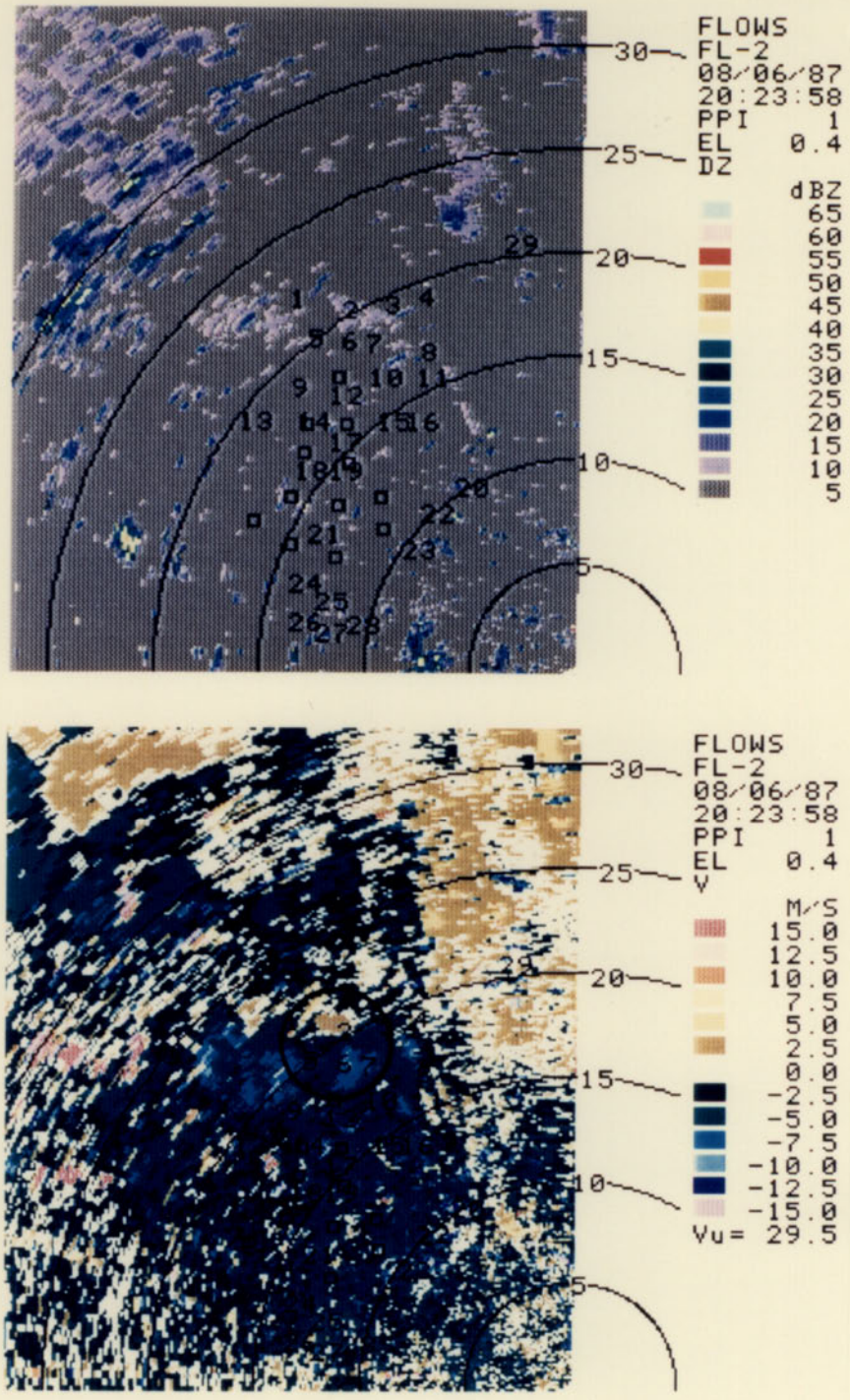

Figure V-6. FL-2 reflectivity and Doppler velocity fields for August 6, 1987 at 2023 (UT). Microburst is located within black circle. Elevation angle for both plots is 0.4°. Range rings are every 5 km and location of mesonet stations are overlaid (squares denote LLWAS sensors).

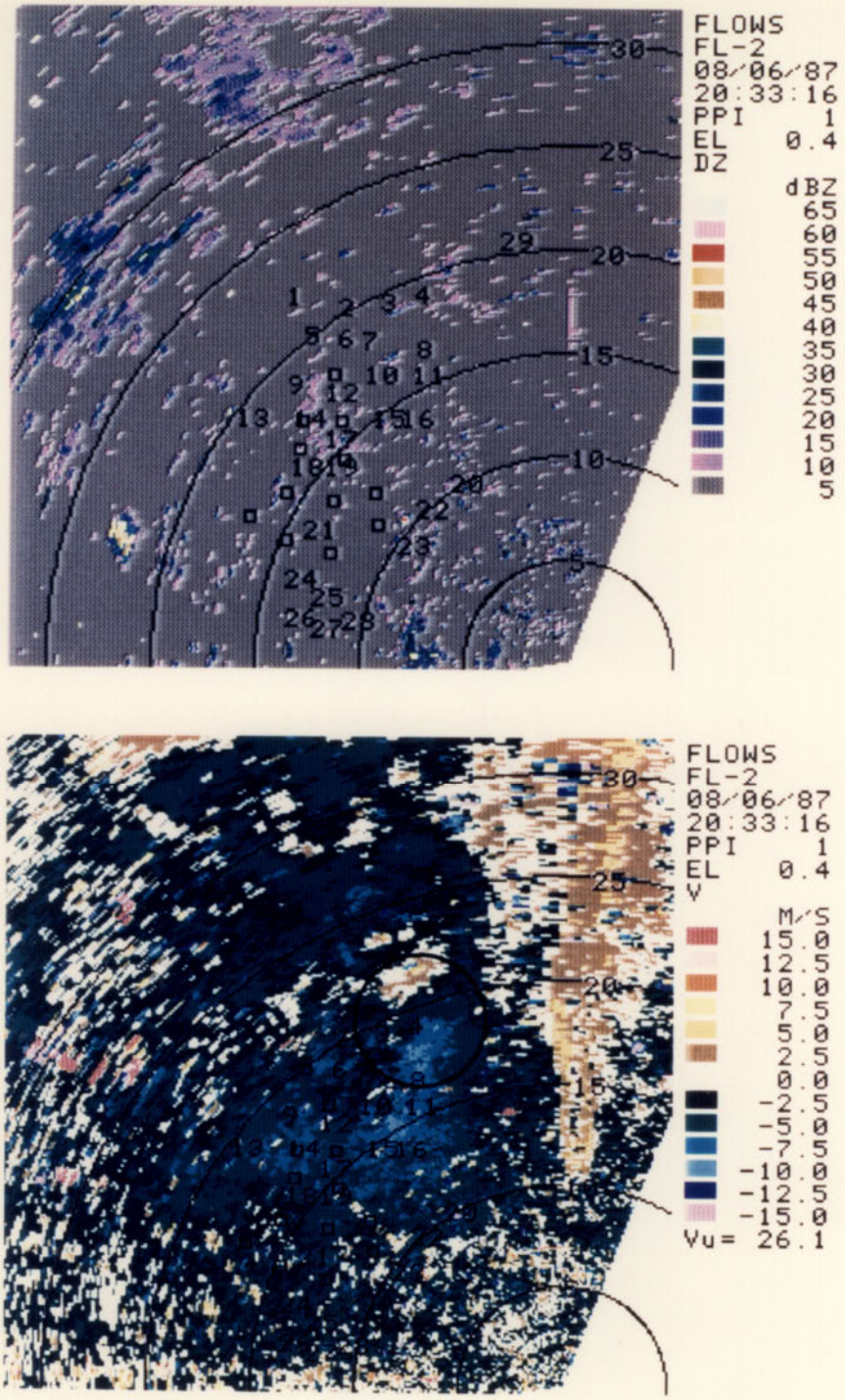

Figure V-7. Same as Figure V-6 except at 2033 (UT).

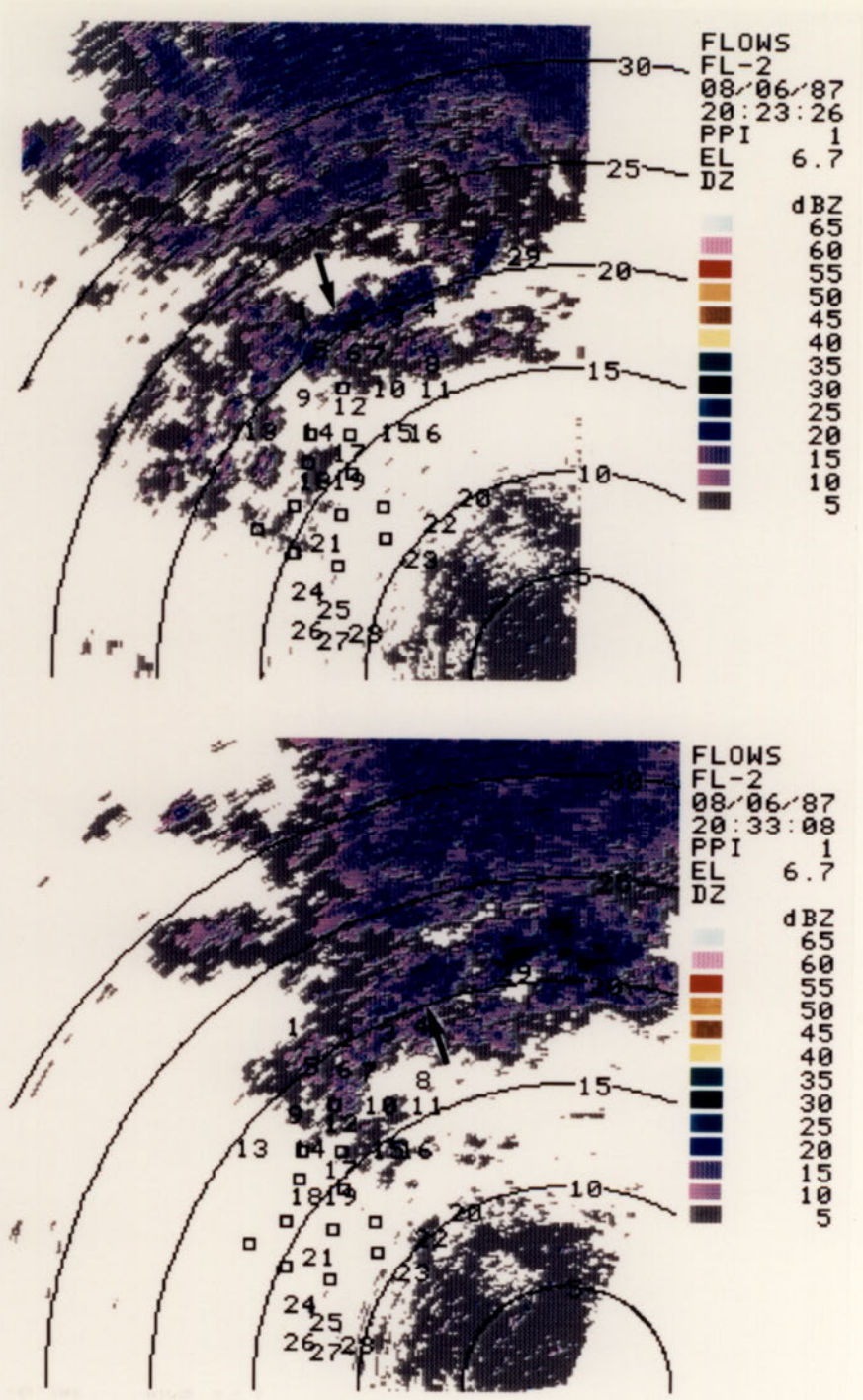

Figure V-8. FL-2 reflectivity fields at 2023 (UT) and 2033 (UT) on August 6, 1987. Arrow points to microburst producing cell. Elevation angle for both plots is 6.7°. Range rings are every 5 km and location of mesonet stations are overlaid (squares denote LLWAS sensors).

SEP 16 2218(UT)

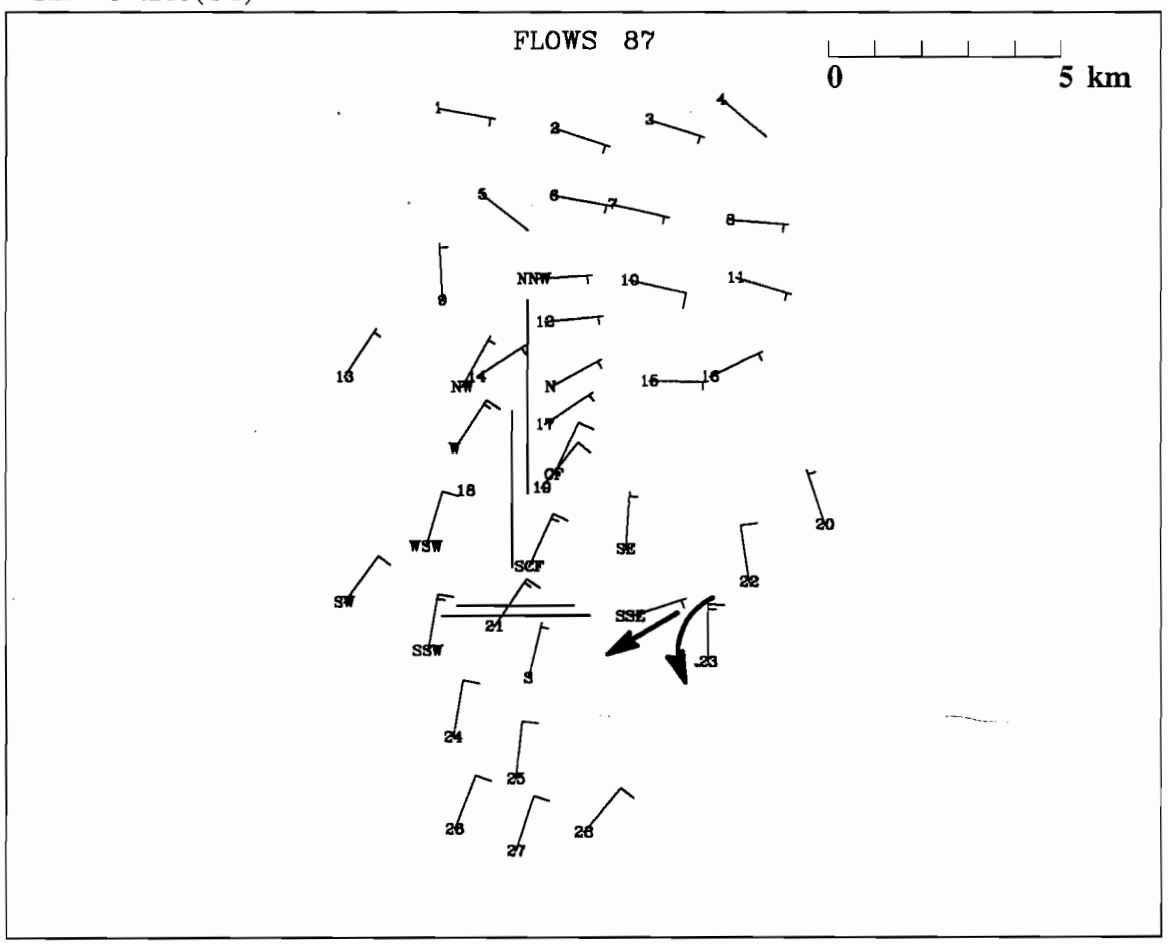

Figure V-9. *Mesonet plot showing the surface wind field at 2218 (UT) on September 16, 1987. Arrows indicate divergent flow and full barb represents 5 m/s and half-barb 2.5 m/s.*

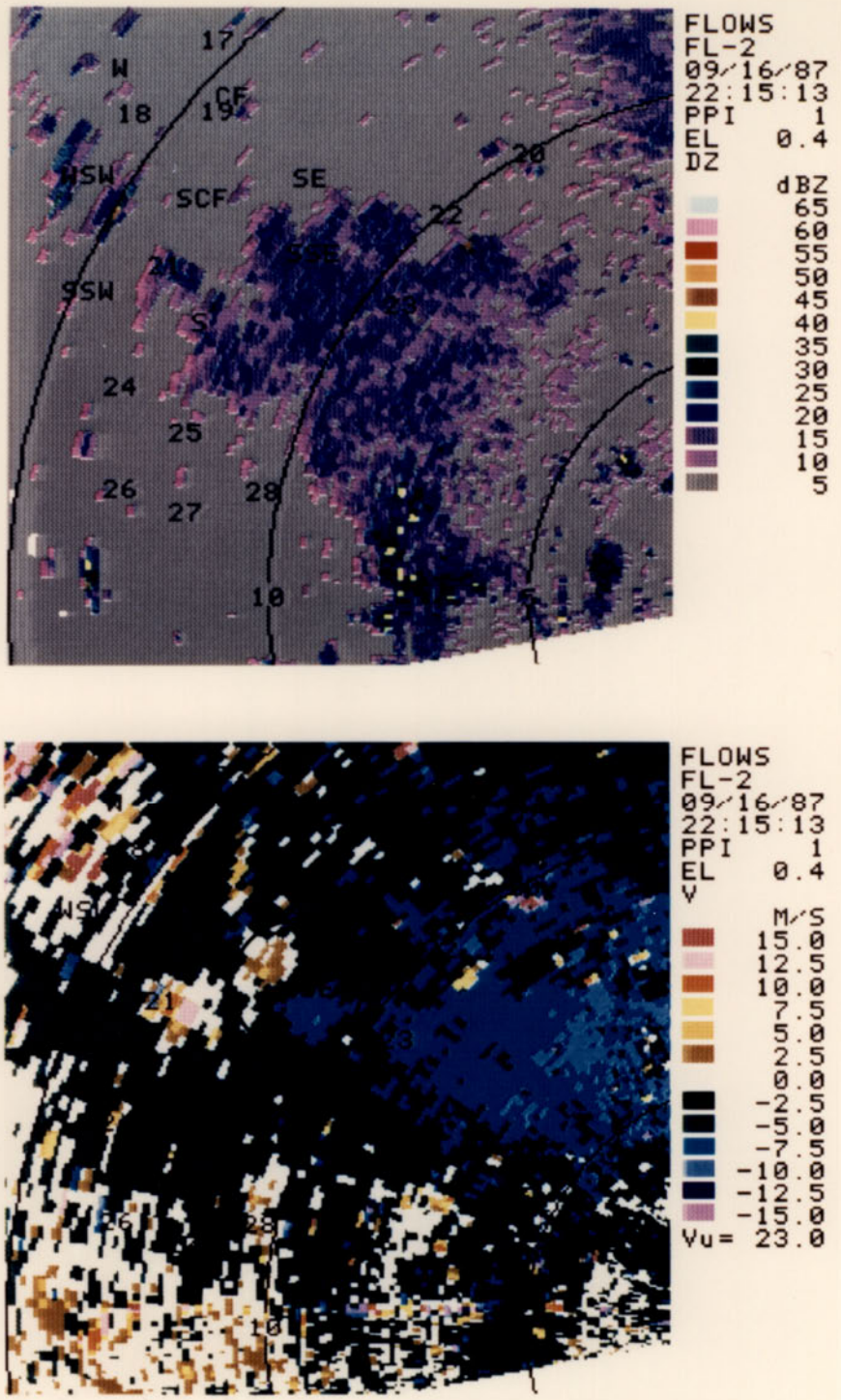

Figure V-10. FL-2 reflectivity and Doppler velocity fields for September 16, 1987 at 2215 (UT). Microburst is located within black circle. Elevation angle for both plots is 0.4°. Range rings are every 5 km and location of mesonet and LLWAS stations are overlaid.

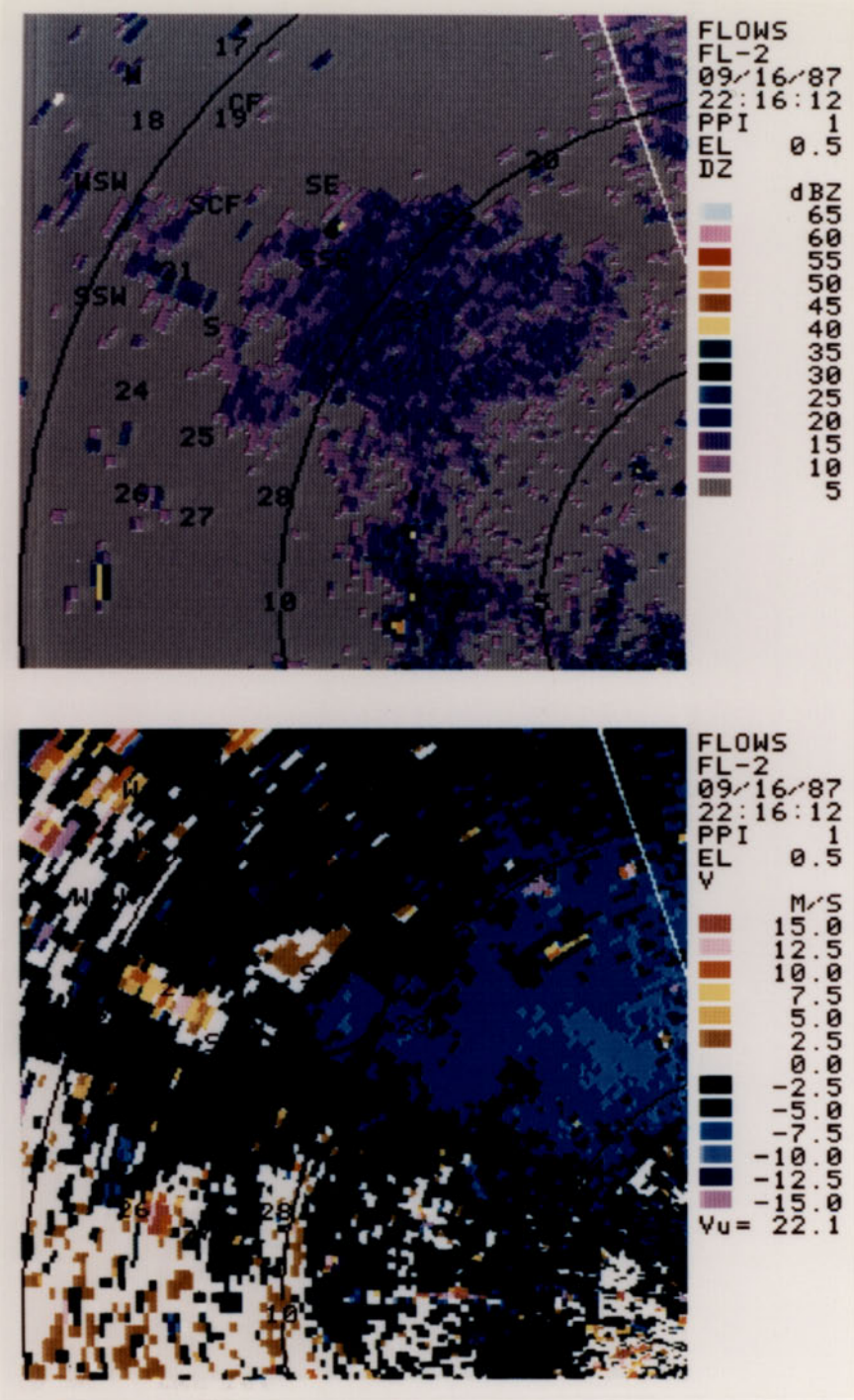

Figure V-11. Same as Figure V-10 except at 2216 (UT). Elevation angle for both plots is 0.5°.

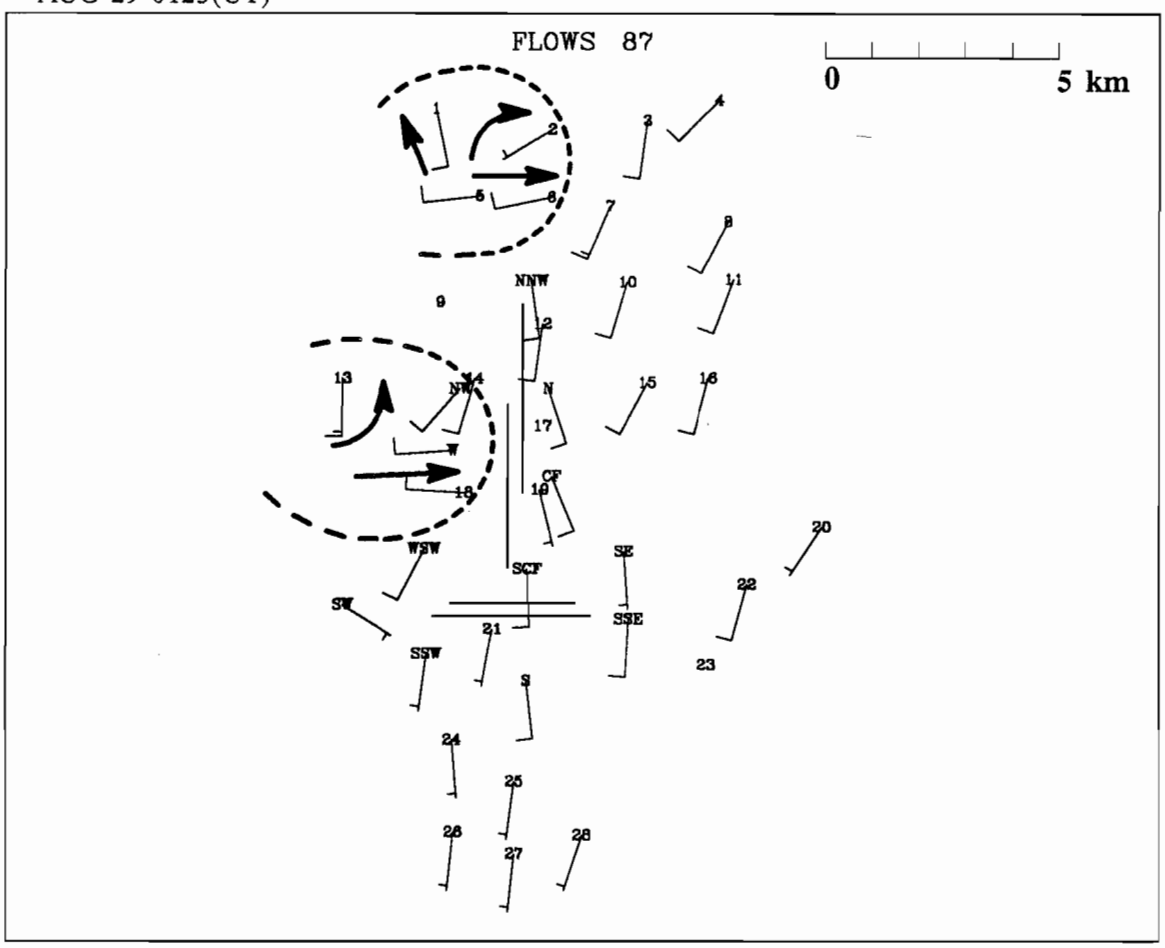

Figure V–12. *Mesonet plot showing the surface wind field at 0123 (UT) on August 29, 1987. Microburst outflow boundaries denoted by dashed lines. Full barb represents 5 m/s and half–barb 2.5 m/s.*

AUG 29 0125(UT)

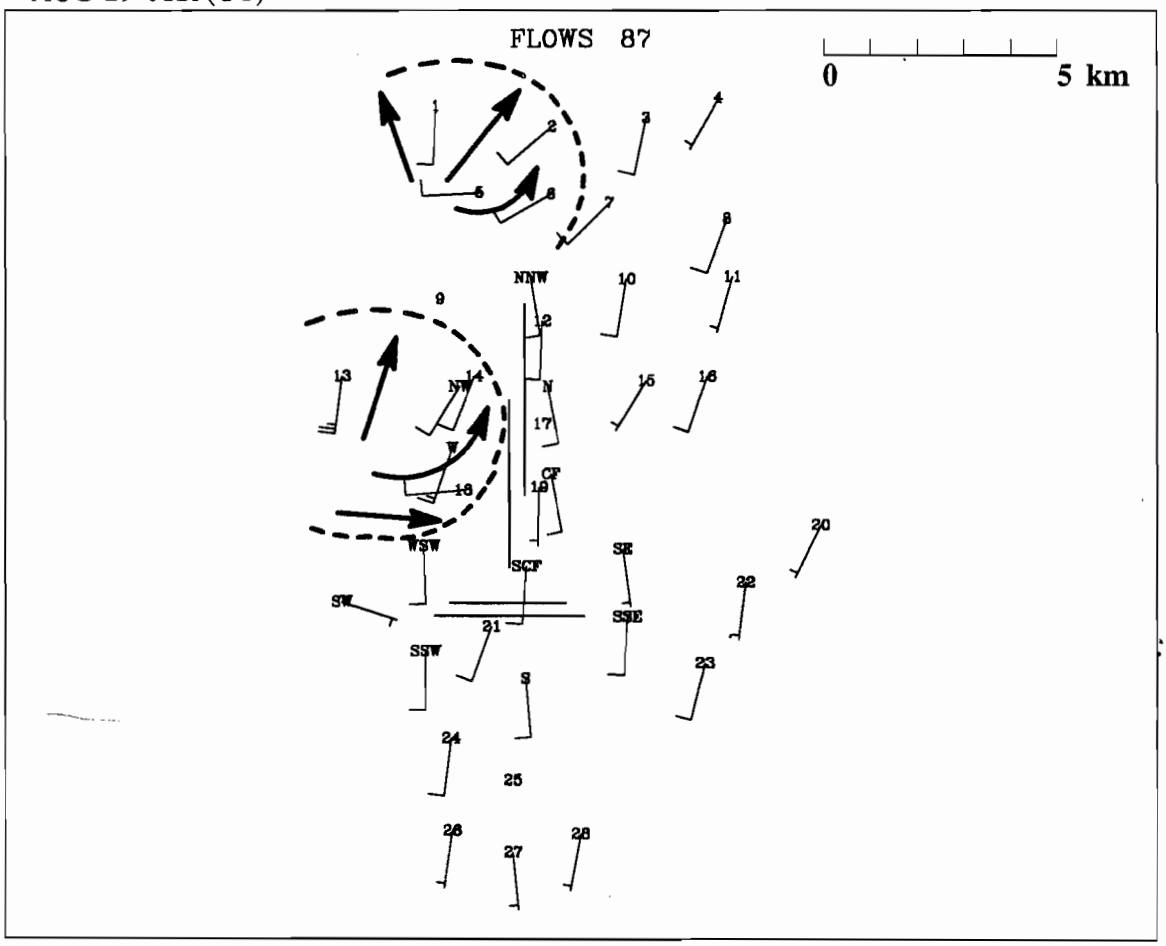

Figure V–13. *Same as figure V–12 except at 0125 (UT). At this time, the microburst in the northern sector of the mesonet was dissipating.*

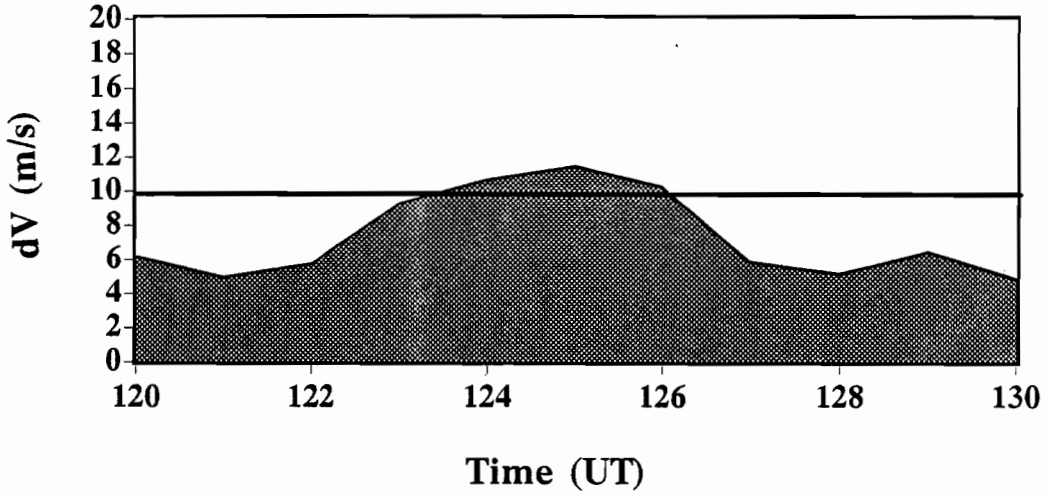

Figure V-14. *Maximum dV values that were computed over the mesonet using the actual measured winds for a specified period during August 29, 1987.*

at only the radial component of the mesonet surface winds (with respect to the FL-2 radar), it was observed that maximum dV values just barely exceeded 10 m/s as shown in Figure V-15. These values were only somewhat weaker when compared with the values calculated from the actual wind measurements. This would suggest that asymmetry (from FL-2's viewing angle) was not a significant factor in this event.

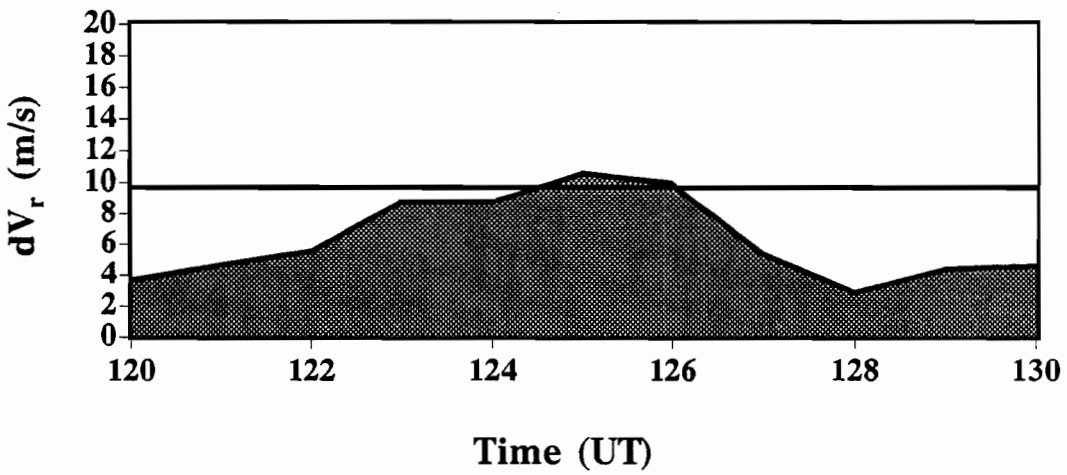

Figure V-15. *Maximum dV values that were computed over the mesonet using the radial wind measurements (w.r.t. the FL-2 radar site) for a specified period during August 29, 1987.*

The lower level tilts (0.4°-1.0°) from the FL-2 radar data exhibited no identifiable weather echoes during this event. It was not until the radar was scanning higher that the echo became evident. Figure V-16 shows the reflectivity cell located at approximately 2.5 km AGL at a range of 17.5 km northwest of the radar. The return signal, as observed from plots of the signal-to-noise ratio (SNR), was weak in the vicinity of this event (at lower levels). Figure V-17 shows the Doppler velocity field, at 0119(UT), with the SNR threshold at 6 dB so that only the stronger signal in the vicinity of the event could be observed. Differential velocities were identified as having reached 8 m/s just southwest of station #13. This plot, however, taken at a 1.0° antenna tilt angle, represented the strongest radar observed divergence during the event. The UND radar data was not useful in analyzing this case because too much data was missing in the area of interest.

Several factors contributed to this very dry microburst being unobserved by the radar:

(1) No precipitation was measured by the surface mesonet stations in the vicinity of the event.

(2) Radar reflectivity plots and thermodynamic data from the mesonet surface data as well as that provided by the NWSFO in Denver indicated that the cloud base during this event was approximately 2.5 km AGL. This would allow for any precipitation, which may have fallen from the cloud, to evaporate well before reaching the surface.

(3) Mesonet stations 13 and 18 measured a temperature increase (warming) and a relative humidity decrease (drying), an obvious indication that no evaporative cooling occurred, but that a process of adiabatic compression* did. It is conceivable that precipitation may have fallen into this deep sub-cloud layer, evaporated well before reaching the surface, and then descended to the ground as a dry air parcel, therefore triggering surface warming.

(4) The signal strength as observed by the radar from the low-level scans during this event were very weak.

This was a marginal event whereby the mesonet surface sensors identified a very weak microburst signature and the FL-2 radar did not. The radar did identify a divergent signature but it was not strong enough to be classified as a microburst. In fact, the strongest radar observed divergence was not at the lowest level surface scan but was a couple of hundred meters above, which was the next scanning level.

---

* Adiabatic compression, in meteorology, is where a parcel of dry air descends such that there is no transfer of heat or mass across its boundaries and the result is warming of the air parcel.

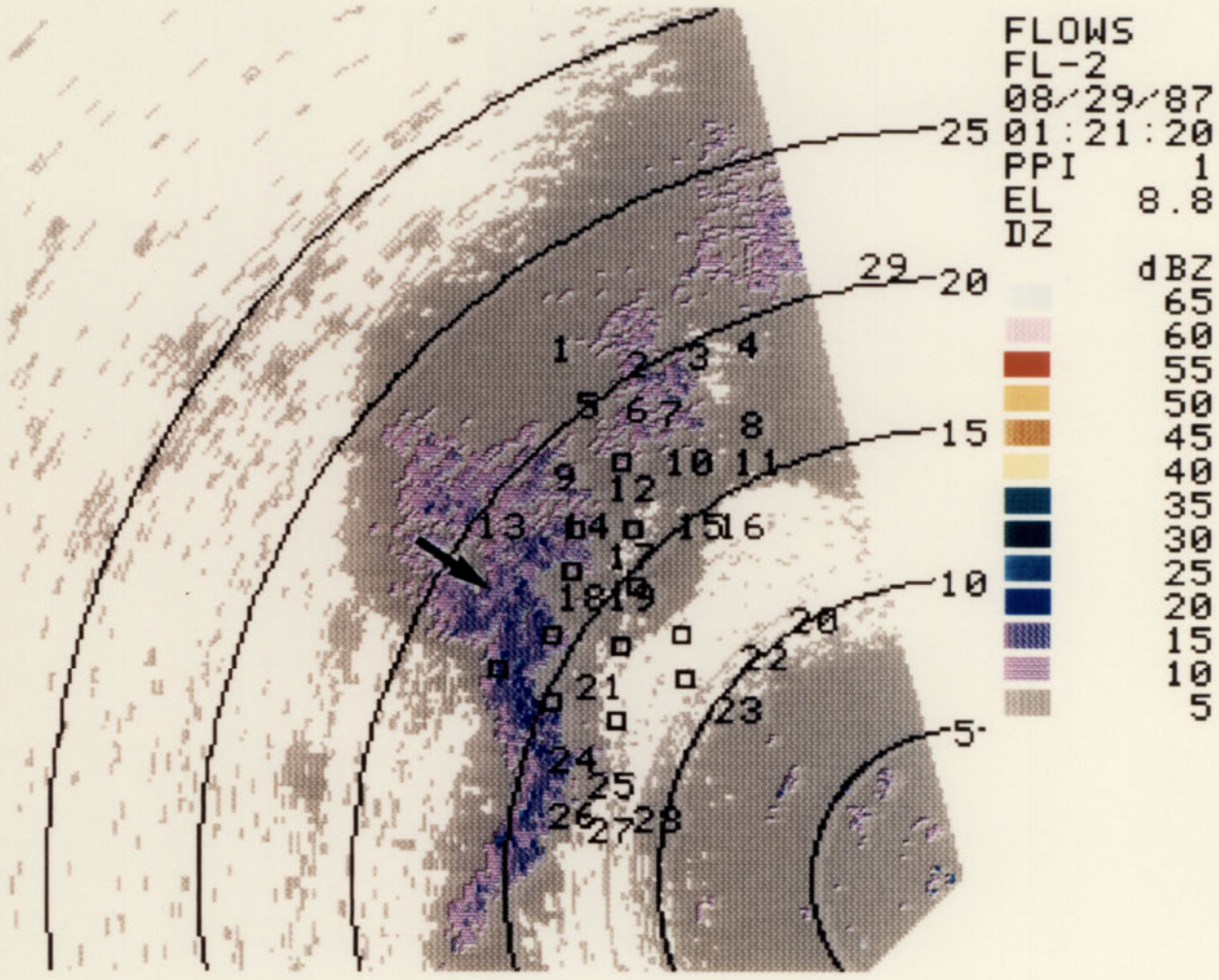

Figure V-16. FL-2 reflectivity field at 0121 (UT) on August 29, 1987. Arrow points to microburst producing cell. Elevation angle is 8.8°. Range rings are every 5 km and location of mesonet stations are overlaid (squares denote LLWAS sensors).

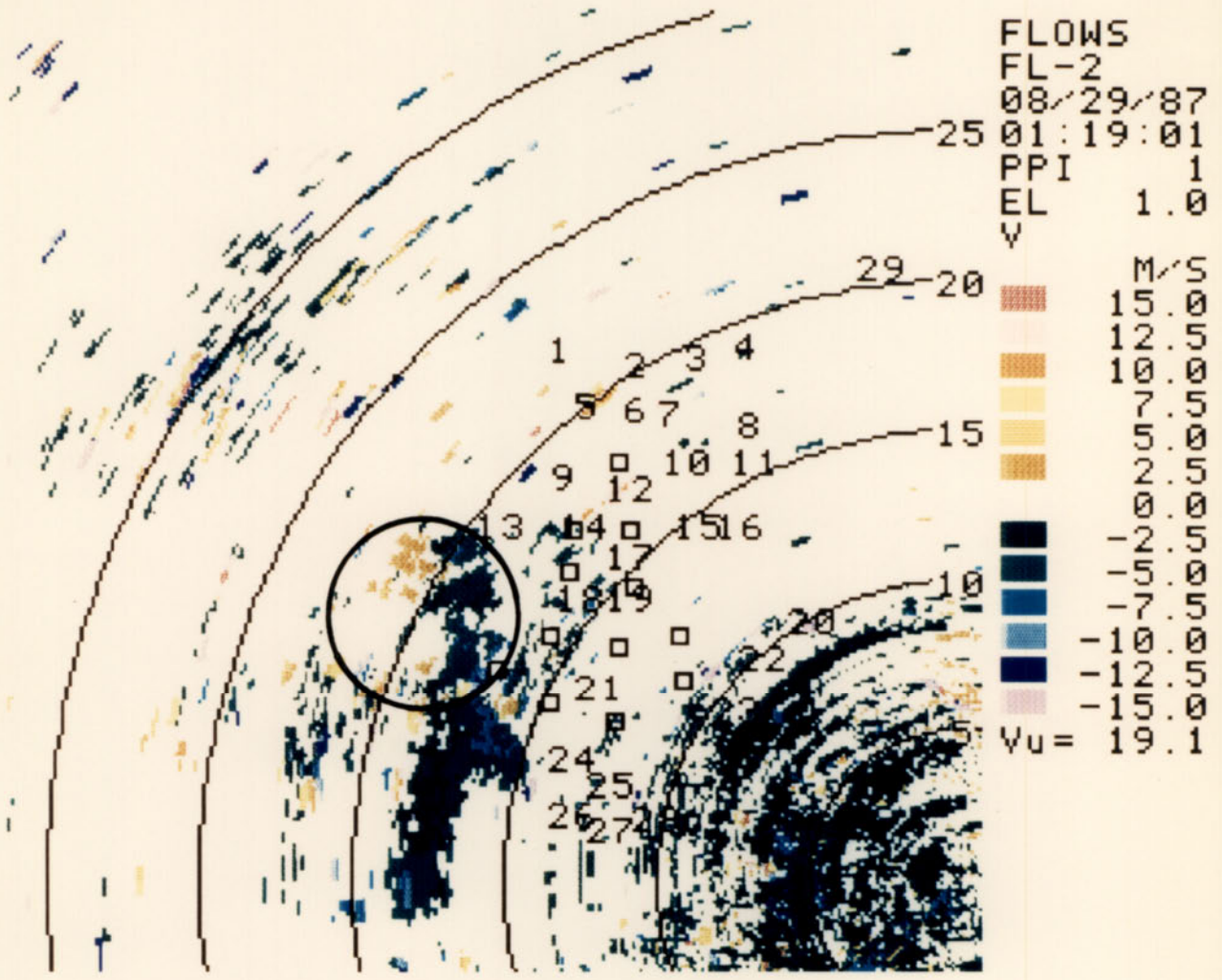

Figure V-17. FL-2 Doppler velocity field (SNR thresholded at 6 dB) at 0119 (UT) on August 29, 1987. Divergent area, associated with the mesonet identified microburst, is located within the black circle. Elevation angle is 1.0°. Range rings are every 5 km and location of mesonet stations are overlaid (squares denote LLWAS sensors).

2. *Case 2: 13 September 1987*

On September 13, a microburst wind shear event was identified by the surface mesonet sensors. It was located in the northern portion of the network between 2113 and 2118(UT) in the vicinity of stations 7 and 10 (Figures V–18 and V–19). The event was short lived and rather small in diameter (affecting, at the most, three surface stations), but it was well defined with maximum dV's, as measured by both the actual and radial (w.r.t. the FL–2 radar) winds, in the order of 16 m/s (Figure V–20). Thus, asymmetry (from the perspective of FL–2) was not a factor that contributed to this event being unobserved by the radar.

The FL–2 radar data shows that the cell responsible for this wind shear event is located approximately 17 km north–northwest of the radar, between mesonet stations 7, 8 and 10 (Figure V–21). According to the thermodynamic information provided by the NWSFO in Denver and that available through the mesonet surface data set, this cell had a base at ~3.3 km AGL and, according to the FL–2 radar reflectivity data, was not very deep. Maximum reflectivity associated with this cell appeared to be 20 dBz.

The surface scans, during the times associated with this microburst, portrayed very low reflectivity values. To determine whether these values were representative of legitimate meteorological targets, the SNR for these scans was assessed. It was determined from both the velocity and SNR data that:

(1) the signal, for part of the area affected by the microburst, appears to be dominated by some ground clutter residue located near mesonet station 10 (see Figure V–22), and

(2) the signal, throughout the rest of the area associated with the microburst, was near or below the 10 dB SNR threshold used in the automated algorithms.

It became apparent from the above, that the signal, as observed by the radar surface scans, was extremely weak and not associated with this microburst. Therefore, it was no surprise to see that the FL–2 Doppler velocity field (even after thresholding the SNR at 6 dB) showed no discernible signature of a shear event in the area identified above. Neither did the UND radar observe this event, although it should be noted that part of their data were missing because UND's data processor could not keep up with the specified azimuthal scanning rate, thereby dropping blocks of data.

3. *Case 3: Missed Events on 2 September 1987*

September 2 was a very active day with regards to wind shear occurrences over the mesonet. Seven (7) microbursts and two (2) gust fronts were observed within a one hour

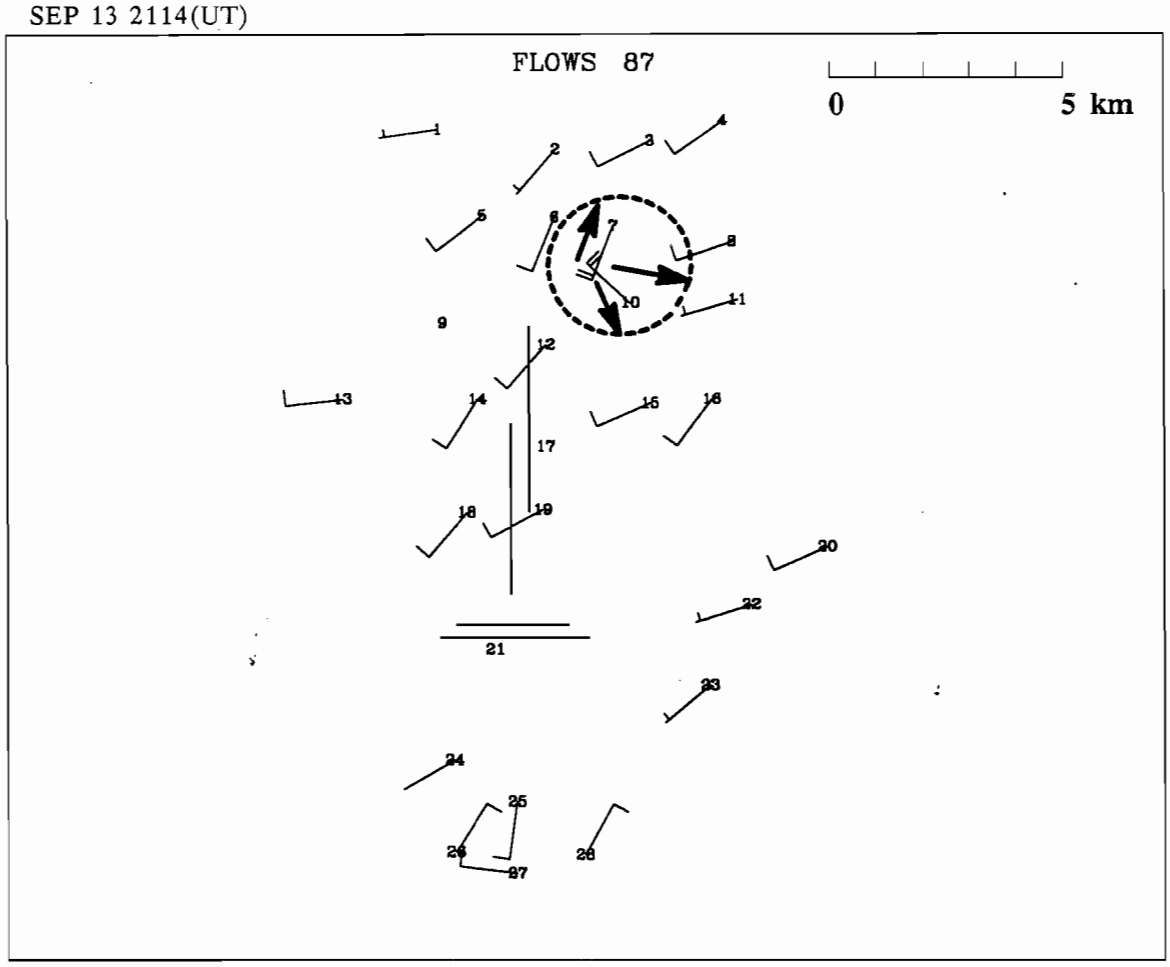

Figure V-18. *Mesonet plot showing the surface wind field at 2114 (UT) on September 13, 1987. Microburst outflow boundary denoted by dashed line. Full barb represents 5 m/s and half-barb 2.5 m/s.*

SEP 13 2116(UT)

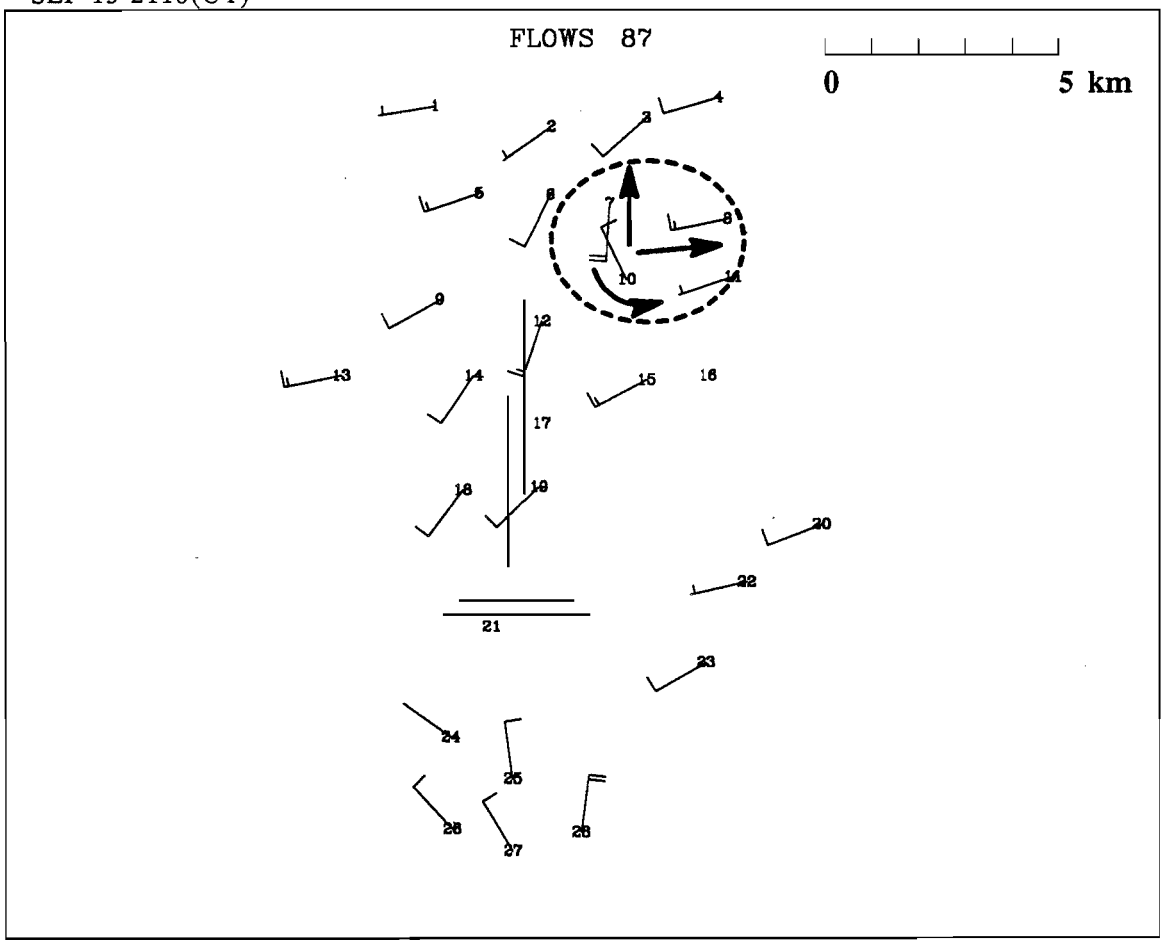

Figure V–19. *Same as figure V–18 except at 2116 (UT).*

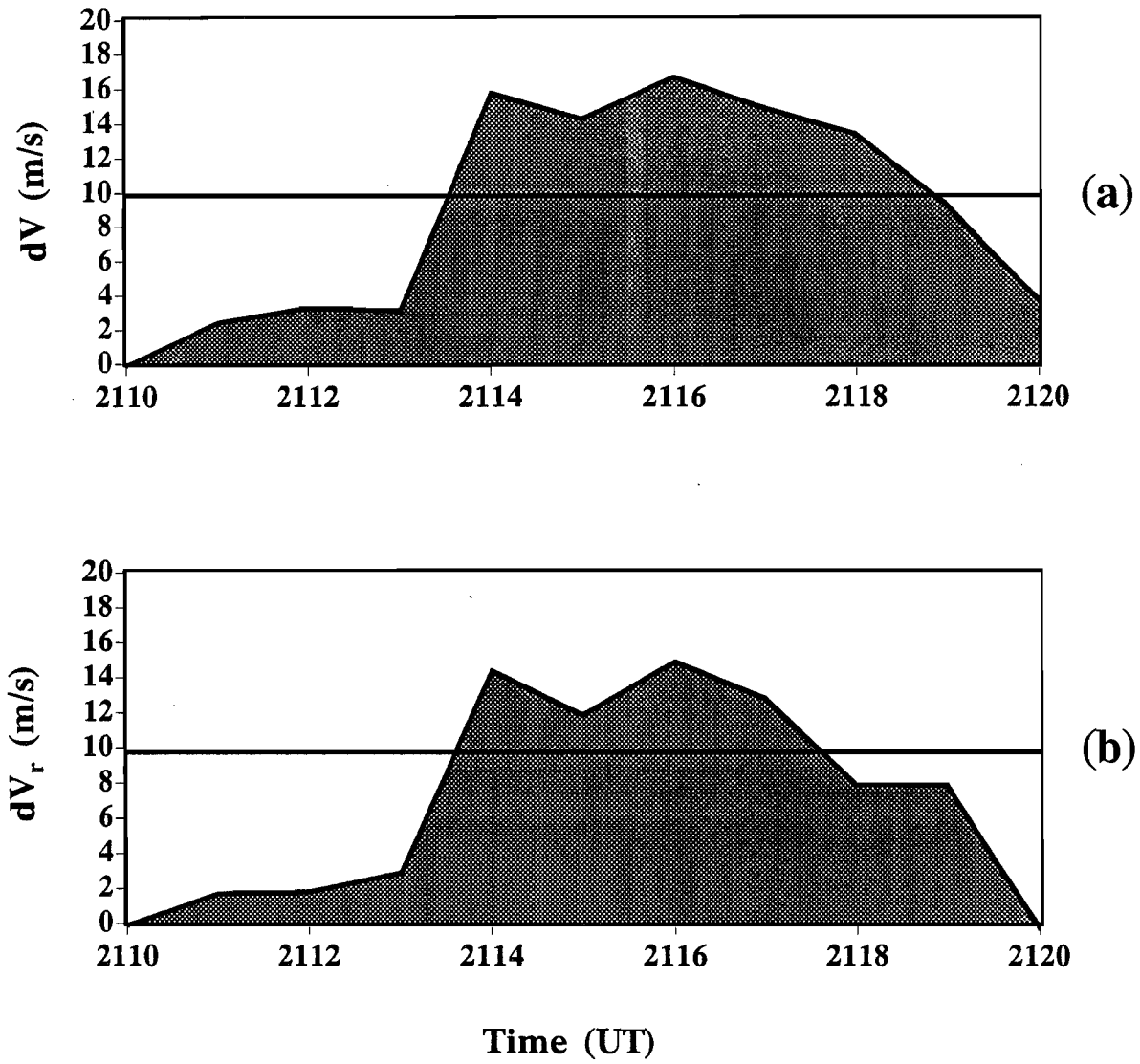

Figure V-20. *Maximum dV values that were computed over the mesonet using (a) the actual, and (b) the radial measured winds for a specified period during September 13, 1987. The radial winds were calculated with respect to the FL-2 radar site.*

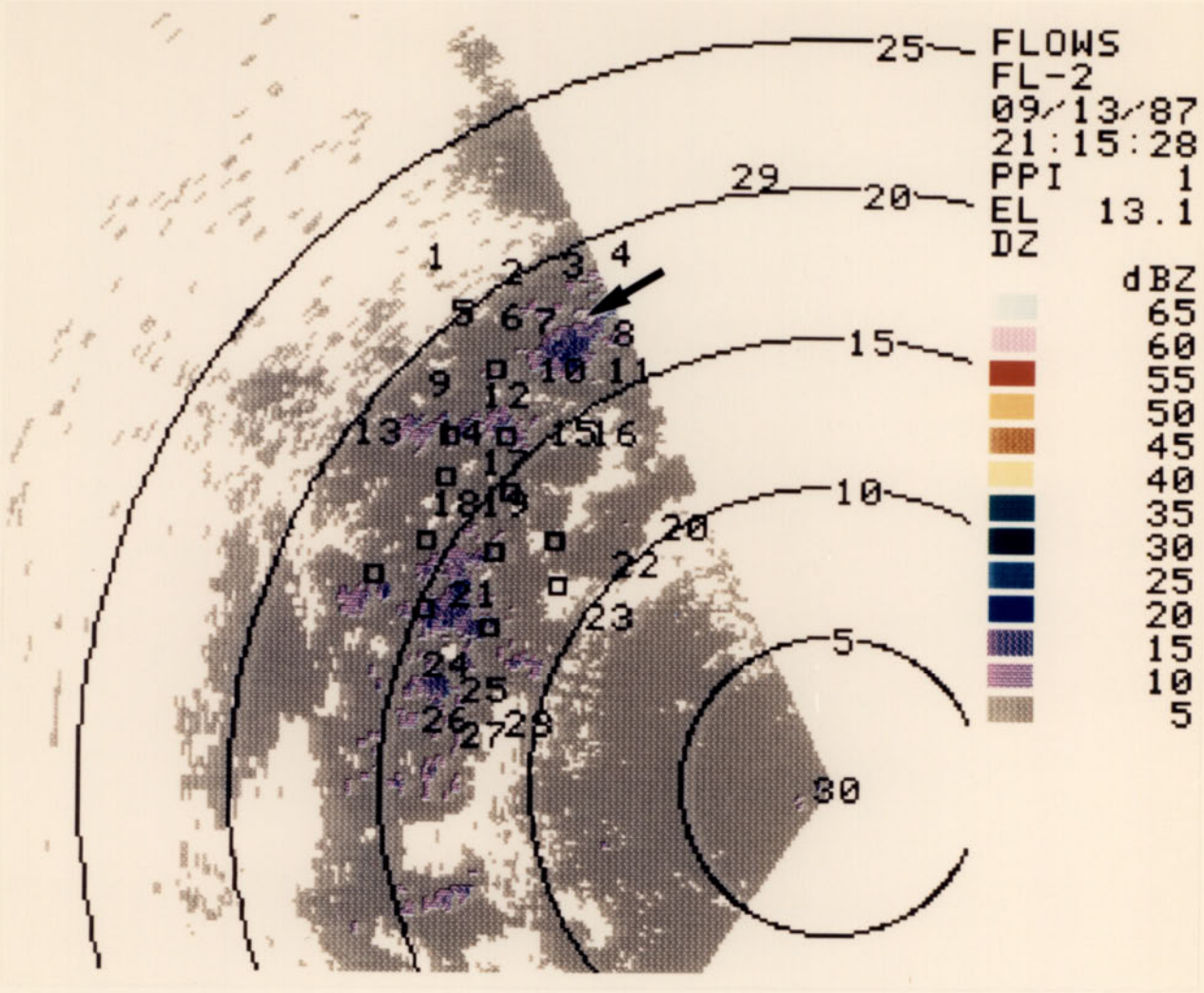

Figure V-21. FL-2 reflectivity field at 2115 (UT) on September 13, 1987. Arrow points to microburst producing cell. Elevation angle is 13.1°. Range rings are every 5 km and location of mesonet stations are overlaid (squares denote LLWAS sensors).

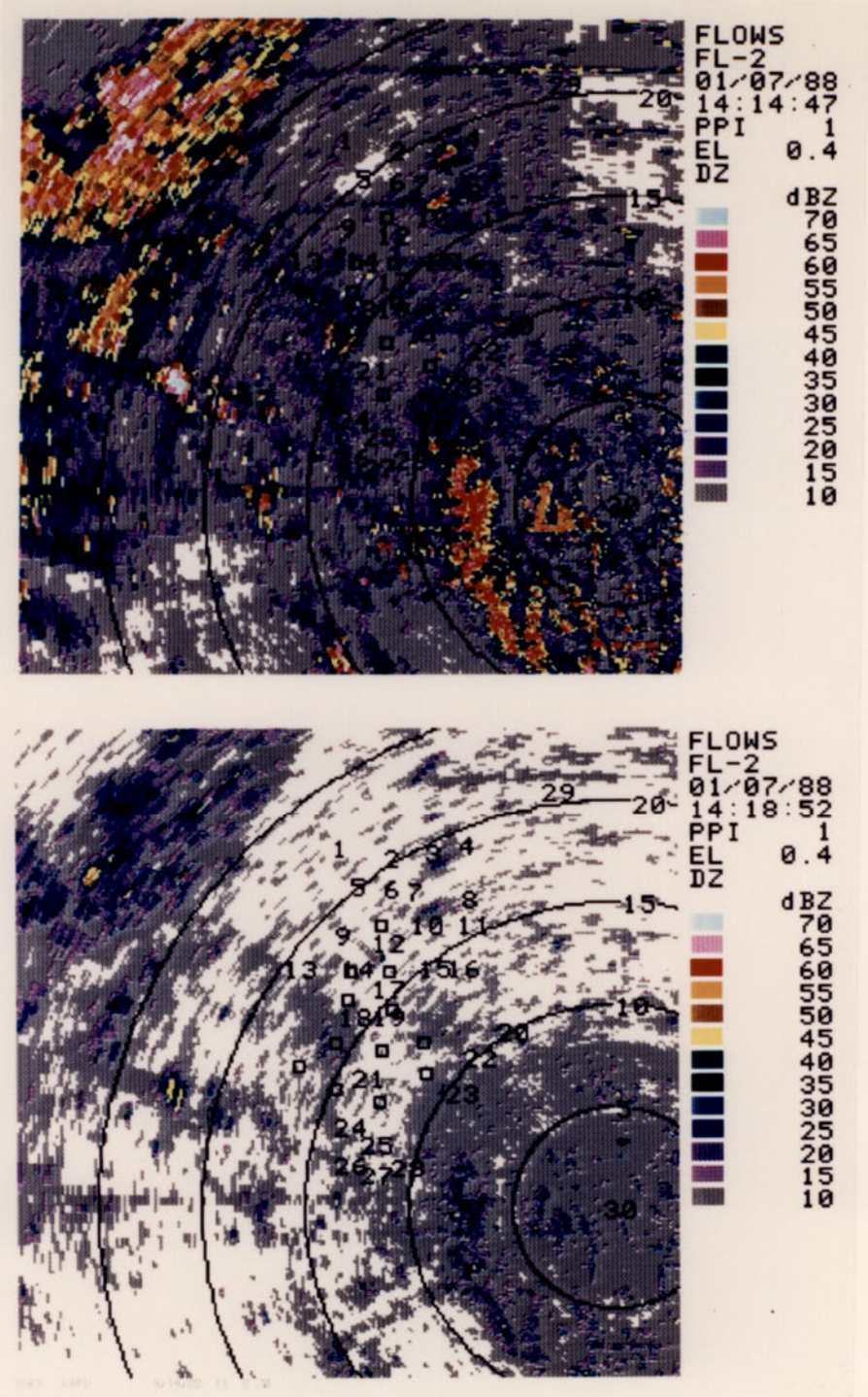

Figure V-22. FL-2 reflectivity field showing clutter (top) and filtered clutter residue (bottom) at an elevation angle of 0.4° on January 7, 1988 in Denver Colorado. Range rings are every 5 km and location of mesonet stations are overlaid (squares denote LLWAS sensors).

time span (2230–2330(UT)). Figure V–23 shows the times for which these events existed. Microbursts #78 and #81 were the two events that were not observed as such by the radar on this day and for which this case study focussed. The figure shows that for most of this hour, especially during the times that these two events were observed, two or more wind shear events were occurring simultaneously over the mesonet.

Microburst #78 was first observed near mesonet station 13. At 2245(UT), Figure V–24 showed the microburst to be approximately 3 km west of the north–south runways at Stapleton Airport. Another microburst was also evident at this time just north of the airport. Microburst #78 moved slowly eastward, and by 2250(UT) was located between LLWAS sensors "NW" and "W" (Figure V–25). At this time, two other microbursts were positioned to the north of the airport and a gust front began to move into the mesonet from the southwest. The center of the microburst, which was located between the LLWAS sensors, continued to move slowly eastward over the next few minutes, but did not appear to have ever reached the airport runways. Meanwhile, the other microburst of concern (microburst #81) was first observed at 2253(UT) just to the east–northeast of mesonet station 13. This microburst appeared at the surface approximately 1 km from microburst #78. This newly developing microburst began to impact the stations that had previously been affected by microburst #78 (i.e., appearing to merge with this previous outflow). Figure V–26 shows its distinct divergent signature positioned a few kilometers west of the airport's north–south runways. This microburst traveled a couple of kilometers east–northeastward to be located between mesonet stations 9 and 12, where, after 2304(UT), it became non–existent.

According to the mesonet surface sensors, these two microbursts exhibited impressive differences with respect to their strength. Figure V–27 shows the maximum dV values for these events as observed by the actual and radial (with respect to the FL–2 radar) components of the mesonet surface winds. The first event exhibited dV values in a range approaching 24 m/s from both the actual and radial wind measurements. The second event was much weaker. It did exceed 10 m/s (dV value) for several minutes as noted by the actual measured winds. However, the plot of the radial measured winds revealed, from the viewpoint of FL–2, that its strength, as determined by the dV values, did not reach this threshold level of 10 m/s.

Radar data, for this day, were available for both FL–2 and UND. However, missing data was prevalent in the UND data set, therefore prompting a decision to use only FL–2's data when dealing with single Doppler analysis during this case study.

The reflectivity fields for microburst #78, as observed by FL–2, were rather weak, where maximum values of only 25 dBz, at an elevation angle of 6.7°, were noted. Figure V–28 identified the cell as it moved eastward over the mesonet. The portion of the cell that extended along a north–south line between mesonet stations 13 and 18 was where this microburst emanated. While this cell moved over the area of the mesonet that was

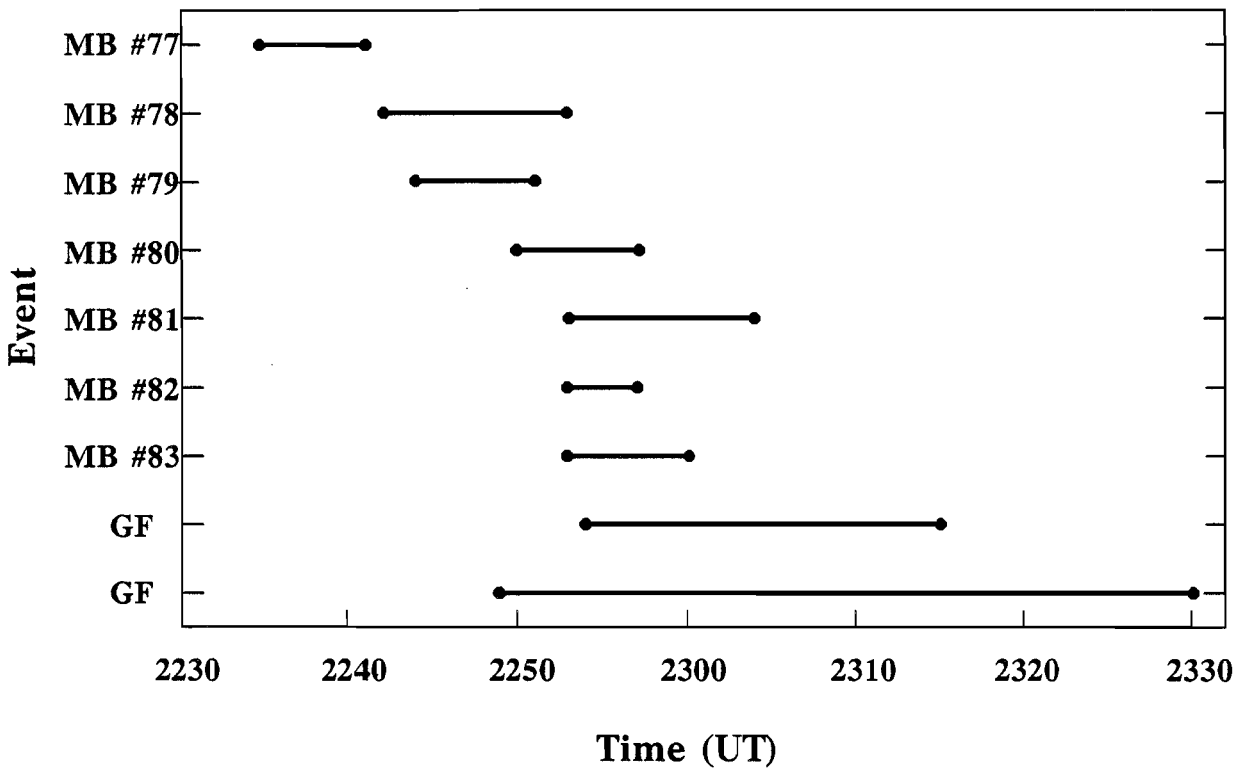

Figure V-23. *Time histories of wind shear events (microbursts (MB) and gust fronts (GF)) that impacted the Denver mesonet during the period 2230–2330 (UT) on September 2, 1987.*

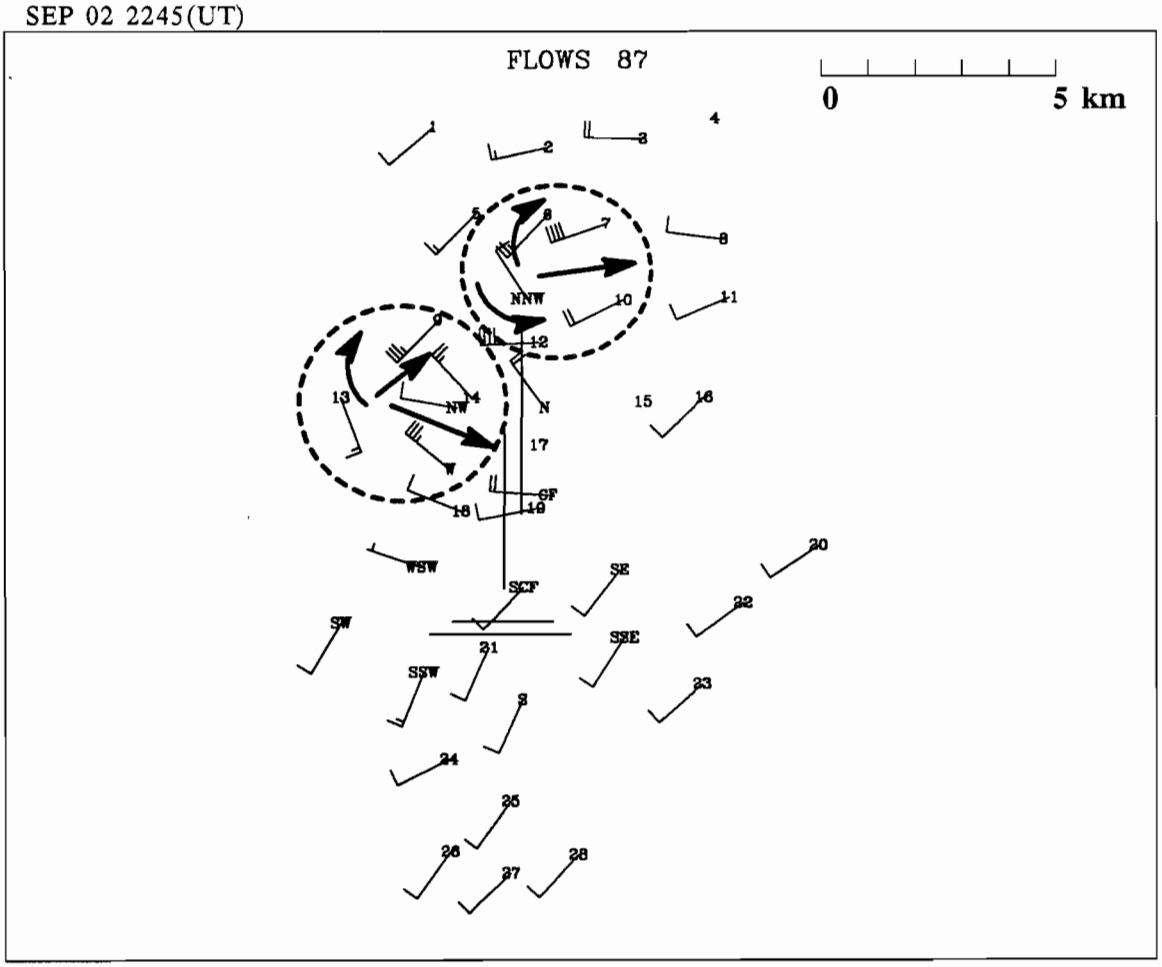

Figure V–24. *Mesonet plot showing the surface wind field at 2245 (UT) on September 2, 1987. Microburst outflow boundaries denoted by dashed lines. Full barb represents 5 m/s and half-barb 2.5 m/s.*

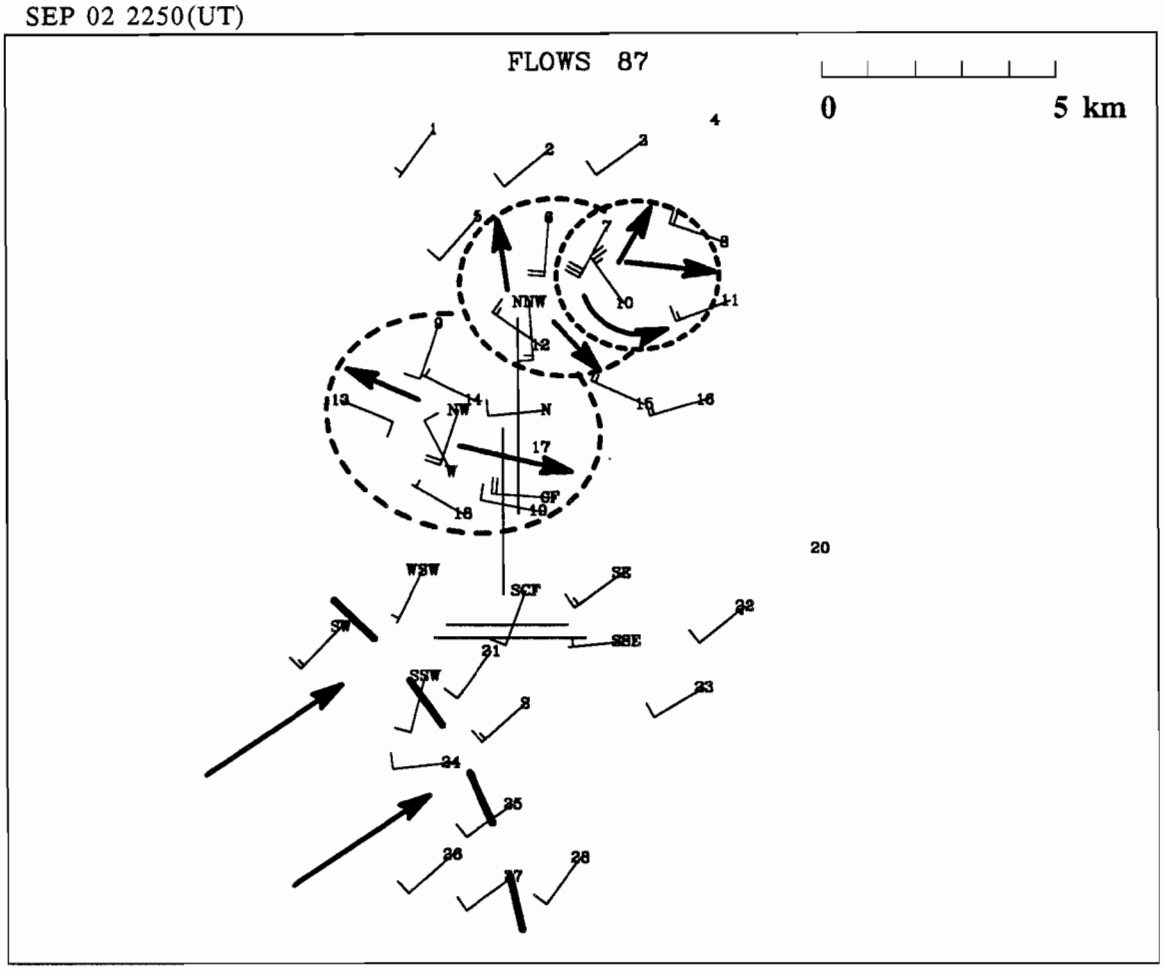

Figure V–25. *Same as figure V–24 except at 2250 (UT). Gust front has moved into the southwest portion of the mesonet.*

SEP 02 2255(UT)

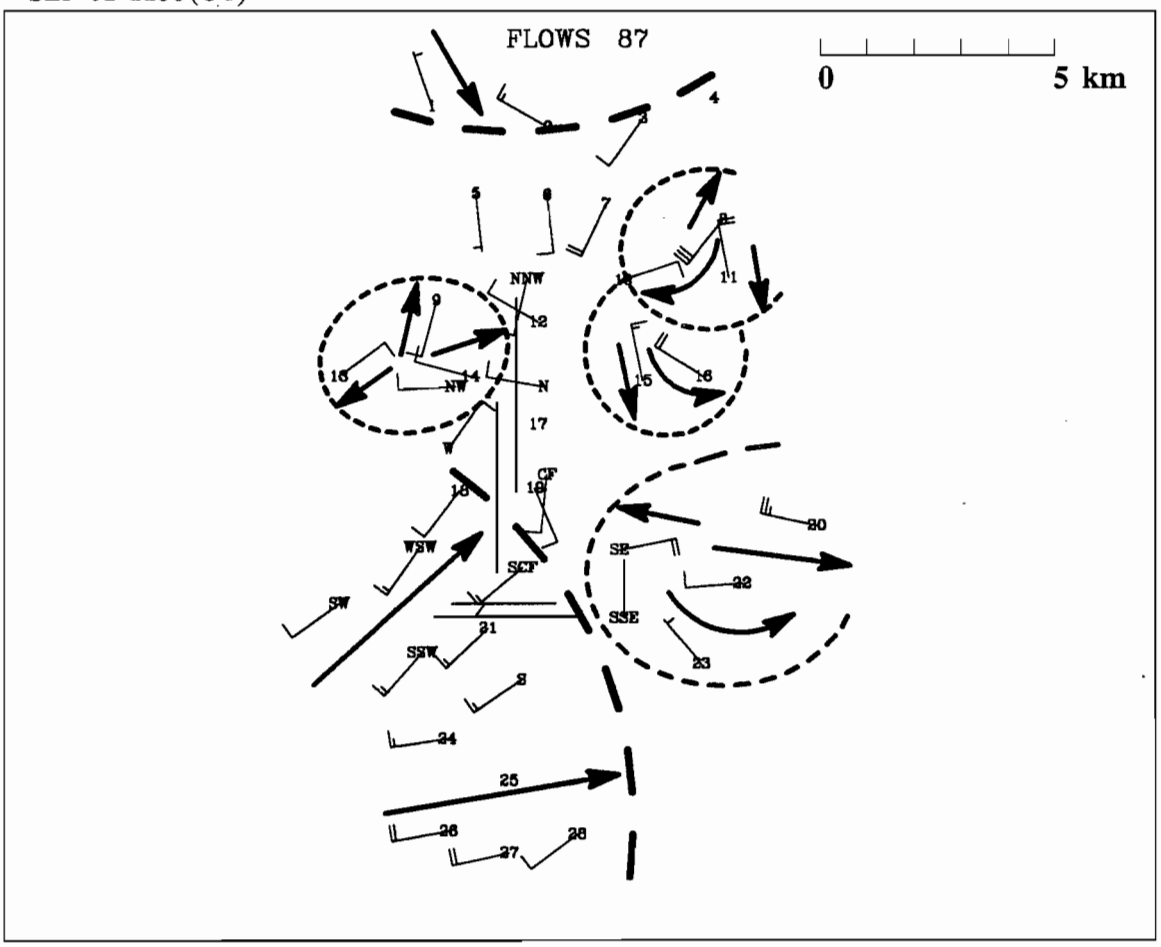

Figure V-26. *Same as figure V-25 except at 2255 (UT). Another gust front has penetrated into the mesonet (northern portion).*

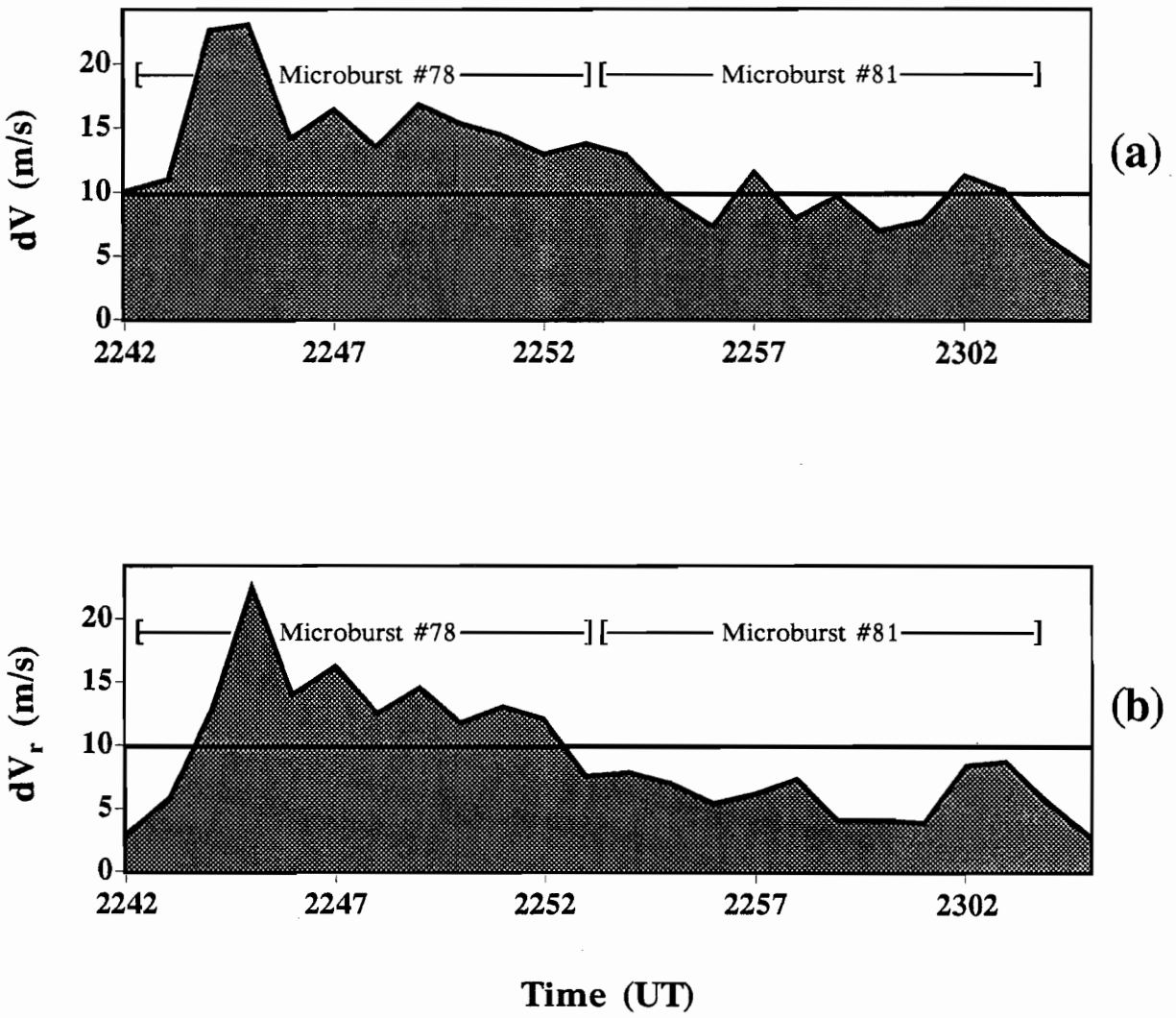

Figure V-27. *Maximum dV values that were computed over the mesonet using (a) the actual, and (b) the radial measured winds for a specified period during September 2, 1987. The radial winds were calculated with respect to the FL-2 radar site.*

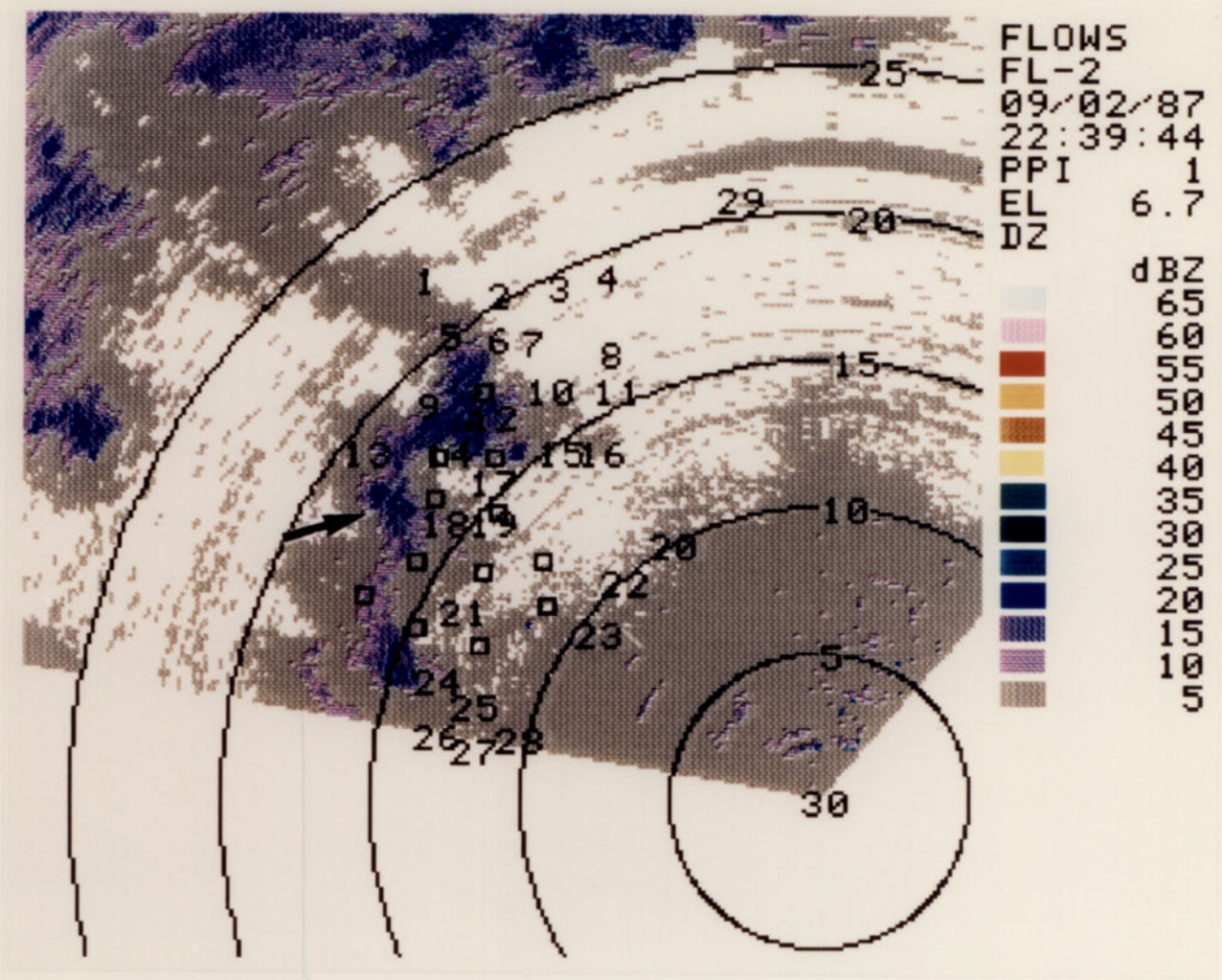

Figure V-28. FL-2 reflectivity field at 2239 (UT) on September 2, 1987. The arrow points to the cell that produced microburst #78. The elevation angle is 6.7°. Range rings are every 5 km and location of mesonet stations are overlaid (squares denote LLWAS sensors).

affected by this microburst, it showed signs of weakening (see Figure V-29). By 2245(UT), the depth of the cell had diminished considerably. The reflectivity values corresponding to microburst #81 were also rather weak, where a maximum of only 30 dBz was observed. Figure V-30 shows the reflectivity fields at an elevation angle of 13.1° for the times 2250 and 2258(UT). The cell that produced microburst #81 was just beginning to enter into the western portion of the mesonet (near station 13) at 2250(UT). The cell which produced microburst #78 can be seen as it continued moving eastward, positioned approximately 13 km northwest of FL-2 and apparently strengthening again. By 2258(UT), the newer microburst producing cell could be seen as it moved over the mesonet in the vicinity of station 13. According to thermodynamic information supplied by the NWSFO in Denver, the cloud base for these cells in the vicinity of Stapleton Airport was approximately 2.7 km AGL.

Low-level plots of SNR were analyzed for the period 2235-2300(UT). The SNR field at 2240(UT)* clearly identified two distinct regions (located 18 km's northwest of the FL-2 radar) where microbursts were occurring (Figure V-31). Also noticeable in this figure is the east-west oriented line of higher signal which was located about 20 km's north of the radar and was identified with a gust frontal boundary. The next several minutes saw the regions of higher SNR that were northwest of the radar, move eastward. The region that was just south of mesonet station 13 in Figure V-31 was representative of microburst #78. The SNR values associated with this system decreased considerably with time. So by 2245(UT), the signal in this area was either near or below the 10 dB SNR threshold used in the automated algorithms or (at the lowest scanning angles) associated with ground clutter. As for microburst #81, the analysis of the SNR field indicated that the signal remained near or below this 10 dB threshold level throughout its history.

The Doppler velocity fields were thresholded with the SNR at 6 dB. This eliminated the velocities that were associated with very weak signals (near the noise level) and therefore allowed a more representative picture of the wind field to be observed. Although higher signals associated with stationary ground clutter would not be eliminated, their corresponding Doppler velocities would be identified by the '0' m/s isodop. During the period between 2240-2244(UT), the velocity fields indicated divergence just to the south and southeast of mesonet station 13. This was obviously associated with microburst #78.

---

* The FL-2's radar elevation angle for this scan was positioned at 1.0°. The lower elevation angles of 0.4° and even 0.5° were contaminated with signals from ground clutter returns. Therefore, the data at 1.0 ° was used to give a better representation of the return signal from weather targets.

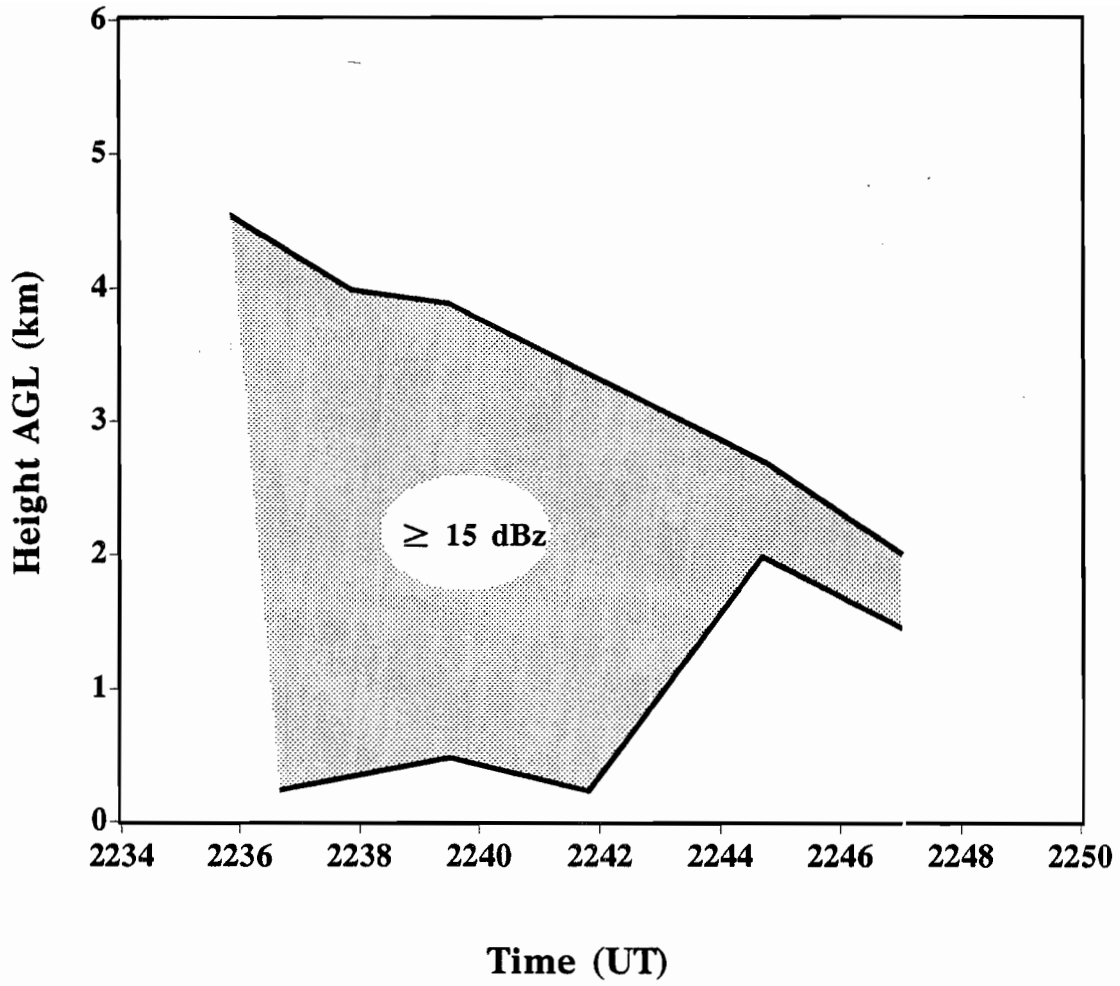

Figure V-29. *Time-height profile of the 15 dBz reflectivity contours from the cell that produced microburst #78 on September 2, 1987. Note the shrinking of the cell when the surface outflow commenced.*

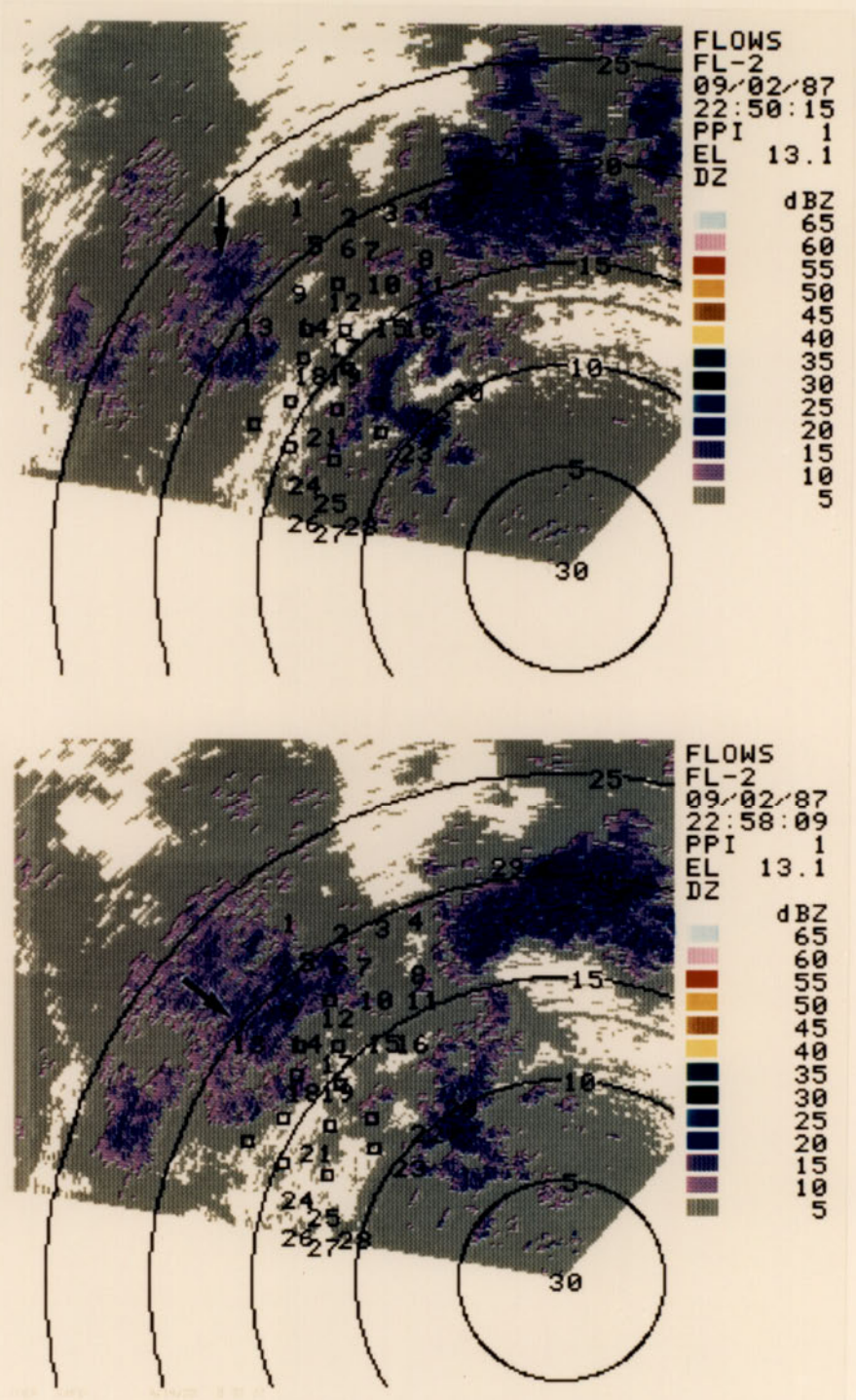

Figure V-30. FL-2 reflectivity fields at 2250 (UT) and 2258 (UT) on September 2, 1987. The arrow points to the cell that produced microburst #81. The elevation angle is 13.1°. Range rings are every 5 km and location of mesonet stations are overlaid (squares denote LLWAS sensors).

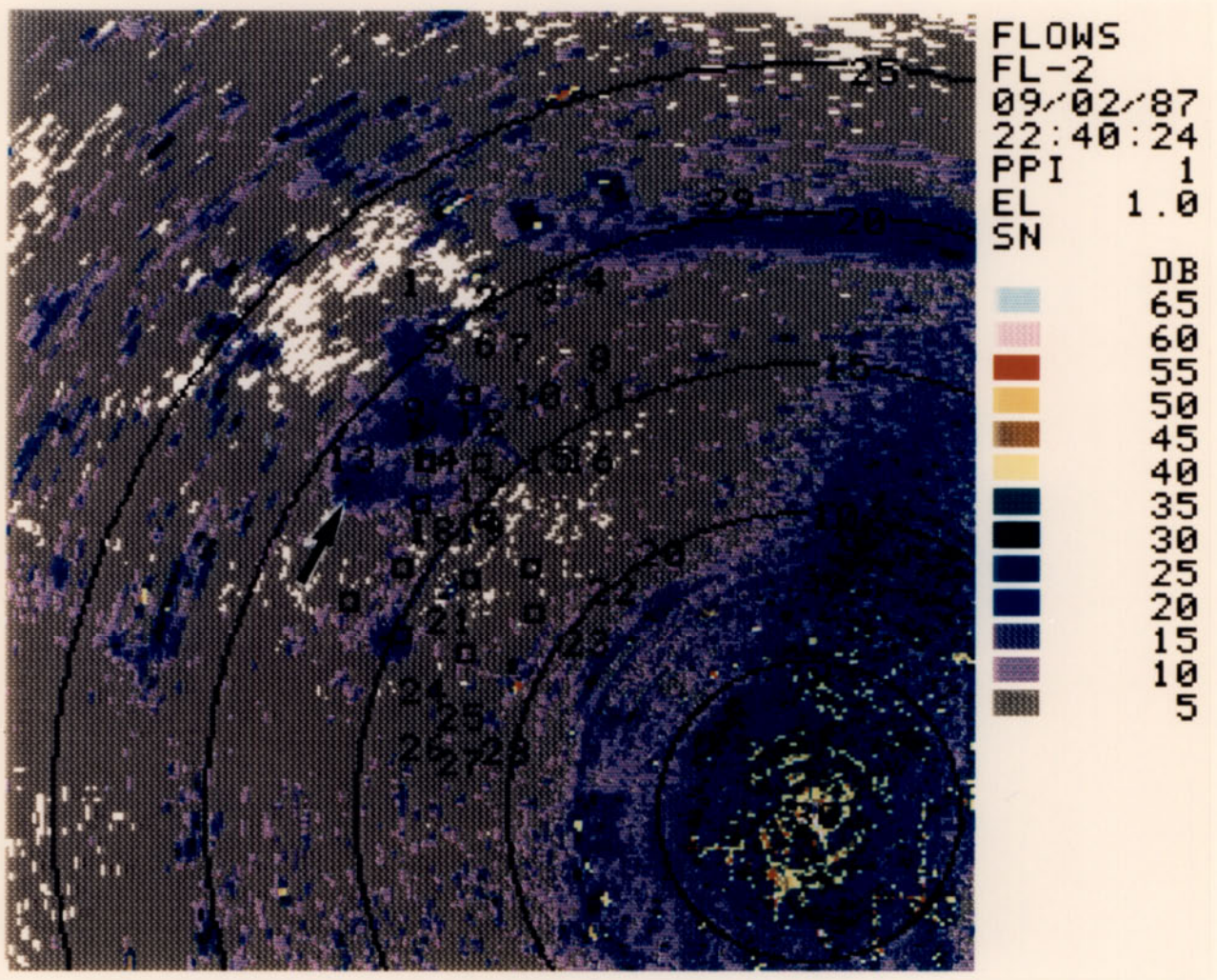

Figure V-31. FL-2 SNR field at 2240 (UT) on September 2, 1987. The region south of mesonet station 13, where SNR values approach 25 dB, is associated with microburst #78 and is indicated by the arrow. The elevation angle is 1.0°. Range rings are every 5 km and location of mesonet stations are overlaid (squares denote LLWAS sensors).

The strongest dV, associated with this event, of 15 m/s was observed at 2241(UT) * at an elevation angle of 0.4°. A comparable value of dV was observed several seconds earlier but at an elevation angle of 1.0°. A broader area of divergence was observed at this somewhat higher elevation angle (Figure V-32). This, however, is not where TDWR scans for microbursts. Also, this radar observed divergence area, especially at the lowest scans, was much smaller than that observed by the mesonet at the surface. From 2245-2300(UT), there was absolutely no indication of any microburst divergence signatures that would be associated with either microbursts #78 or #81. Even when performing Dual-Doppler analysis on thresholded (SNR @ 6 dB) FL-2 and UND data over this same period of time, microbursts #78 and #81 could still not be identified.

It seemed apparent that these two microbursts on September 2 were unquestionably identified by the mesonet surface sensors. It was also obvious that microburst #81 went completely unobserved by the FL-2 radar. From the data provided in this section, it would seem reasonable to assert that the extremely weak signal, or lack thereof, as indicated by the radar at low levels, was the reason microburst #81 was unobserved. A very deep sub-cloud layer existed with this microburst producing cell, allowing any precipitation that may have fallen from the cloud to totally evaporate before reaching the surface.

Microburst #78 was categorized as unobserved by the radar even though, for a short period of time, divergence near the surface was evident. There seemed to be two distinct phases associated with this microburst:

(1) that before 2245(UT), where an area of reliable weather signal was identified near the surface, and

(2) that from 2245(UT) and on, where the observed signal was extremely weak and apparently not associated with weather.

During this second phase, beginning at 2245(UT), microburst #78 obviously was unobserved by the radar because of the lack of signal. However, in the period before

* There was a 4 minute time lag between the time at which the maximum differential velocity (dV) was observed by radar (2241(UT)) and the surface mesonet sensors (2245(UT)). The average time delay observed for 5 of the microbursts that impacted the mesonet on September 2 was slightly more than '3' minutes (microburst #79 and #81 were excluded from this sampling; microburst #79 because its' center remained outside the periphery of the mesonet, thereby not allowing a reasonable comparison, and microburst #81 because the radar did not observe this event). Other mesonet impacting microbursts from the 1987 Denver data set also showed similar lag times. The clocks for both the radar and mesonet sensors were syncronous with the GOES satellite clock. Therefore, the probability that this lag can be attributed to a timing difference between the radar and mesonet clocks is small.

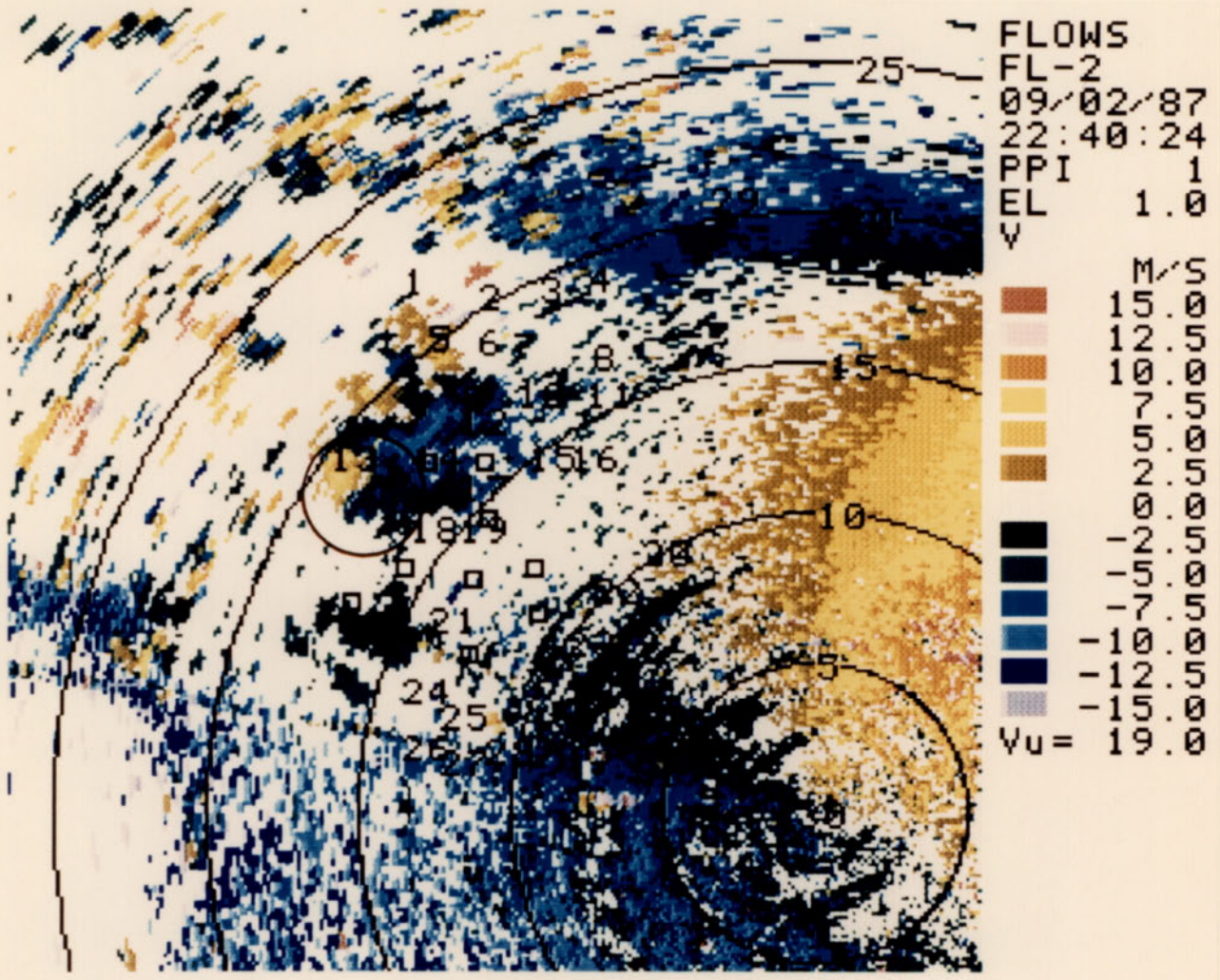

Figure V-32. FL-2 Doppler velocity field (SNR threshold at 6 dB) at 2240 (UT) on September 2, 1987. Divergent area associated with microburst #78 is identified within the black circle. The elevation angle is 1.0°. Range rings are every 5 km and location of mesonet stations are overlaid (squares denote LLWAS sensors).

2245(UT), divergence in the Doppler velocity field was observed, yet when compared with the strength and duration that was noted in the mesonet data, no similarities were evident (see Table V–1). So the decision on how to classify this microburst ultimately came down to how three specific questions were answered:

(1) Did the mesonet surface sensors observe this event?

(2) Did the radar observe this event?

(3) If the event was seen by both systems, was what was seen comparable?

The answers to the first two questions were yes, but it was obvious from the analysis that the radar data significantly underestimated the strength, duration, and area of microburst #78, and thus we have classified this event as unobserved by the radar.

As to the question of why only a small area of divergence was observed at FL–2's lowest scans, a couple of possible explanations are presented:

(1) the surface outflow signature was obscured by the signature of weather above the surface outflow, or

(2) there was some blockage to the beam which prevented the surface outflow from being measured, and/or

(3) the surface outflow reflectivity was so low that the noisiness in the velocity estimates obscured the divergence signature.

With regards to the possibility of beam blockage, the Fitzsimons medical facility, which was located approximately 10 km northwest of FL–2, was a target first suspected in the matter. Figure V–33 shows, however, that at the lowest elevation angle of 0.4°, the half–power beam of the FL–2 radar, with a width of approximately 1.0° (Rinehart, et al., 1986) did not appear affected by even the highest point of this target, but at such a low elevation angle, a portion of the main lobe most likely did intercept this target. The only other probable source that could be responsible for blocking a portion of the beam would be ground clutter targets in the vicinity of the microburst impact point (near mesonet station 13). Figure V–22 (top) indicates just how visible the clutter is in this area when the clutter suppression filter is disabled.

The possibility also existed for the hazardous microburst outflow to be shallow in depth and located close to the surface. Wilson *et al.* [1984] indicated that from single Doppler observations at close range (4–10 km) the height of maximum differential velocity associated with microbursts is ~75 m AGL. According to Figure V–33, this height, near

Table V-1. *Comparative statistics between the FL-2 radar and surface mesonet data sets regarding the strength, duration, and area impacted from microburst #78 on September 2, 1987.*

	MESONET	FL-2 RADAR
Duration (min.) Where Max dV ≥ 10 m/s	12	3
Duration (min.) Where Max dV ≥ 20 m/s	2–3	0
Max dV (m/s)	23.5	15
Area (km^2)	38	5

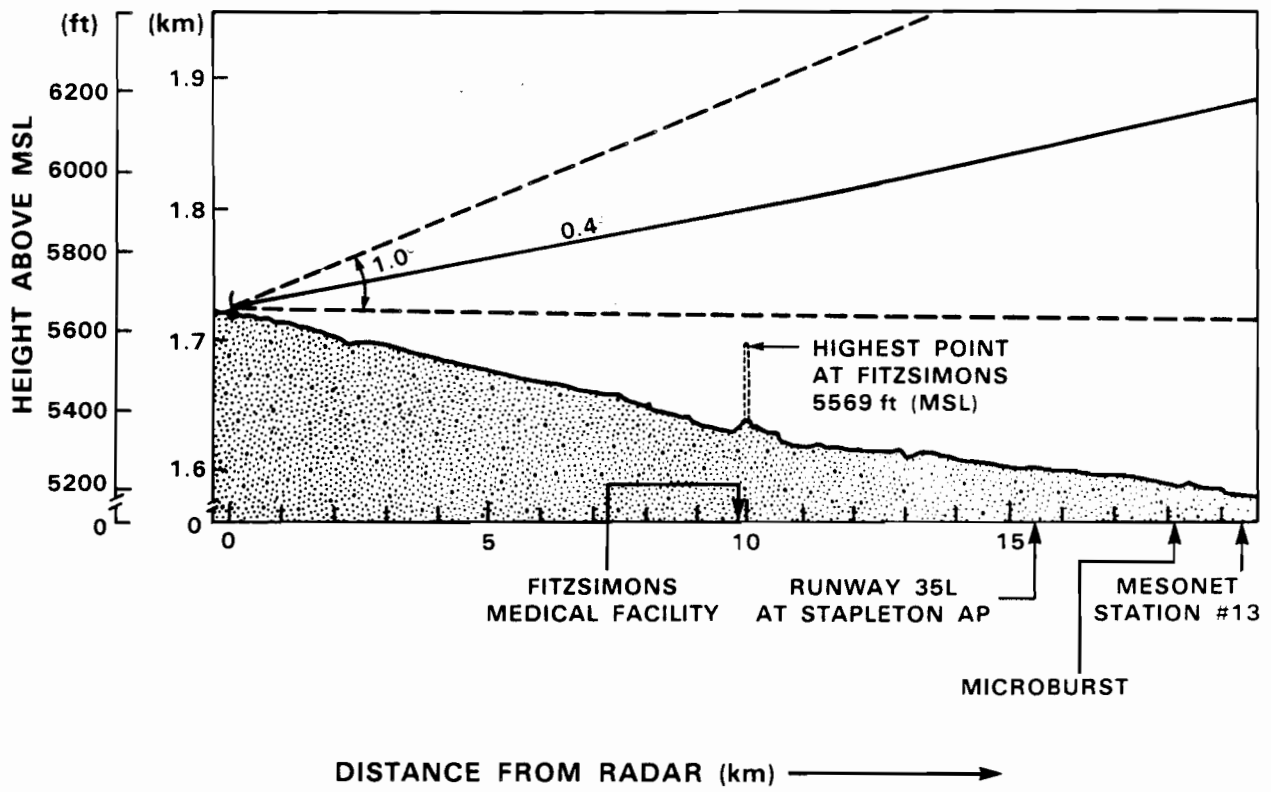

Figure V-33. Vertical profile of the topography between the FL-2 radar and points northwest along the 306° azimuth. With the radar scanning at an elevation angle of 0.4°, the bottom and top of the half-power beam, assuming no blockage, are noted by dashed lines.

the vicinity of microburst #78, would correspond to an area below that which was scanned at the lowest antenna tilt angle (0.4°). So in order to appropriately estimate the differential velocity profile between the area scanned by the lowest antenna tilt angle and the surface, a simulation of the wind profile with height was needed. To generate this, an apparent profile of the velocity field with altitude (including observations from the surface mesonet) was needed as input. But as mentioned earlier in this section, most of this event was identified with low SNR values and consequently, the reflectivity and Doppler velocity fields in the area of this microburst appeared riddled with noise. To alleviate this problem without deleting any data points, a median filter was applied. Figures V–34 through V–36 show results of this filter. Note the difference between the thresholded velocity data in Figure V–32 and the smoothed, non–thresholded velocity field in Figure V–34.

Figure V–37 shows the results of the simulation as well as the apparent profile with height of the differential velocity associated with microburst #78. It was obvious that the simulation provided a closer estimate to the maximum differential velocity which had been observed by the surface mesonet, but it was still an underestimate. This seems to suggest that if the antenna tilt angle was adjusted lower than 0.4°, a better representation of the intensity of this microburst could have been obtained. Keeping in mind that the lowest effective elevation angle used for scanning weather is typically 0.2° above the average terrain slope, figure V–33 would indicate that scanning in this area could be done at an elevation tilt angle of approximately –0.2°. However, the problem that would be encountered by implementing this lower altitude scan strategy would be an increased probability of encountering high level ground clutter due to increased main lobe illumination of ground clutter targets. Figure V–38 shows by lowering the antenna tilt angle just 0.2 of a degree from 0.2° to 0.0°, a significant increase in filtered clutter residue results. We conclude that with a 1.0° beam width and the current (NEXRAD) sensitivity, this particular microburst signature could not be effectively detected at this location.

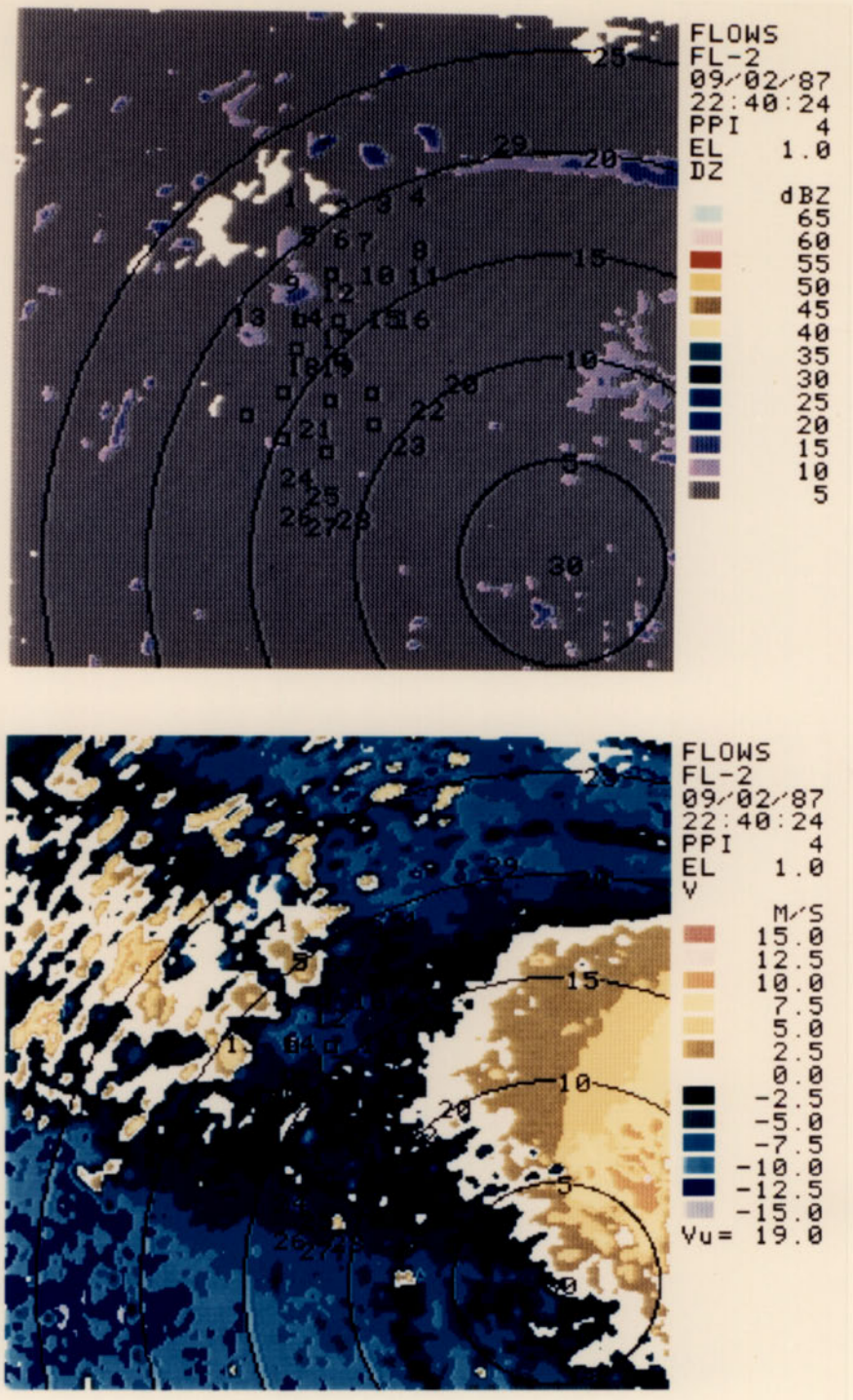

Figure V-34. FL-2 reflectivity and Doppler velocity fields for September 2, 1987 after a median filter has been applied to the data. The time of this plot is 22:40:24 (UT), and the elevation angle is 1.0°. Range rings are every 5 km and location of mesonet stations are overlaid (squares denote LLWAS sensors).

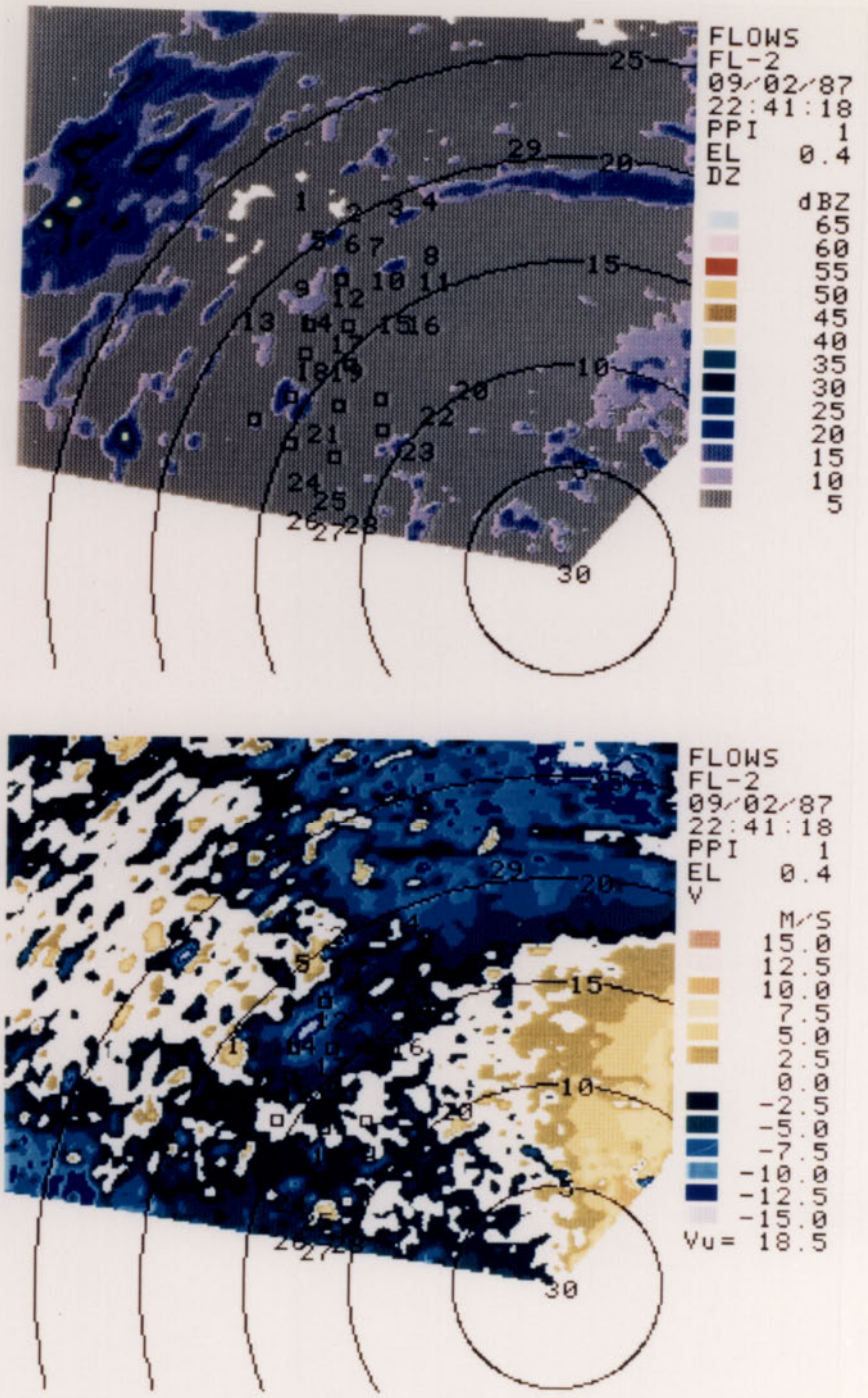

Figure V-35. Same as Figure V-34 except the time is 22:41:18 (UT) and the elevation angle is 0.4°.

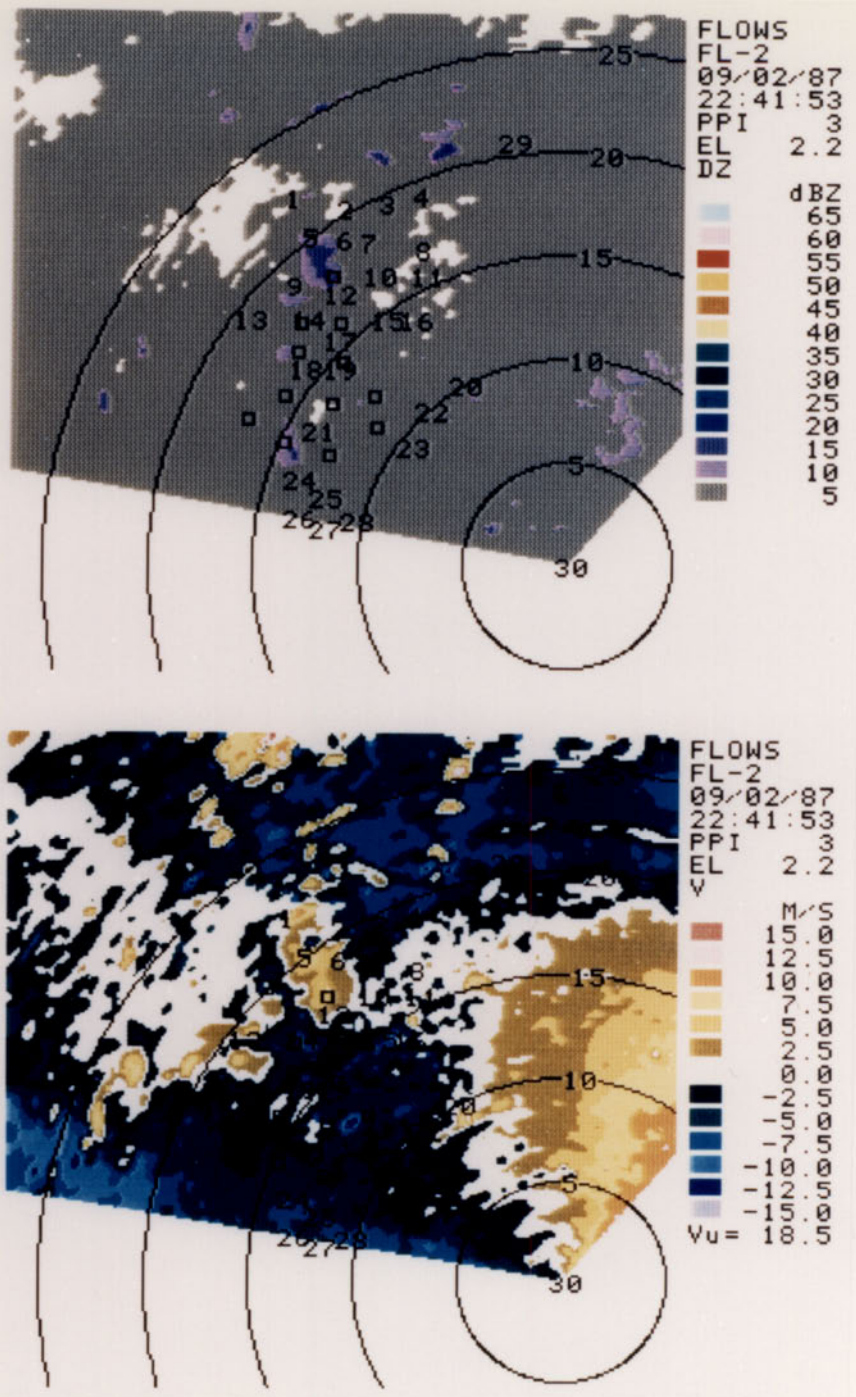

Figure V-36. Same as Figure V-34 except the time is 22:41:53 (UT) and the elevation angle is 2.2°.

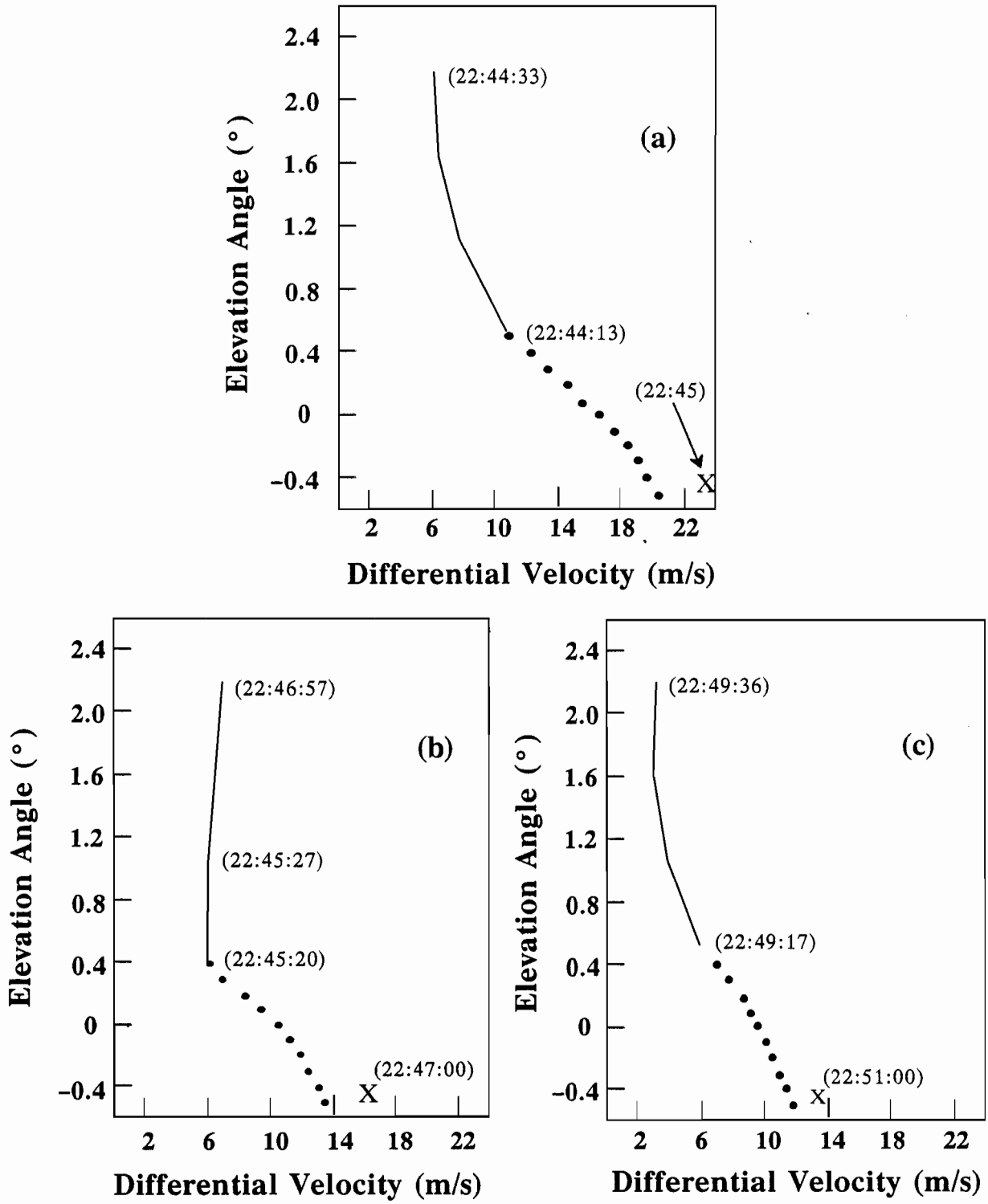

Figure V-37. *Differential velocity profile with height at (a) -22:40:30 (ut), (b) -22:46:30 (UT), and (c) -22:50 (UT) on September 2, 1987. Solid line represents the estimated wind profile from FL-2 radar data, dotted line represents the wind profile generated from the numerical simulation, and 'X' indicates the mesonet observed surface velocity differential.*

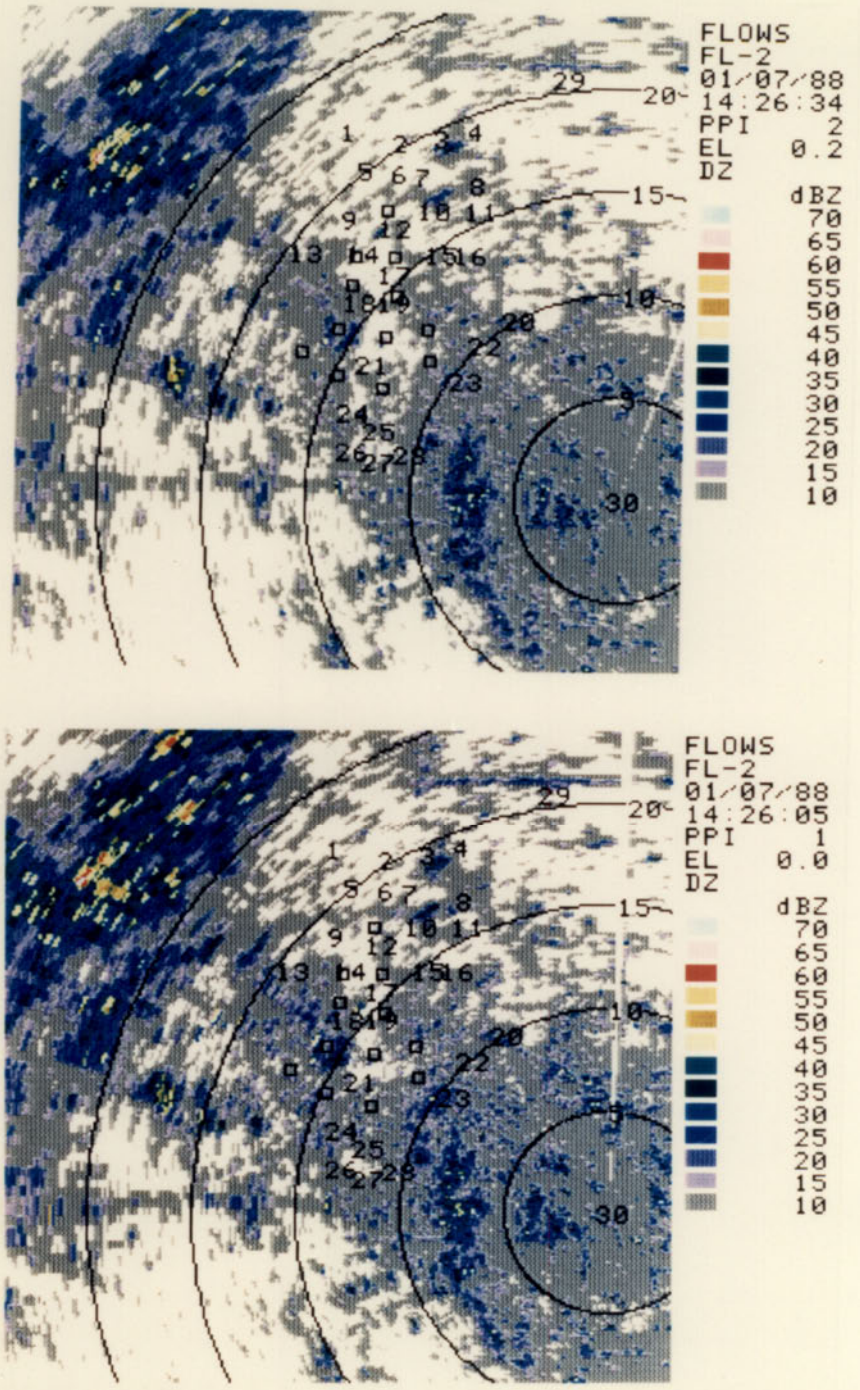

Figure V-38. FL-2 reflectivity showing the filtered clutter residue field on January 7, 1988 at elevation angles of 0.0° and 0.2° in Denver, Colorado. Range rings are every 5 km and location of mesonet stations are overlaid (squares denote LLWAS sensors).

VI. SUMMARY

During 1987, it was estimated based on Doppler radar and surface mesonet data that 102 microbursts impacted the FLOWS mesonet in Denver, Colorado. Relevant to this study were the microbursts that had available both the radar and mesonet surface data from which comparative analysis could be performed. There were 66 of these such microbursts, whereby:

(1) 92.4% (61 of 66) were observed by both the radar and mesonet,

(2) 1.5% (1 of 66) was unobserved by the mesonet surface sensors, and

(3) 6.1% (4 of 66) were unobserved by the radar, corresponding to a radar observed percentage of 93.9%.

Of these 66 events, the probability of detection (P_D) for the stronger microbursts (maximum differential velocity of at least 20 m/s) was 97%.

The one microburst that went unobserved by the mesonet sensors occurred on September 16. According to the FL–2 radar data, this was a short–lived, weak, but well–defined event. However, the portion of the microburst identified by an area of receding values in the Doppler velocity field was, for the most part, contained between three LLWAS sensors. These sensors were separated on the average by less than 2 km, yet this microburst was still effectively small enough to remain unobserved by the surface mesonet sensors.

The four microbursts that were unobserved by the radar* were all classified as dry events. The first of these occurred on August 29 and was identified as a marginal event whereby the mesonet surface sensors indicated the existence of a weak microburst (located in the western portion of the network) but the FL–2 radar did not. According to the mesonet data, when comparing the maximum differential velocities (dV's) as computed from the actual wind field with those from the radially measured winds (w.r.t. FL–2), only slight differences were noted. This indicated that assymetry from the viewpoint of FL–2 would not be a problem. Divergence, however, was observed in the FL–2 Doppler velocity field, but it was below the threshold for microburst classification ($dV \geq 10$ m/s within a distance of 4 km). As mentioned above, this was a dry event in that no precipitation was measured by the surface sensors and not only was none measured, but the relative humidity sensors in the area of the microburst indicated surface conditions were

* Radar data from both FL–2 and UND existed for these missed events. The quality of the FL–2 data for these events was fine. However, the only acceptable UND data, from these four days, was found on September 13 (see Table IV–2a).

becoming even drier. Most likely, any precipitation which fell from the cell, which was identified by the radar, evaporated before reaching the surface. This was reflected in the radar data whereby the observed signal at low–levels was very weak.

Another microburst that was unobserved by the radar occurred in the northern portion of the mesonet on September 13. According to the mesonet surface data, it was a short–lived event that affected just a small area (only three stations were impacted), but was easily detected. Maximum differential velocity values of 16 m/s were observed by the surface sensors. The FL–2 radar identified a small but weak cell (maximum reflectivity of 20 dBz) located above the impacted mesonet stations, and with a cloud base of ~3.3 km AGL. According to the radar data, the signal observed in the surface scans was extremely weak and apparently not associated with the microburst. Understandably then, the Doppler velocity field showed absolutely no sign of any shear event.

September 2 was the day on which two microbursts went unobserved by the FL–2 radar. This was a very active day in which seven (7) microbursts and two (2) gust fronts impacted the mesonet within a one hour period. The first microburst (#78) that was unobserved by the radar on this day, according to the mesonet data, appeared just west of the airport and moved slowly eastward. The center of this divergent event did not cross the runways. The second microburst (#81) not observed by the radar appeared at the surface about 1 km from the first microburst. It moved a few kilometers east–northeastward and impacted the same stations that had been affected by microburst #78. According to the mesonet wind analysis, maximum dV values, computed from the actual wind field, clearly identified microburst #78 as the stronger of the two with computed values of differential velocity approaching 24 m/s, whereas microburst #81 just barely exceeded threshold. When examining the radial component of the mesonet winds (w.r.t. FL–2), it was observed that microburst #78 was still quite strong, but dV values for microburst #81 had failed even to reach threshold. This suggested a possible assymetry problem. However, the FL–2 radar data, after identifying the microburst producing cell, indicated that the signal observed by the lower–level scans was extremely weak, thus providing the reason for the event going unobserved. Assymetry, therefore, was not a determining factor in this case.

As for microburst #78, the cell responsible for producing this event was clearly identified by the radar. Further analysis showed that there were two distinct parts to this storm's history:

(1) the first few minutes of its existence when some reliable signal and consequently an area of divergence was observed, and

(2) the remaining minutes of its existence when the signal was extremely weak and no associated shear was identified.

Upon further comparison between the mesonet and radar data regarding the viewing of this event, it was realized that the radar highly underestimated the strength, duration, and impacted area of this microburst. Thus it was classified as unobserved by FL–2.

Another question arose during the analysis of microburst #78 on September 2, which was why only a small area of divergence was observed at FL–2's lowest scanning angles when the corresponding mesonet data identified a much broader area of divergence. The response to this question pointed to two possible explanations:

(1) the signal observed by the radar was, in fact, all the signal that reached through to the lowest scanning levels, and/or

(2) there was some blockage to the beam which prevented the event from being better identified.

Regarding the possibility of beam blockage, the Fitzsimons medical facility, which was located about 10 km northwest of the FL–2 radar, was the target first suspected as the probable source of this blockage. However, analysis showed that the half–power beam was not affected by the presence of this target, but at such low scanning angles, a portion of the main lobe most likely did intercept this target. The other probable source region responsible for blocking a portion of the beam would be ground clutter targets in the vicinity of where this microburst impacted the surface (near mesonet station 13).

The possibility of this hazardous microburst outflow being shallow in depth and located close to the surface was also examined. It was thought that this hazardous outflow occurred below the lowest levels scanned by FL–2. In order to estimate what the velocity profile below this level looked like, a numerical simulation of the wind with height was generated. This simulation provided a closer estimate to the maximum differential velocity which had been observed by the surface mesonet. Though close, this was still an underestimate of the intensity of microburst #78 that occurred on September 2. It could be suggested from this information that if the antenna tilt angle was adjusted lower than 0.4°, a better representation of the intensity of this microburst could have been obtained. However, the problem encountered by pointing the antenna lower than 0.4° would be to increase the probability of blockage to the beam by ground clutter targets.

Overall, it appeared that the dominant problem, which was visible during the four events that were unobserved by the radar, was the absence of adequate signal–to–noise ratio at low–levels.

VII. FUTURE WORK

Subsequent studies will determine how the observed microbursts, as identified in this study, compare with the detections by the current microburst algorithm. Also, there are plans to further compare the radar and mesonet observed microburst wind fields. The wind histories as well as the wind magnitudes versus time will be analyzed for select cases. In operational detection systems, timeliness is very important. The qualitative impression is that the mesonet lags by one or two minutes, but this report identified lags greater than three minutes between observations of maximum velocity differences measured by radar and surface (mesonet and LLWAS) sensors. Therefore, an event by event comparison must be made in order to determine and better understand the problem of lag time between when maximum shears are observed by radar and surface mesonet/LLWAS sensors.

ACKNOWLEDGMENTS

I first want to thank Jim Evans for his guidance and assistance during the time this report was being written. I also wish to acknowledge the work of Chuck Curtiss who maintained the surface mesonet system throughout 1987, and the continued diligence of Charles LeBell who processed all the mesonet and LLWAS data that had been collected throughout the year. I wish to thank John Anderson, Marilyn Wolfson, Mark Merritt, and Dan Hynek for their input to the September 2nd case study. I especially thank Mark Weber who generated the numerical simulation that was used in this report. Thanks and appreciation also goes to Paul Biron who often assisted in the resampling and plotting of radar data, and to Tom Morton for his help in processing both radar and mesonet data. Special thanks goes to Barbara Forman for the software support that she provided which made possible the in-depth analysis of surface data that was required in this report.

REFERENCES

Campbell, S. D., and M. Merritt, 1987: Advanced Microburst Recognition Algorithm. MIT, Lincoln Laboratory Weather Radar Project Report ATC-145, FAA Report DOT/FAA/PM-87-23.

Clark, D. A., 1988: Observability of Microbursts with Doppler Weather Radar During 1986 in Huntsville,Alabama. MIT, Lincoln Laboratory Project Report ATC-160.

DiStefano, J. T., 1987: Study of Microburst Detection Performance During 1985 in Huntsville, Alabama. MIT, Lincoln Laboratory Project Report ATC-142.

Eilts, M. D., and R. Doviak, 1987: Oklahoma Downbursts and Their Asymmetry. J. Climate Appl. Meteor., 26, 69-78.

Evans, J. E., and D. Turnbull, 1985: The FAA/MIT Lincoln Laboratory Doppler Weather Radar Program. Preprints, 2nd International Conference on the Aviation Weather System. Montreal, Canada, American Meteorological Society, pp. 76-79.

Fujita, T. T., 1980: Downbursts and Microbursts - An Aviation Hazard. Preprints, 9th Conference on Radar Meteorology. Boston, MA, American Meteorology Society, pp. 94-101.

Fujita, T. T., 1983: Microburst Wind Shear at New Orleans International Airport, Kenner, Louisiana on July 9, 1982. University of Chicago, Department of Geophysical Sciences, Satellite and Mesometeorology Research Project. The University of Chicago, IL, SMRP Research Paper 199.

Fujita, T. T., 1985: The Downburst - Microburst and Macroburst. Department of Geophysical Sciences, The University of Chicago, IL, 122 p.

Fujita, T. T., 1986: DFW Microburst. Department of Geophysical Sciences, The University of Chicago, IL, 154 p.

Merritt, M. W., 1987: Automated Detection of Microburst Windshear for Terminal Doppler Weather Radar. Preprints, Digital Image Processing and Visual Communications Technologies in Meteorology. Bellingham, WA, Society of Photo-Optical Instrumentation Engineers (SPIE), pp. 61-68.

National Research Council, 1983: Low Altitude Wind Shear and its Hazard to Aviation. National Academy Press, 112 p.

Rinehart, R. E., J. T. DiStefano, and M. M. Wolfson, 1986: Preliminary Memphis FAA Lincoln Laboratory Operational Weather Studies Results. MIT, Lincoln Laboratory Project Report ATC-141.

United States General Accounting Office (GAO), 1987: Aviation Weather–Status of of FAA's New Hazardous Weather Detection and Dissemination Systems. Resources, Community, and Economic Development Division, Washington, DC Report GAO/RCED–87–208, 28 p.

Wilson, J. W., R. D. Roberts, C. Kessinger, and J. McCarthy, 1984: Microburst Wind Structure and Evaluation of Doppler Radar for Airport Wind Shear Detection. J. Climate Appl. Meteor., 23, pp. 898–915.

Wolfson, M. M., J. T. DiStefano, and B. E. Forman, 1986: The FLOWS Automatic Weather Station Network in Operation. MIT, Lincoln Laboratory Project Report ATC–134, FAA Report DOT–FAA–PM–85/27, 284 pp.